Pyruvate Carboxylase: The Protein & Gene in Yeast

by
Filip Lim, B.Sc.(Hons)*

A thesis submitted to the
University of Adelaide, South Australia
for the degree of
Doctor of Philosophy.

April, 1988
Department of Biochemistry,
University of Adelaide,
South Australia.

*Supported by a Commonwealth Postgraduate Research Award

Contents

STATEMENT

This thesis contains no material which has been accepted for the award of any other degree or diploma in any university. To the best of my knowledge it contains no material that has been previously published by any other person except where due reference is made in the text.

Signed:

.....

Filip Lim

ACKNOWLEDGEMENTS

I wish to thank Professor W.H. Elliott for permission to undertake research in the Department of Biochemistry, University of Adelaide. I sincerely thank my supervisor, Dr. John C. Wallace for his advice, enthusiasm and friendly support at all times.

I would like to thank Dr. Phil Morris for his work, careful criticisms and guidance throughout the project. I thank Dr. Manfred Rohde for many useful discussions and expert help in electron microscopy. Many thanks to past and present colleagues in the biotin enzyme project — Dr. Ian Cassady, Dr. John Carver, Karen Oliver, David Mottershead, Chris Bagley, Grant Booker, Alison Whittle, Fil Occhiodoro and Hu Bing — for advice and technical help, and to all of the other inhabitants of Labs 109, 110 and 112 who made it so enjoyable to work here:

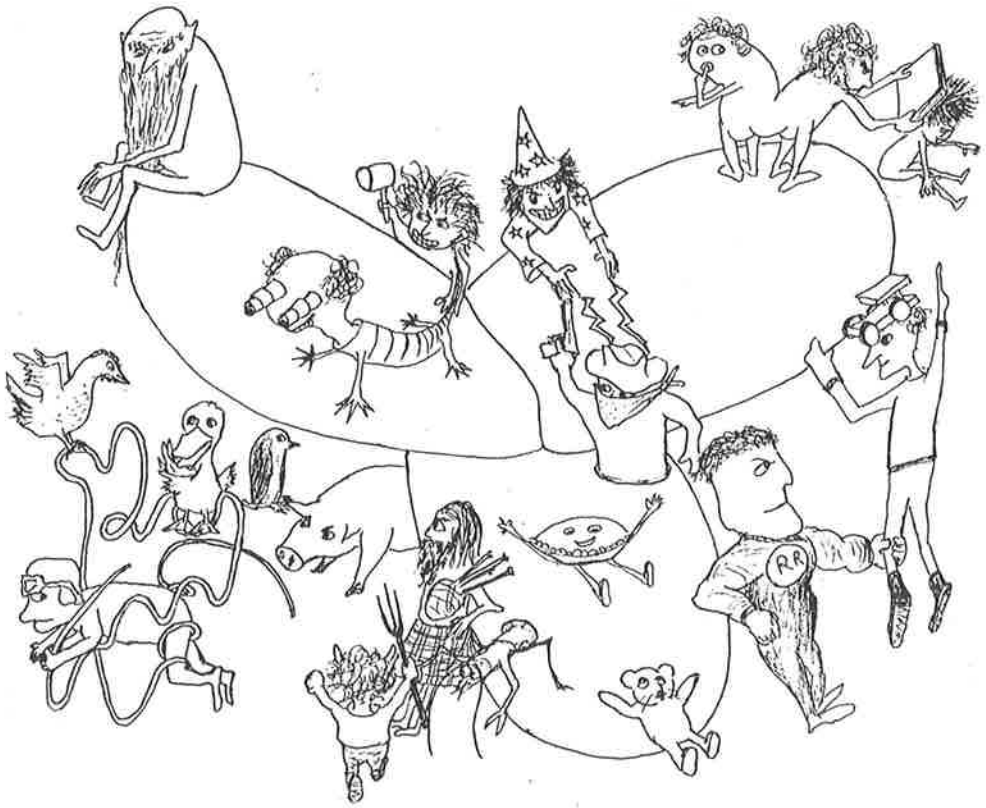

I am grateful to Jenny Brazier and Yvonne Riese for expert technical assistance and to Joan Rowe, Steve Rogers, Denise Turner and Mark Snoswell for their expertise in protein sequencing. I would also like to thank all other members of the Biochemistry Department who gave their time and effort so freely.

Finally I am indebted to my parents for their continued support, understanding and tolerance.

ABBREVIATIONS

In addition to the abbreviations accepted by *The Journal of Biological Chemistry* the following have been used:

A_λ	.....	absorbance at wavelength λ nm
NEM	.....	N-ethyl-morpholine
oATP	.....	2′, 3′ dialdehyde periodate oxidation product of ATP
PEG	.....	polyethylene glycol
PMSF	.....	phenylmethanesulphonyl fluoride

ERRATA

page	line	
1	11	"Fersht, 1985" should read "reviewed in Fersht, 1985".
1	18	"Fersht, 1985" should read "reviewed in Fersht, 1985".
14	24	The solvent for 50 mM PMSF was ethanol.
16	1	"....precipitation with...." should read "....precipitating the protein with...."

The following two references should be inserted into the bibliography:

1. Dale, R.M.K., McClure, B.A. and Houchins, J.P. (1985) *Plasmid* **13**, 31–40.

2. Hardie, D.G. and Coggins, J.R. (1986) *Multidomain Proteins - Structure and Evolution.* Elsevier, Amsterdam.

SUMMARY

Pyruvate carboxylase from yeast was chosen as a model to study the structure, function, control and evolution of multidomain proteins. The enzyme was purified to homogeneity from baker's yeast and electron microscopy showed that it is structurally similar to vertebrate pyruvate carboxylases. The native protein consists of four subunits, each containing one biotin molecule, arranged in a tetrahedron-like configuration. The activators acetyl-CoA and palmitoyl-CoA enhance tetramer formation whereas the inhibitors L-aspartate and 2-oxo-glutarate are detrimental to the native structure. Crystallisation of the enzyme was attempted and a number of conditions have been screened by a vapour diffusion method. Electron microscopy using the immunogold technique showed that yeast pyruvate carboxylase is a cytosolic enzyme, in contrast to the vertebrate enzymes, which reside in the mitochondria. Chicken and sheep pyruvate carboxylases cross-reacted with anti-yeast pyruvate carboxylase antibodies but the determinants involved are inaccessible in the native enzymes and only become exposed upon denaturation.

The nucleotide sequence of the yeast pyruvate carboxylase gene was determined from a cloned fragment of yeast genomic DNA. The identity of the clone and sections of the inferred amino acid sequence were confirmed by peptide sequencing. The deduced translation product codes for a polypeptide of 1 178 amino acids, having a calculated relative molecular mass of 130 100. The protein shows strong sequence homology to other biotin carboxylases, lipoamide transferases and carbamyl phosphate synthetases. The homologous regions suggest the presence of three subsites linearly distributed along the enzyme sequence: a biotin attachment site, a ketoacid-binding site and an ATP/HCO_3-binding site. Partial proteolysis with a variety of proteases under non-denaturing conditions indicates the presence of structural domains corresponding to these subsites and two affinity labels of the ATP-binding site were characterised.

Chapter 1

Introduction

1.1 MULTIDOMAIN PROTEINS

It is a widely accepted view that proteins are composed of discrete globular components called domains. Each of these distinct, folded regions is made up of a continuous stretch of polypeptide chain and usually has a specific catalytic or binding function (Hardie and Coggins, 1986). Detailed three-dimensional data has been obtained for a large number of the smaller proteins and it is apparent that many of these molecules share common motifs in structure as well as sequence. When the structures of crystalline serine proteases were solved, it was found that the polypeptide backbones of the members of this family were virtually superimposable (Fersht, 1985). Differences in their specificities were due to amino acid changes in the substrate binding pocket.

Another way in which diversity of function appears to have been generated during evolution is by gene fusion. The pyridine nucleotide-linked dehydrogenases form a functionally related family of proteins which all bind the same cofactor. Although the structures of the complete intact enzymes are extensively different in some cases, all contain a nucleotide-binding domain with a similar three-dimensional configuration (Fersht, 1985). Thus it seems that the linkage of domains via gene fusion has led to the evolution of more complex proteins from simpler primitive ancestors. Some of the introns found in eukaryotic structural genes may be remnants of untranslated DNA flanking these progenitor genes. Indeed, the correspondence of exons to structural do-

mains in families such as the hemoglobins (Blake, 1981) and the lysozymes (Artymiuk *et al*, 1981) supports such a hypothesis.

Large enzymes which carry several catalytic functions per subunit appear to consist of a complicated mosaic of interacting domains but so far detailed three-dimensional structural data is sparse for these multifunctional enzymes. However, one way in which the analysis of such complex molecules could be simplified would be to identify and characterise separately the individual domains. Total function could then be deduced by studying the interaction between these domains.

1.2 THE BIOTIN ENZYMES

The biotin enzymes provide an ideal system to study multidomain proteins. This family consists of the carboxylases, the decarboxylases and transcarboxylase (Wood and Barden, 1977; Moss and Lane, 1971). These enzymes all contain a covalently attached prosthetic group *biotin* (Vitamin H), which serves as a carrier of activated CO_2. The carboxyl group of biotin is linked to the ϵ-amino group of a specific lysine residue in the apoenzyme by a holoenzyme synthetase. Catalytic function in the biotin enzymes is accomplished by a combination of two out of three basic activities: biotin carboxylase (equation 1), carboxyltransferase (equation 2) and carboxybiotin decarboxylase (equation 3).

$$\text{ENZ-biotin} + HCO_3^- + ATP \rightleftharpoons \text{ENZ-biotin-}CO_2^- + ADP + P_i \quad (1)$$

$$\text{ENZ-biotin} + \text{R-}CO_2^- \rightleftharpoons \text{ENZ-biotin-}CO_2^- + \text{R-H} \quad (2)$$

$$\text{ENZ-biotin-}CO_2^- + H^+ + 2Na^+_{in} \rightleftharpoons \text{ENZ-biotin} + CO_2 + 2Na^+_{out} \quad (3)$$

All biotin enzymes contain a carboxyltransferase activity; in the carboxylases this is combined with biotin carboxylase, in decarboxylases, with carboxybiotin decarboxylase and in transcarboxylase, with another carboxyltransferase activity of a differ-

ent substrate specificity. Thus different members of the biotin enzyme family, while catalysing different overall reactions, may nevertheless share similar, if not identical, partial functions stemming from a common evolutionary origin. Obermayer and Lynen (1976) reviewed the structure of several biotin-containing enzymes and proposed that the large multifunctional polypeptides of this family have evolved by fusion of smaller, simpler components. According to this hypothesis the successive stages in the evolution of the biotin enzymes are represented by *E.coli* acetyl-CoA carboxylase and *P.shermanii* transcarboxylase with their three unifunctional polypeptide components, followed by the two component polypeptide enzymes such as propionyl-CoA carboxylase and *P.citronellolis* pyruvate carboxylase, and finally the single multifunctional polypeptides such as the eukaryotic acetyl-CoA carboxylases and pyruvate carboxylases.

1.3 PYRUVATE CARBOXYLASE

Pyruvate carboxylase catalyses the ATP-dependent attachment of a carboxyl group from bicarbonate to pyruvate to form oxaloacetate. In vertebrates this has an anaplerotic function: when intermediates of the citric acid cycle are withdrawn to be built into anabolic products, oxaloacetate is synthesised by pyruvate carboxylase to maintain the levels of these intermediates. Pyruvate carboxylase also serves as an anaplerotic enzyme in numerous microorganisms including *Bacillus stearothermophilus* (Sundaram, 1973), *Pseudomonas citronellolis* (O'Brien *et al*, 1972), *Saccharomyces cerevisiae* (Losada *et al*, 1964), and *Aspergillus nidulans* (Skinner and Armitt, 1972). The higher eukaryotic pyruvate carboxylases are mitochondrial whereas in all filamentous fungi studied so far and in most, but not all, yeasts, the enzyme appears to have a cytosolic localisation. It should be noted though that at the time when this project was started there was still some controversy over the subcellular localisation of pyruvate carboxylase in some

species.

Purification of pyruvate carboxylase has been reported from many vertebrate and microbial sources (Wallace, 1985) but there has been considerable confusion over the structural properties of this enzyme due to studies of nonhomogeneous preparations. The information given in this section represents what was known when this project was initiated in February 1985. As will be shown in the following chapters much of **this data has now been extensively revised.**

1.3.1 Physicochemical Properties

The active enzyme isolated from all species appears to have a molecular weight in the range of 440 000 to 600 000. In *Pseudomonas citronellolis* the enzyme is an octamer of the form $\alpha_4\beta_4$ where the individual α and β polypeptides have molecular weights of 65 000 and 54 000 respectively. In all other species investigated the enzyme is a tetramer of four identical subunits, each with a molecular weight in the range 110 000 to 150 000. Each subunit (in *Pseudomonas citronellolis* each α subunit) contains a single biotin moiety and a divalent metal ion. Manganese is the metal normally found tightly bound in vertebrate pyruvate carboxylases though magnesium may substitute for manganese in manganese deficiency (Wallace and Easterbrook-Smith, 1985). In yeast (Scrutton *et al*, 1970) and *Bacillus stearothermophilus* (Libor *et al*, 1979) zinc has been identified as the tightly bound divalent cation.

1.3.2 Sequence Data

When this study was begun only a limited amount of sequence data for the biotin enzymes was available. The N-termini of all pyruvate carboxylases sequenced so far have been blocked. However, Rylatt *et al* (1977) used the high affinity of avidin for biotin to detect and isolate biotin-containing tryptic peptides from sheep, chicken and turkey pyruvate carboxylases. Rather more sequence data around the biotin attach-

HUMAN PC	Gly	Gln	Pro	Leu	Cys	Val	Leu	Ser	Ala	Met	BCT	Met	Glu	Thr	Val	Val	Thr	Ser	Pro	Met
CHICK PC	Gly	Ala	Pro	Leu	—	Val	Leu	Ser	Ala	Met	BCT	Met	Glu	Thr	Val	Val	Thr	Ala	Pro	Arg
SHEEP PC	Gly	Gln	Pro	Leu	—	Val	Leu	Ser	Ala	Met	BCT	Met	Glu	Thr	Val	Val	Thr	Ser	Pro	Val
PS TC	Gly	Gln	Thr	Val	Leu	Val	Leu	Glu	Ala	Met	BCT	Met	Glu	Thr	Glu	Ile	Asn	Ala	Pro	Thr
EC ACC	Gly	Asn	Thr	Leu	Cys	Ile	Val	Glu	Ala	Met	BCT	Met	Met	Asn	Gln	Ile	Glu	Ala	Asp	Lys

Figure 1.1 **Sequence homology around the biotin attachment site of pyruvate carboxylase and two other biotin enzymes.** PC = pyruvate carboxylase, the human enzyme (Freytag and Collier, 1984) the chicken and turkey enzymes, and the sheep enzyme (Rylatt *et al*, 1977 - the two avian sequences were identical). PS TC = *Propionibacterium shermanii* transcarboxylase. EC ACC = *E. coli* acetyl-CoA carboxylase. BCT = biocytin = biotinyl-ϵ-lysine.

ment site of human pyruvate carboxylase was reported by Freytag and Collier (1984) who used the oligonucleotide probing approach to obtain a cDNA clone of human pyruvate carboxylase mRNA. The only other sequences available for biotin enzymes at the beginning of this project were those for the 1.3S biotinyl subunit of *Propionibacterium shermanii* transcarboxylase (Maloy *et al*, 1979) and a fragment of the biotinyl subunit of *E. coli* acetyl-CoA carboxylase (Sutton *et al*, 1977). Both were determined by peptide sequencing but the 1.3S transcarboxylase subunit gene was also cloned (Murtif *et al*, 1985). Considerable homology was observed in all of the above sequences (Figure 1.1). This was taken as good evidence firstly that these enzymes shared some common evolutionary origin, and secondly that there was strong selective pressure to conserve the amino acid sequence in the region around the biotin site.

1.3.3 Three-dimensional Structure

Although crystals of pyruvate carboxylase have not been obtained for three-dimensional analysis by X-ray diffraction the quaternary structure of the enzyme from several

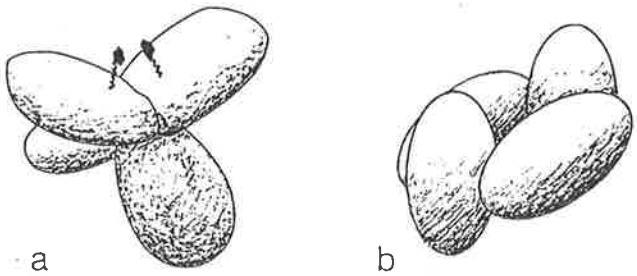

Figure 1.2 **Models for the three-dimensional configuration of pyruvate carboxylase.** The subunits of pyruvate carboxylases from all species studied are arranged in a tetrahedral manner (a) (Mayer *et al*, 1980; Osmani *et al*, 1984; Libor *et al*, 1979) except in the yeast enzyme where a rhomboidal configuration (b) has been proposed (Cohen *et al*, 1979). In (a) the location of the biotin moieties as determined by binding studies with avidin (Johannssen *et al*, 1983) on the upper two subunits has been indicated.

species has been examined by electron microscopy of negatively stained samples. In sheep, chicken, rat, (Mayer *et al*, 1980) *Aspergillus nidulans* (Osmani *et al*, 1984) and *Bacillus stearothermophilus* (Libor *et al*, 1979) the native tetramer has a tetrahedron-like arrangement (Figure 1.2a) whereas the four subunits of yeast pyruvate carboxylase have been reported (Cohen *et al*, 1979) to be prolate ellipsoids located at the corners of a rhombus such that diagonally opposite pairs of protomers lie in orthogonal planes (Figure 1.2b).

Electron microscopy was also used to locate the active site of vertebrate pyruvate carboxylases and the *Aspergillus* enzyme. In these studies the geometry of the binding of avidin, a 68-kDa protein, to biotin on the enzyme enabled the prediction of the position of the prosthetic group within the three-dimensional structure of the tetramer. To account for the polymerisation of pyruvate carboxylase and avidin into linear unbranching chains, Johannssen *et al* (1983) proposed a model in which the biotin moieties are localised on the midline of each subunit, within approximately 3 nm

of the intersubunit junction (Figure 1.2a).

1.3.4 Mechanism

The conversion of pyruvate to oxaloacetate proceeds via two partial reactions which may be assayed independently:

$$\text{ENZ-biotin} + HCO_3^- + \text{ATP} \rightleftharpoons \text{ENZ-biotin-}CO_2^- + \text{ADP} + P_i$$

$$\text{ENZ-biotin-}CO_2^- + \text{pyruvate} \rightleftharpoons \text{ENZ-biotin} + \text{oxaloacetate}$$

The carboxyl group is temporarily carried by the prosthetic group biotin, which is covalently attached to the protein via the ϵ-amino group of a lysine residue. It is envisaged that this long flexible linkage enables the biotin moiety to swing between two catalytic subsites transporting a carboxyl group from one to the other. On the basis of isotopic exchange studies and experiments using ^{32}P- and ^{14}C-labelled enzyme-bound intermediates Wallace *et al* (1985) have described the first partial reaction (see also Chapters 5 and 6) as follows:

$$\text{ENZ-biotin} + \text{ATP} \overset{Mg^{2+}}{\rightleftharpoons} \text{ATP-ENZ-biotin}$$

$$\text{ATP-ENZ-biotin} + HCO_3^- \rightleftharpoons \left[\begin{matrix} Pi \\ \vdots \\ COO^- \end{matrix}\!\!>\!\text{ENZ-biotin}\right] + \text{ADP}$$

$$\left[\begin{matrix} Pi \\ \vdots \\ COO^- \end{matrix}\!\!>\!\text{ENZ-biotin}\right] \overset{\text{acetyl CoA}}{\rightleftharpoons} \text{ENZ-biotin-}COO^- + Pi$$

According to these authors the binding of pyruvate to the enzyme then induces the translocation of carboxybiotin from the first to the second partial reaction site. In the scheme proposed by Goodall *et al* (1983) the second partial reaction proceeds via an enolate-ion relay mechanism:

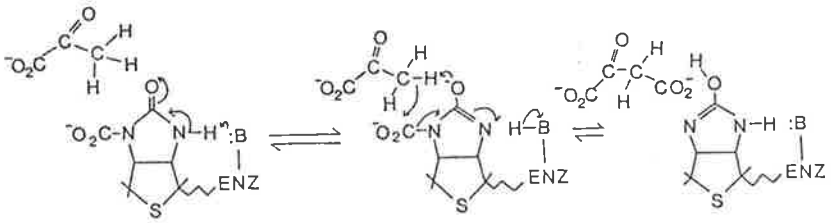

Such partitioning of function in this enzyme should facilitate the identification of its component structural units.

1.3.5 Regulation

Allosteric proteins are capable of responding to changes in the environment by the binding of effector molecules. This leads to conformational changes which alter the orientation and function of domains. In pyruvate carboxylase catalytic activity is regulated by the presence of acetyl-CoA, although the vertebrate, fungal and bacterial pyruvate carboxylases differ in their regulatory properties. The vertebrate forms are highly dependent on the presence of acetyl-CoA whereas many of the bacterial enzymes exhibit considerable activity in its absence and some, such as those from *Pseudomonas citronellolis* and *Azotobacter vinelandii* are not activated by this ligand at all. The fungal pyruvate carboxylases are active in the absence of acetyl-CoA but are stimulated by a wide range of acyl-CoA compounds and inhibited by L-aspartate.

1.4 PROJECT RATIONALE

Due to the large size of pyruvate carboxylase (well over 1000 amino acids per subunit) obtaining the full primary structure by direct protein sequencing would be a long and cumbersome task. A more profitable approach would be to clone and sequence the relevant gene, and obtain the protein sequence by inference. Much of the past work in this laboratory has been conducted on chicken and sheep pyruvate carboxylases. However, the genes for these enzymes are likely to be as large as 10 kb since in addition

to the large size of the coding region, they would almost certainly contain extensive regions of intervening DNA. One way in which this problem may be circumvented is by making cDNA clones. The cloning and sequencing of the yeast pyruvate carboxylase gene is simplified compared to vertebrate genes since not only is the yeast genome is relatively small but also yeast genes, apart from a few rare exceptions, do not contain introns.

Yeast is also an ideal experimental organism in that while it has the characteristics of a eukaryotic organism, both stringent environmental and genetic control are possible. An obvious advantage of these qualities is that large quantities of cloned enzyme could be produced, perhaps by overexpression of its gene on suitable yeast plasmids. This would enable large amounts of enzyme to be committed to "protein-expensive" work such as crystallisation studies. The ease of experimental manipulation of yeast would also facilitate the expression and characterisation of mutant pyruvate carboxylases, making it possible to study the functional effects of specific changes introduced genetically. The knowledge gained by experimentation with such a system would shed light not only on the many aspects of protein structure and evolution, but also on the mechanisms and problems involved in protein design and expression.

1.5 AIMS

For a complete understanding of the molecular mechanism of pyruvate carboxylase a detailed structural description of the enzyme is necessary. Specifically, the main aims in this analysis of yeast pyruvate carboxylase were:

1. To purify and characterise the enzyme directly.

2. To obtain the full primary structure of the enzyme by gene sequencing.

3. To identify the component domains of the enzyme.

Chapter 2

Materials and Methods

2.1 MATERIALS

2.1.1 Yeast

Compressed yeast (1kg blocks) was a generous donation from Mauri Foods Company (South Australia). The GP001 haploid yeast strain (mat α, ura3-52) was kindly supplied by Dr. Glenn Pure while the *pyc* mutant was obtained as a gift from Dr. C. Wills (Wills and Melham, 1985).

2.1.2 Radiochemicals

NaH[^{14}C]O_3 (50–60 mCi/mmol), D[carbonyl-^{14}C]biotin (40–60 mCi/mmol) and [5′,8-^{3}H]ATP (40–60 mCi/mmol) were purchased from Amersham while [α-^{32}P]dATP, [α-^{32}P]dCTP and [γ-^{32}P]ATP (all three nucleotides at 3000 Ci/mmol) were from Bresatec, South Australia.

2.1.3 Proteins

T4 DNA polymerase and terminal transferase were purchased from PL Biochemicals while T4 DNA ligase and restriction enzymes were obtained from Bresatec, South Australia. Protein molecular mass standards, avidin, the nonspecific protease from *Streptomyces griseus*, trypsin and thermolysin were from Sigma while proteinase K and calf intestinal phosphatase were from Boehringer Mannheim. Chicken pyruvate carboxylase was purified as described by Goss *et al* (1979), sheep and rat pyruvate

carboxylases were gifts from Ms. K.J. Oliver and transcarboxylase was a gift from Dr. N. Phillips.

2.1.4 Immunochemicals

Nitrocellulose (0.2 μm pore size) was obtained from Sartorius (Göttingen, West Germany), Nitro Blue Tetrazolium, 5-bromo-4-chloro-3-indolyl phosphate and avidin-alkaline phosphatase conjugate were purchased from Bresatec, South Australia while goat anti-rabbit alkaline phosphatase was from Sigma (St. Louis, MO, USA).

2.1.5 Chromatographic Media

Sephadex G-10 and G-50, DEAE-Sephacel, protein A-Sepharose, the Superose 6 and the Superose 12 column were purchased from Pharmacia. Monomeric avidin-Sepharose was made by coupling avidin to cyanogen bromide-activated Sepharose CL-4B (Pharmacia) as described by Kohanski and Lane (1985). The Aquapore RP300 C_8 column was from Brownlee Labs, the TSK3000 SW column from Toya Soda and the Nova Pak C_{18} column from Waters.

2.1.6 Miscellaneous

All standard reagents used were of analytical grade. Acetyl-CoA was prepared from acetic anhydride by the method of Simon and Shemin (1953). The oligonucleotide primer used for generating deletion subclones (Dale *et al*, 1985), M13mp19 vector and dideoxynucleotide sequencing kits were from Bresatec, South Australia. LR gold resin from Sigma Pharmaceuticals Ltd. (Victoria, Australia) and benzoyl-peroxide from Polaron Equipment Ltd. (Hertfordshire, England). The Gamma A nucleotide labelling kit was obtained from Bresatec, South Australia and 8-azido-ADP was from Sigma (St. Louis, MO, USA).

2.2 METHODS

2.2.1 Protein Assays

Three methods were used to estimate protein concentrations of samples:

Biuret Assay

The following is a microtitre plate adaptation of the method described by Layne (1957). To 50µl of sample (1 - 10 mg/ml protein) 200µl of biuret reagent (0.15% (w/v) $CuSO_4$, 0.6% (w/v) sodium tartrate, 3% (w/v) NaOH) were added. After 5 minutes the A_{540} of the sample was measured on a microtitre plate spectroscopic reader. The protein concentration of test samples was determined from a standard curve of bovine serum albumin. Although this method of protein estimation was the most independent of amino acid composition and least subject to artifacts, it had the disadvantage of being quite insensitive.

Ultraviolet Absorbance

The absorbance of samples (1ml) at 280nm and 260nm was measured and the protein concentration calculated according to Layne (1957):

$$\text{protein concentration (mg/ml)} = (1.55 \times A_{280}) - (0.76 \times A_{260})$$

This method was unreliable for samples containing particulate or 260nm-absorbing material, or below protein concentrations of 0.1mg/ml. For pure samples of yeast pyruvate carboxylase an extinction coefficient of $\epsilon_{280nm}^{1mg/ml} = 0.725$ (Section 3.2.2) was used.

Bradford Assay

The microtitre plate adaptation (Rylatt and Parish, 1982) of the method of Bradford (1976) was used. Since the binding of Coomassie Brilliant Blue G_{250} is influenced

by amino acid composition, for the purposes of determining protein concentrations of purified yeast pyruvate carboxylase the following formula was used:

$$\text{pyruvate carboxylase concentration} = \begin{array}{l}0.867 \times \text{concentration determined using} \\ \text{bovine serum albumin standards.}\end{array}$$

This scale factor was experimentally determined (Section 3.2.2) by a calibration curve using known amounts of purified yeast pyruvate carboxylase (determined by the biuret method).

2.2.2 Biotin Assay

Biotin content was estimated using the avidin/[^{14}C]-biotin assay described by Rylatt *et al* (1977). To eliminate steric interference of avidin/biotin interactions by protein, pyruvate carboxylase samples were pretreated with a nonspecific protease from *Streptomyces griseus* ($\frac{1}{100}$ protease/substrate mass ratio) for 1 hour at 37°C followed by 5 minutes at 90°C.

2.2.3 Pyruvate Carboxylase Activity Assays

Yeast pyruvate carboxylase activity was measured at 30°C and pH 8.0 in the presence of 250μM acetyl-CoA by either the isotopic incorporation assay or the enzyme-linked spectrophotometric assay (Young *et al*, 1969). One unit of enzyme is defined as that quantity which catalyses the carboxylation of 1 μmol of pyruvate to oxaloacetate in one minute. The final reaction mix contained 100 mM Tris-chloride pH 8.0, 8 mM $MgCl_2$, 2.5 mM ATP (sodium salt), 10 mM sodium pyruvate, and 10 mM $NaHCO_3$. The spectrophotometric assay mix also contained 0.125 mM NADH and 1 U/ml malate dehydrogenase. The final specific activity of $H^{14}CO_3^-$ used in isotopic assays was 250–300mCi/mol.

Where the activity of samples prepared for electron microscopy was measured (Sections 3.2.5 and 3.2.6), the spectrophotometric assay was started by the addition of the concentrated reactants to an aliquot of the pre-diluted enzyme rather than the usual

procedure of adding enzyme to pre-diluted reactants. The assay was conducted while another aliquot was simultaneously mounted for examination in the electron microscope. This method enabled the measurement of activity of the enzyme at the same dilution and after the same incubation period (15 minutes) as mounted samples.

2.2.4 SDS Gel Electrophoresis

Proteins were electrophoresed on polyacrylamide gels in the presence of SDS and β-mercaptoethanol according to the method of Laemmli (1970). Gels were stained with Coomassie Brilliant Blue R_{250} (1g in 1 litre of 50% (v/v) methanol, 10% (v/v) acetic acid) and destained with 5% (v/v) methanol, 10% (v/v) acetic acid. The high molecular weight markers consisted of myosin (205 kDa), β-galactosidase (116 kDa), phosphorylase b (97.4 kDa), bovine serum albumin (66 kDa), ovalbumin (45 kDa) and carbonic anhydrase (29 kDa) while the low molecular mass markers were bovine serum albumin (66 kDa), ovalbumin (45 kDa), carbonic anhydrase (29 kDa), trypsinogen (24 kDa), β-lactoglobulin (18.4 kDa) and lysozyme (14.3 kDa).

2.2.5 Purification of Yeast Pyruvate Carboxylase

Throughout the purification procedure, particularly during the addition of protamine sulphate, ammonium sulphate and PEG, the pH was maintained between 7.2 – 7.4 by the addition of 1 M Tris. All operations were carried out at room temperature. Either 500 g or 1 kg samples of compressed yeast were normally processed: the quantities in the following method were doubled for a 1 kg preparation.

Cell Disruption

Baker's yeast (500 g) was mixed with 50 g sucrose and 300 ml TM buffer (100 mM Tris-acetate pH 7.2, 10 mM $MgCl_2$) and incubated overnight at room temperature. In the following morning 6 mg DTE and 1 ml 50 mM PMSF was added and the cells

disrupted by either one of the following two methods:

1. Passage through a French press at 12 000 lb/in^2 (83 MPa).

2. The yeast cell suspension was diluted twofold with TM buffer and pumped through a 700 ml *Dynomill* bead mill (Willy Bachofen, Basel) at 7 l/hr using a blade speed of 3000 revolutions per minute. The chamber was loaded to 80% volume with 0.5–0.75 mm glass beads.

Cell debris was removed by centrifugation at 18000 $\times g$ for 15 minutes and the pH of the supernatant adjusted to 7.2. After the addition of 4 ml 10 mM biotin the extract was incubated for a further 15 minutes before assay.

Lysates obtained by both methods of cell disruption contained approximately the same amount of enzymatic activity.

Clarification

Lipids were removed from the lysate by extraction with an equal volume of 1,1,2-trichloro-1,2,2-trifluoro-ethane. Nucleic acids were precipitated by the addition of 100 ml of 2.5% protamine sulphate and removed by centrifugation at 18000 $\times g$ for 15 minutes.

Salt Fractionation

The crude extract was fractionated by stirring with 1.8 M ammonium sulphate for 30 minutes. After centrifugation at 18000 $\times g$ for 15 minutes the pellet containing the pyruvate carboxylase was resuspended in approximately 60 ml TM buffer containing 0.01 mM PMSF.

Desalting

Ammonium sulphate was removed from the enzyme preparation by precipitation with 14.5% (w/v) PEG 8000 (after stirring for 5 minutes). The pellet was collected by centrifugation at 22000 $\times g$ for 5 minutes and resuspended in 25 mM potassium phosphate pH 7.2, 1 mM EDTA, 20 mM ammonium sulphate (approximately 50 ml). Insoluble material was removed by centrifugation at 22000 $\times g$ for 5 minutes.

Ion Exchange Chromatography

The protein extract was chromatographed on a 200 ml DEAE-Sephacel column with a linear gradient from 20 mM ammonium sulphate to 200 mM ammonium sulphate in 25 mM potassium phosphate pH 7.2, 1 mM EDTA (Goss *et al*, 1979) at a flow rate of 1 ml/min. Fractions of 12 ml were collected and assayed. Those containing pyruvate carboxylase activity were pooled and concentrated by precipitation with 1.8 M ammonium sulphate. The enzyme pellet was resuspended in 50 mM potassium phosphate pH 7.2 containing 0.01 mM PMSF.

Affinity Chromatography

Chromatography on monomeric avidin-Sepharose was performed in 50 mM potassium phosphate pH 7.2 as described by Henrikson *et al* (1979). The A_{280} of the effluent was monitored and the protein peak obtained by elution with 1 mM biotin was collected by precipitation with 1.8 M ammonium sulphate.

Gel Filtration

This step was only necessary if contaminants were still evident after avidin-Sepharose chromatography. Aliquots of enzyme (500 μl maximum volume) were purified by gel filtration in 100 mM Tris-acetate pH 7.2, 10 mM $MgCl_2$ on Superose 6 or Superose

12 (30 ml columns) using the Pharmacia FPLC system. The pyruvate carboxylase activity eluting immediately after the void volume was collected and precipitated with 1.8 M ammonium sulphate.

Storage and Assay

Enzyme activity during the purification procedure was monitored using the spectrophotometric assay. All samples prior to the PEG precipitation step were assayed in the presence and absence of avidin (final conc. $\sim$ 1 mg/ml) to determine biotin-dependent activity, since other NADH-using enzymes present caused an overestimation of activity.

Protein concentration was estimated by the A_{260}/A_{280} spectrophotometric method of Layne except for the first 3 stages of the purification. These samples contained too much 260 nm absorbing material and were assayed by the biuret method.

Enzyme purity was determined by SDS polyacrylamide gel electrophoresis. The material used for experiments contained less than 5% contaminants as measured by densitometry of Coomassie-stained gels. Yeast pyruvate carboxylase was stored snap-frozen at -70°C at concentrations above 3 mg/ml in 50 mM Tris-acetate pH 7.2 containing 5 μM PMSF.

2.2.6 Protein Crystallisation

Figure 2.1 shows the hanging drop method (J. Priestle, personal communication) employed to screen over 150 conditions for the crystallisation of yeast pyruvate carboxylase. The wells of a 24-place multiwell tray were filled with a 1 ml reservoir of buffer containing precipitant over a range of concentrations. The droplet was made up by mixing 5 μl of the reservoir solution with 5 μl of enzyme (dissolved in the same buffer as the precipitant) on a siliconised coverslip which was then inverted over a well. The lips of the well were covered with grease to ensure an airtight seal.

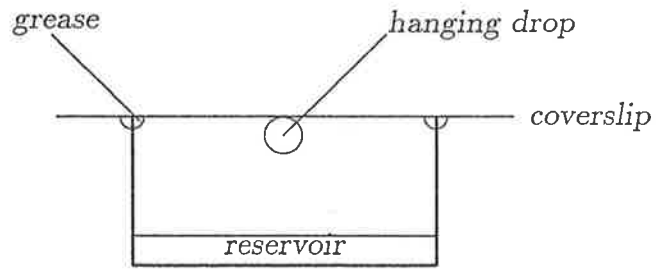

Figure 2.1: **The hanging drop vapour diffusion method.**

2.2.7 Electron Microscopy with Negative Stain

Thin carbon support films, approximately 4-6 nm thick, were prepared by direct sublimation of carbon on to freshly cleaved mica. Samples of yeast pyruvate carboxylase in the presence or absence of activators, inhibitors or avidin were prepared at final enzyme concentrations in the range 8–80 μg/ml. Using 400 mesh copper grids, these samples were then negatively stained with 4% (w/v) uranyl acetate dissolved in water (pH 4.5) according to the method of Valentine *et al* (1968). Enzyme samples were diluted in 100 mM Tris acetate, pH 7.2 containing 10 mM $MgCl_2$ together with the additions indicated in the figure and table legends. The avidin titration series was performed using the protocol described by Johannssen *et al* (1983). Specimens were examined and micrographs taken with a Philips EM 300 electron microscope at an acceleration voltage of 80 kV using Kodak Electron Microscope Film 4489. Tilting of samples was performed using a Philips EM 400 electron microscope with an eucentric goniometer. Magnifications were calibrated using a lined-grating replica. Primary magnifications ranged from 19000 × to 60000 ×.

2.2.8 Polyclonal Antibodies

Rabbit polyclonal antibodies were raised against purified yeast pyruvate carboxylase according to established procedures (Brown, 1967). The antiserum was purified by precipitation with 30% (w/v) ammonium sulphate followed by protein A-Sepharose chromatography (Ey *et al*, 1978). Non-denaturing Ouchterlony immunodiffusion was performed in 50 mM sodium phosphate pH 7.2, 0.02% (w/v) sodium azide, 1% agarose as described by Radding and Shreffler (1966).

2.2.9 Western Blotting

After SDS gel electrophoresis of samples, protein bands were transferred to nitrocellulose according to Svboda *et al* (1985). To detect biotin-containing proteins, the nitrocellulose blots were incubated with 1 μg/ml avidin/alkaline phosphatase conjugate in Buffer 1 (100 mM Tris Cl pH 7.0, 100 mM NaCl, 2 mM $MgCl_2$, 0.5% (v/v) Tween 20) for 1 hour at room temperature, washed twice with Buffer 2 (100 mM Tris pH 9.5, 100 mM NaCl, 5 mM $MgCl_2$) and developed in 0.3 mg/ml Nitro Blue Tetrazolium and 0.2 mg/ml 5-bromo-4-chloro-3-indolyl phosphate in Buffer 2 for 5 minutes in subdued lighting. The same procedure was followed to achieve immunochemical staining except that 1 μg/ml rabbit anti-yeast pyruvate carboxylase antibody replaced the avidin conjugate and a second incubation with goat anti-rabbit antibody/alkaline phosphatase conjugate ($\frac{1}{1000}$ dilution in Buffer 1) preceded the colour development process.

2.2.10 Fixation and Embedding of Yeast Protoplasts

Yeast protoplasts were prepared as described by Cryer *et al* (1975) and suspended in 1.5% (w/v) agar; after solidification the agar was cut into small cubes. Fixation was performed by immersion for 60 minutes in a solution containing 0.5% (v/v) formaldehyde and 0.3% (v/v) glutaraldehyde in 0.1M potassium phosphate buffer pH 7.0 held on ice. Dehydration was achieved by equilibration with a series of graded ethanol so-

lutions (10, 25, 50, 70, 90, 100% (v/v)) on ice. Samples were then embedded in LR gold resin: a) in 50% (w/v) LR gold resin and 50% ethanol for 60 minutes; b) in 70% LR gold resin and 30% ethanol for 60 minutes at room temperature. These were left overnight in pure LR gold resin at 4°C, followed by an incubation in the embedding mixture consisting of LR gold resin and 1.5% (w/v) benzoyl-peroxide paste (60% in dibutyl phthalate) for 8 hours or overnight at 4°C. Fresh embedding mixture was added prior to polymerisation for 36 - 48 hours at room temperature.

2.2.11 Immunocytochemical Labelling

Colloidal gold particles were prepared as described by Slot and Geuze (1981) and covered with goat anti-rabbit IgG according to de Mey *et al* (1981). Thin sections were mounted on formvar covered 300 mesh nickel grids. The grids were then incubated for 3 hours at room temperature on a drop of various dilutions of rabbit anti-yeast pyruvate carboxylase polyclonal antibodies. Sections were rinsed in phosphate-buffered saline and incubated with goat anti-rabbit gold (GARG) for 1 hour at room temperature. Finally, the sections were rinsed with phosphate-buffered saline and water prior to poststaining with aqueous 4% (w/v) uranyl acetate for 4 minutes.

The specificity of labelling was demonstrated by use of the following controls: a) incubation of the sections with GARG only; b) incubation of the sections with nonspecific (rabbit anti-bacterial carbon monoxide dehydrogenase) IgG antibodies followed by GARG.

2.2.12 Reverse Phase HPLC

C_8 reverse phase HPLC was conducted on a Brownlee Labs Aquapore RP-300 column (220 mm × 4.6 mm internal diameter) while C_{18} reverse phase HPLC was performed on a Waters Nova Pak column (100mm × 4 mm internal diameter). The gradient used in both cases was 0–60% acetonitrile in aqueous 0.1% trifluoroacetic acid over 60

minutes, at a flow rate of 1 ml/min.

2.2.13 Isolation of Tryptic Peptides

Yeast pyruvate carboxylase (3mg/ml) was digested to completion with trypsin at an enzyme to protease mass ratio of 10 in 10 mM Tris-Cl pH 8.0, 2 M urea at 37°C for 2 hours. The tryptic peptides were separated by reverse phase high performance liquid chromatography on a C_8 column.

2.2.14 Protein Sequencing

The amino-terminal sequences of peptides were determined by automated Edman degradation with an Applied Biosystems gas phase sequencer (Hunkapiller *et al*, 1983).

2.2.15 Isolation of the Biotin-containing Peptide

Sephadex G-50 Gel Filtration

This was a slight modification of the method of Rylatt *et al* (1977). Yeast pyruvate carboxylase (126 nmol, 20 mg/ml in 200 mM potassium phosphate pH 7.2) was treated with trypsin at a substrate to protease mass ratio of 50. After 1 hour at 37°C a second amount of trypsin was added and incubation continued for another hour. The trypsin was inactivated by heating at 90°C for 5 minutes and insoluble material removed by centrifugation. The digest was then incubated with 10 mg of avidin for 30 minutes and chromatographed on Sephadex G-50 (38 cm × 1.3 cm diameter column) in 10 mM potassium phosphate pH 7.2. Fractions (1 ml) were collected, lyophilised and the biotin-containing peptide dissociated from the avidin by the addition of 100 μl 70% formic acid. After lyophilisation the samples were resuspended in 200 mM potassium phosphate pH 7.2 and residual formic acid in some of the samples neutralised with 1 M NaOH. Fractions found to contain biotin (by the ^{14}C-biotin/avidin assay) were pooled and rechromatographed on Sephadex G-50 using conditions identical to the first run.

Fractions (1ml) were collected and assayed for biotin content. The 3 peak fractions were pooled and purified by C_{18} reverse phase HPLC.

Avidin-Sepharose Chromatography

Yeast pyruvate carboxylase (31 nmol, 3mg/ml in 10 mM Tris-chloride pH 8, 2 M urea) was treated with trypsin at a substrate to protease mass ratio of 10. After 1 hour at 37°C the trypsin was inactivated by heating at 90°C for 10 minutes and insoluble material removed by centrifugation. The tryptic digest was diluted 4-fold with Buffer A (10 mM Tris-chloride pH 7.5, 500 mM NaCl) and loaded on to a 10 ml avidin-Sepharose column at 1ml/min. The column was washed with Buffer A until the absorbance of the eluate at 280 nm had returned to baseline. The biotin-containing material was eluted from the column with Buffer B (10 mM HCl, 200 mM NaCl) and the absorbance peak at 280 nm collected. The peptides were then purified by C_8 reverse phase HPLC.

2.2.16 Isolation of the Yeast Pyruvate Carboxylase Gene

High molecular weight wild type yeast DNA was partially digested with Sau 3A to yield fragments ranging in size from 8–25 kb. Fragments within the size class 12–17 kb were selected by agarose gel electrophoresis and treated with calf intestinal phosphatase. The vector (λEMBL3) DNA was prepared by complete digestion with Bam HI and Eco RI followed by precipitation with propan-2-ol to remove the short cohesive ends of the middle fragment. After ligation of vector and size-selected yeast DNA fragments, recombinant λEMBL3 molecules were packaged *in vitro* using extracts from defective λ lysogens. The recombinant phage (total of 4×10^5) were then used to infect *E.coli* NM539. Since the strain NM539 is a host lysogen for the bacteriophage P1, transformants were selected for the Spi^- phenotype, and thus for the absence of the λEMBL3 middle fragment.

The yeast genomic library was screened for pyruvate carboxylase gene sequences

using the plaque transfer procedure of Benton and Davis (1977). The probe was a fragment from the 3'-end of the yeast pyruvate carboxylase gene (Morris *et al*, 1987) radiolabelled to high specific activity by nick translation (Rigby *et al*, 1977) in the presence of [α-^{32}P]dCTP. Hybridisation was performed at 42°C in 50% formamide, 5× Denhardt's solution (1× = 0.02% Ficoll, 0.02% bovine serum albumin, 0.02% polyvinylpyrrolidone), 5× SSPE (1× = 0.15M NaCl, 4 mM sodium phosphate, 1 mM EDTA pH 7.4), 0.1% SDS and 100 μg/ml denatured salmon sperm DNA. Filters were washed in a final solution 0.5× SSC (1× = 150 mM NaCl, 15 mM sodium citrate pH 7.0), 0.1% SDS at 65°C for 30 minutes.

2.2.17 Sequencing of the Pyruvate Carboxylase Gene

The purification, analysis and cloning of DNA was carried out according to standard procedures (Maniatis *et al*, 1982). A series of overlapping subclones of both orientations of the 4kb Hind III yeast pyruvate carboxylase DNA insert in M13mp19 was generated by the method of Dale *et al* (1985). The DNA sequences of these subclones were determined by the chain termination method of Sanger *et al* (1977).

2.2.18 Partial Proteolysis

Thermolysin and proteinase K digestions of native yeast pyruvate carboxylase were carried out at an enzyme to protease mass ratio of 12.5 at 20°C in 100 mM NEM-Cl pH 8.0. Chymotrypsin was used at an enzyme to protease mass ratio of 30 at 30°C in 100 mM NEM-Cl pH 8.0. After various time intervals an aliquot of the reaction was stopped by removal into 5 mM PMSF (chymotrypsin and proteinase K), or 5 mM EDTA (thermolysin). After SDS polyacrylamide gel electrophoresis of the protein samples bands were visualised by staining with Coomassie Brilliant Blue R_{250} and quantified by densitometry with a soft laser scanner. Biotin-containing fragments were

detected by a reduction in electrophoretic mobility after pre-incubation with avidin (Lau *et al*, 1979).

2.2.19 Isolation of Partial Proteolysis Fragments

Fragments derived from partial proteolysis experiments were isolated by gel filtration chromatography on either a TSK-3000 SW column or a Superose 12 column in 10 mM potassium phosphate pH 7.5, 100 mM NaCl. The samples were desalted and concentrated by filtration through a 30K cutoff membrane (Centricon 30 microconcentrator, Amicon) and analysed by SDS polyacrylamide gel electrophoresis.

2.2.20 Synthesis of oATP

The 2′, 3′ dialdehyde oxidation product of ATP (oATP) was synthesised by incubating 200 μl 10 mM ATP + 400 μl 1 mM HCl + 200 μl 100 mM sodium *meta* periodate in the dark at room temperature for 1 hour, by which time the reaction was complete as judged by chromatography of the reaction mixture on polyethylene imine thin layer chromatograms, developed with 0.8 M ammonium bicarbonate. (An ultraviolet light – 254 nm, was used to locate the position of the nucleotide.) The reaction was stopped by the addition of 200 μl 80% (v/v) glycerol and the oATP purified from the mixture by Sephadex G-10 chromatography as previously described (Easterbrook-Smith *et al*, 1976). The yield using this procedure was approximately 80%.

2.2.21 Covalent Modification of Pyruvate Carboxylase with oATP

Pyruvate carboxylase was incubated with Mg-oATP in 0.125 M NEM-acetate buffer pH 8.0, containing 1 mM EDTA and 7.5 mM $MgCl_2$. After 5 minutes sodium borohydride was added in tenfold molar excess over the Mg-oATP used and the solution incubated at room temperature for 40 minutes.

2.2.22 Synthesis of [γ-^{32}P]8-azido-ATP

The radiolabelling of 8-azido-ADP with ^{32}P was achieved by an enzymatic procedure using the "Gamma A " kit marketed by Bresatec, South Australia. The product was purified by chromatography on DEAE-cellulose as recommended by the Bresatec instructions.

2.2.23 Covalent Modification of Pyruvate Carboxylase with [γ-^{32}P]8-azido-ATP

Pyruvate carboxylase was incubated with [γ-^{32}P]8-azido-ATP in 0.125 M NEM-acetate buffer pH 8.0, containing 1 mM EDTA and 7.5 mM $MgCl_2$. After 5 minutes the mixture in an uncovered plastic tray was placed on ice and irradiated for 90 seconds with a broad spectrum white light source (Philips 300 W mercury vapour lamp) placed 5cm from the sample.

2.2.24 Computer Programmes

A nonlinear regression programme (Duggleby, 1980; Duggleby *et al*, 1981) written in BASIC was modified and used to fit data to the following equations:

(1) $\log y = \frac{-b-\sqrt{b^2-4a(c-x)}}{2a}$ parabolic fit for log molecular weight and electrophoretic mobility

(2) $y = Ae^{-kx}$ exponential decay

(3) $y = \frac{Vx}{K+x}$ Michaelis-Menten equation

(4) $y = \frac{Vx_1}{K_m(1+x_2/K_i)+x_1}$ competitive inhibition

where x, x_1, x_2 and y are variables
and a, b, c, A, k, V, K, K_m and K_i are parameters.

Sequencing gel autoradiographs were read using a digitiser (Science Accessories Corporation) with a programme written in PASCAL by Mark Snoswell. Sequence overlaps were obtained by using SPCOMP, a modification (by Dr. A. Sivaprasad) of the FORTRAN programme DBCOMP for the comparison of nucleotide sequences (Staden, 1982).

Database homology searches were conducted with MATCH and MATCHTRANS (Wilbur and Lipman, 1983). Local regions of similarity between proteins were identified by SEQHP (Goad and Kanehisa, 1982; Dayhoff *et al*, 1978) and the degree of homology quantified by SEQDP (Needleman and Wunsch, 1970; Dayhoff *et al*, 1978). ANALYSEQ (a suite of DNA and protein analysis programmes by Staden, 1984) was used to translate nucleotide sequences, calculate protein molecular mass, gene codon usage and predict coding/noncoding boundaries in the yeast pyruvate carboxylase gene.

This thesis and various posters, abstracts and papers were edited using LUDWIG, a screen editor developed at the University of Adelaide for the VAX/VMS and UNIX systems. Typesetting was with TEX(Knuth, 1984) and LATEX(Lamport, 1986).

Chapter 3

Purification and Characterisation of the Enzyme

3.1 INTRODUCTION

The ultimate goal of using yeast as a system to study genetically engineered pyruvate carboxylases necessitates a knowledge of the endogenous enzyme first. Thus the first phase of the project, described in this chapter, was concerned mainly with the characterisation of yeast pyruvate carboxylase and establishing the differences and similarities between the yeast enzyme and those from other species.

Although a purification procedure had been published previously (Young *et al*, 1969) this method required extensive modifications for several reasons. For example, the unavailability of the same cell disruption apparatus (Eppenbach colloid mill) as described by these authors resulted in an altered composition of the cell extract, which affected all subsequent steps. Another consideration in developing a purification scheme was the suitability for scaling-up. Thus such steps as heat denaturation which depend on geometric factors and vary in their effectiveness according to the quantities used were avoided.

The identity of purified yeast pyruvate carboxylase was confirmed by comparison of a number of experimentally determined properties with those of other pyruvate carboxylases as well as previously published data for the yeast enzyme. One of the most striking differences previously reported between pyruvate carboxylase from yeast and

the enzyme from other species was its three-dimensional configuration as determined by electron microscopy. This however seemed to be due to a difference in the interpretation of data rather than a different appearance of the enzyme in electron micrographs. Accordingly, one of the main aims of this work was to establish if the yeast enzyme has a unique structure unlike that of other pyruvate carboxylases. In this section of work I was fortunate in being able to collaborate with Dr. Manfred Rohde who performed the electron microscopy on my enzyme samples.

Vertebrate and fungal pyruvate carboxylases differ in their regulatory properties, reflecting the differences in metabolic organisation and subcellular location of this enzyme in these organisms. For example, the fungal (cytosolic) pyruvate carboxylases appear to be stimulated more effectively by long chain acyl-CoAs (eg. palmitoyl-CoA and oleoyl-CoA) than by acetyl-CoA whereas the vertebrate (mitochondrial) pyruvate carboxylases are activated by acetyl-CoA but not by long chain acyl-CoAs (Osmani *et al*, 1985). Furthermore the mitochondrial pyruvate carboxylases are sensitive to regulatory inhibition by L-glutamate, and in a few instances 2-oxo-glutarate, while for the cytosolic pyruvate carboxylases L-aspartate and 2-oxoglutarate act as the regulatory inhibitors (Osmani *et al*, 1985). To investigate the mode of action of regulatory modifiers, their effect on the structure of yeast pyruvate carboxylase was examined by electron microscopy.

Structural characterisation of the enzyme was also attempted by two other approaches. Firstly, since the complete three-dimensional description of a protein relies heavily upon X-ray diffraction data, a vapour diffusion method was used to screen over 150 crystallisation conditions for yeast pyruvate carboxylase. Secondly, polyclonal antibodies against yeast pyruvate carboxylase were raised and used to study differences between this enzyme and pyruvate carboxylases from other sources.

SAMPLE	ACTIVITY PC (U/ml)	% NONSPEC. ACTIVITY	APPEARANCE OF EXTRACT
Control	1.6	79	cloudy
+ B (after)	1.9	75	cloudy
+ B (before)	3.0	56	cloudy
+ S	1.6	58	clear
+ S + B (after)	2.4	49	clear
+ S + B (before)	2.2	47	clear

Table 3.1 **Effect of preincubation of yeast with sucrose (6.7% w/v) and biotin (50 μg/l) on the cell extract.** The yeast was suspended (10 g yeast + 6 ml 100 mM Tris-chloride, 10 mM $MgCl_2$) and incubated (~16 hours at 22°C) before disruption by the French press.
+ B (before) = biotin added before incubation.
+ B (after) = biotin added after cell disruption.
+ S = sucrose added before incubation.
Enzyme activity was measured by the spectrophotometric method both in the presence and absence of avidin (1 mg/ml) to determine pyruvate carboxylase activity (PC U/ml). Nonspecific activity in the assay was due to the presence of other NADH-utilising systems in the crude extracts.

3.2 RESULTS

3.2.1 Purification from Yeast

Commercial compressed baker's yeast (diploid *Saccharomyces cerevisiae*) was found to be the most convenient source from which to purify pyruvate carboxylase. I have found little difference in the enzymatic content of brewer's yeast or baker's yeast, cultured aerobically or anaerobically, in rich or minimal medium. Initially, the purification procedure of Young *et al* (1969) was followed but the cell lysate obtained by using the French press instead of the colloid mill contained large amounts of cloudy material which could not be separated from pyruvate carboxylase activity. However, overnight incubation of the compressed yeast with 6.7% (w/v) sucrose prior to cell disruption was found to improve the clarity of the supernatant while the addition of biotin (final concentration 50μg/l) to the cell lysate increased the enzymatic activity of the extract (Table 3.1).

The use of 1,1,2-trichloro-1,2,2-trifluoro-ethane extraction to remove lipids and protamine sulphate to precipitate nucleic acids resulted in a clear protein extract from which pyruvate carboxylase was purified to homogeneity. During the purification procedure (Figure 3.1) pyruvate carboxylase activity was followed using the enzyme-linked spectrophotometric assay. Prior to stage 4 (PEG precipitation) all samples were assayed in the presence and the absence of avidin (final concentration 1 mg/ml) to determine biotin-dependent activity, since other NADH-utilising enzymes were present.

Figure 3.2**A** shows the profile obtained by chromatography of the yeast protein extract on DEAE-Sephacel (stage 5). The pooled active fractions from this step were initially further purified by gel filtration on Superose 6 (Figure 3.2**B**). However, affinity chromatography on monomeric avidin-Sepharose (Figure 3.2**C**) was used later because it enabled the processing of larger quantities. The results of a typical purification are summarised in Table 3.2. The final specific activity and recovery varied between preparations but have been as high as 32 U/mg and 48% respectively. Purified yeast pyruvate carboxylase appeared as a single band on SDS polyacrylamide gels and when chromatographed on Superose 6 or Superose 12, a single peak of absorbance at 280 nm coincident with a single peak of enzyme activity was obtained. The pure enzyme snap-frozen at -70°C in 100 mM Tris-chloride, 10 mM $MgCl_2$ has been found to be stable for up to one year with a quantitative recovery of activity.

3.2.2 Properties

The absorbance index determined for yeast pyruvate carboxylase was

$$\epsilon_{280nm}^{1mg/ml} = 0.725.$$

Protein estimations of samples of purified yeast pyruvate carboxylase by ultraviolet absorbance or the Bradford dye-binding assay were standardised against values obtained by the biuret method. It was found that estimations using the A_{280}/A_{260} method of

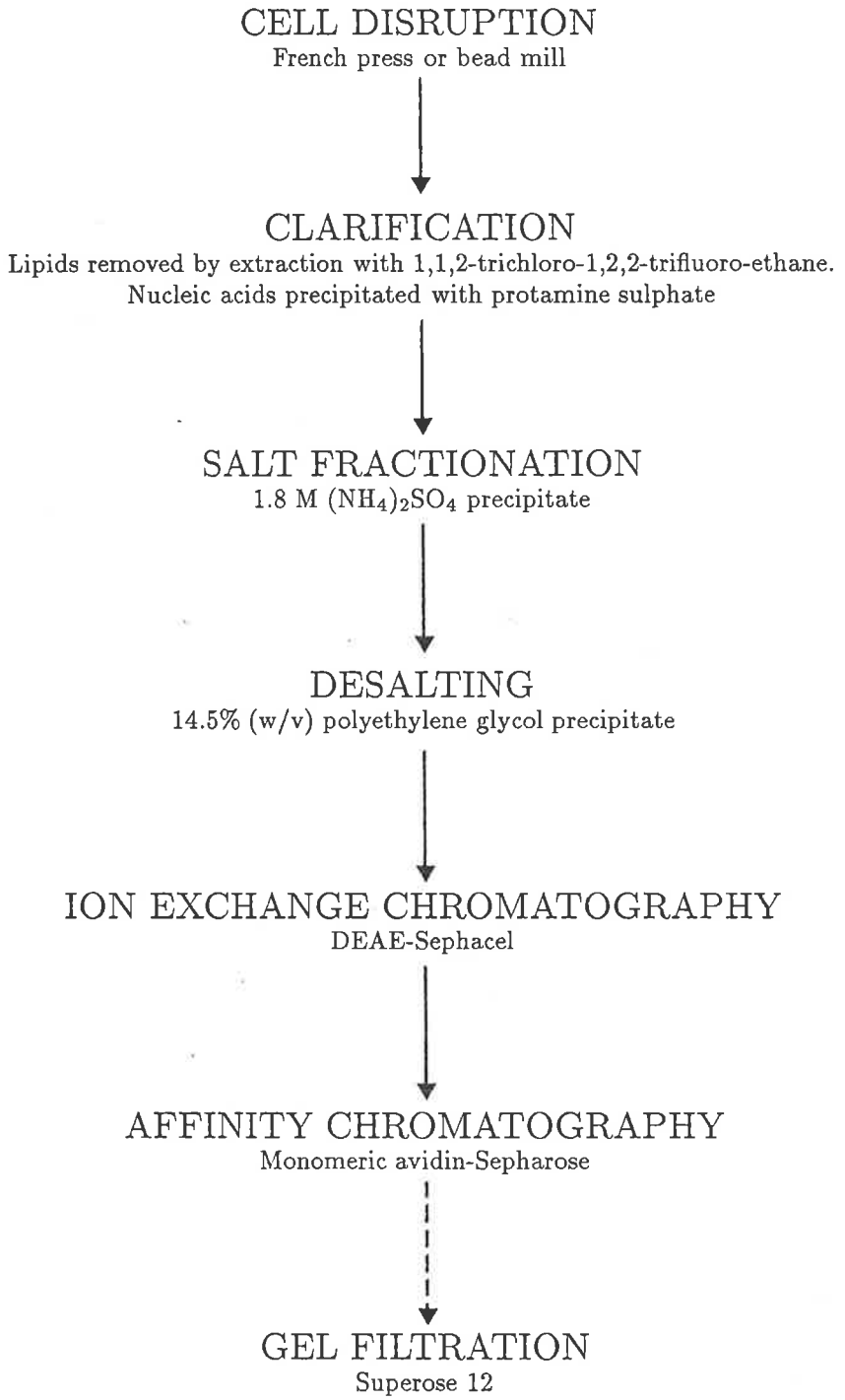

Figure 3.1: **Purification of yeast pyruvate carboxylase** The gel filtration step was only necessary in those preparations containing contaminants after avidin-Sepharose chromatography.

Figure 3.2: **Chromatographic purification of yeast pyruvate carboxylase.** In A and B fractions were collected and pyruvate carboxylase activity (PC U/ml) was measured by the spectrophotometric assay (•—•).

A Ion-exchange chromatography of crude yeast protein extract (1840 mg, 40 ml from polyethylene glycol precipitation step) on DEAE-Sephacel (200 ml column). Eluent = 25 mM potassium phosphate pH 7.2, 1 mM EDTA with a linear gradient of 20 mM – 200 mM ammonium sulphate. Flow rate = 1 ml/min.

B Superose 6 gel filtration (30 ml column) of yeast protein extract (30 mg, 1 ml load) after purification on DEAE-Sephacel. Eluent = 100 mM Tris-acetate pH 7.2, 10 mM $MgCl_2$. Flow rate = 0.8 ml/min.

C Monomeric avidin-Sepharose chromatography (30 ml column) of yeast protein extract (483 mg, 23 ml load) after purification on DEAE-Sephacel. Eluent = 50 mM potassium phosphate pH 7.2. Flow rate = 1 ml/min. Pyruvate carboxylase was eluted from the column with 1 mM biotin (arrow) and concentrated by precipitation with 1.8 M ammonium sulphate. The active fraction is indicated (hatched).

A

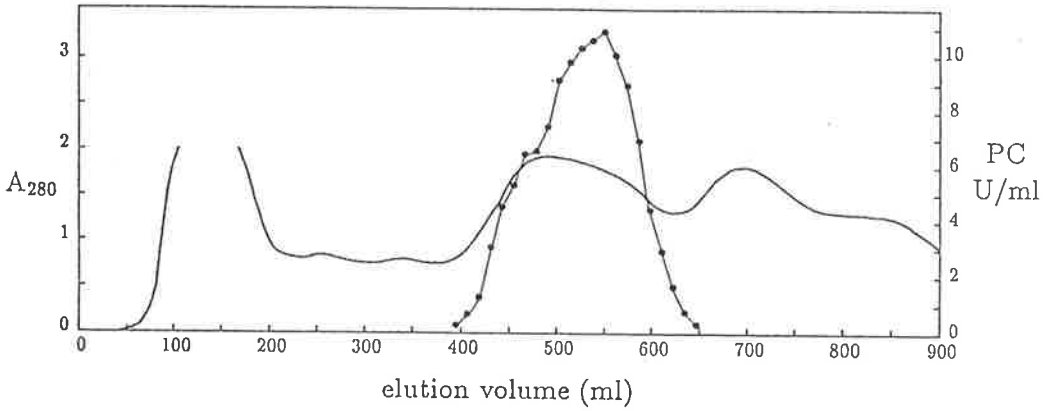
A280
PC
U/ml
elution volume (ml)

B

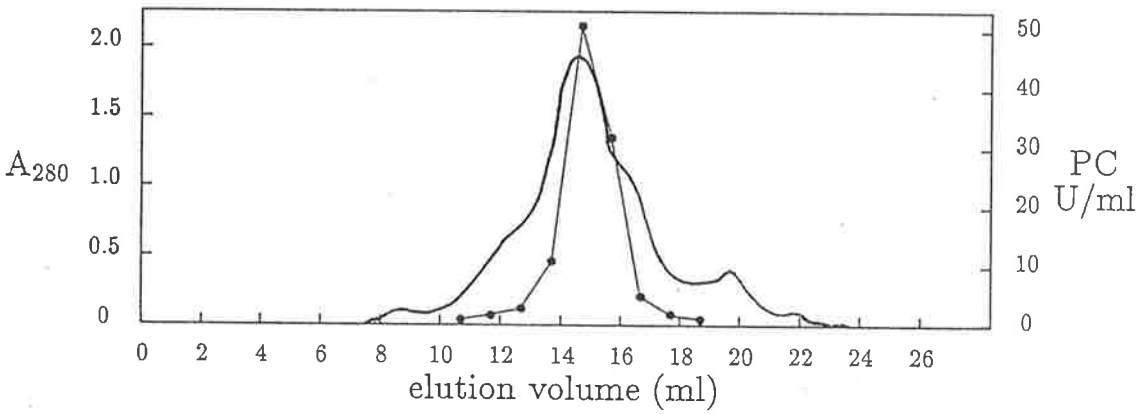
A280
PC
U/ml
elution volume (ml)

C

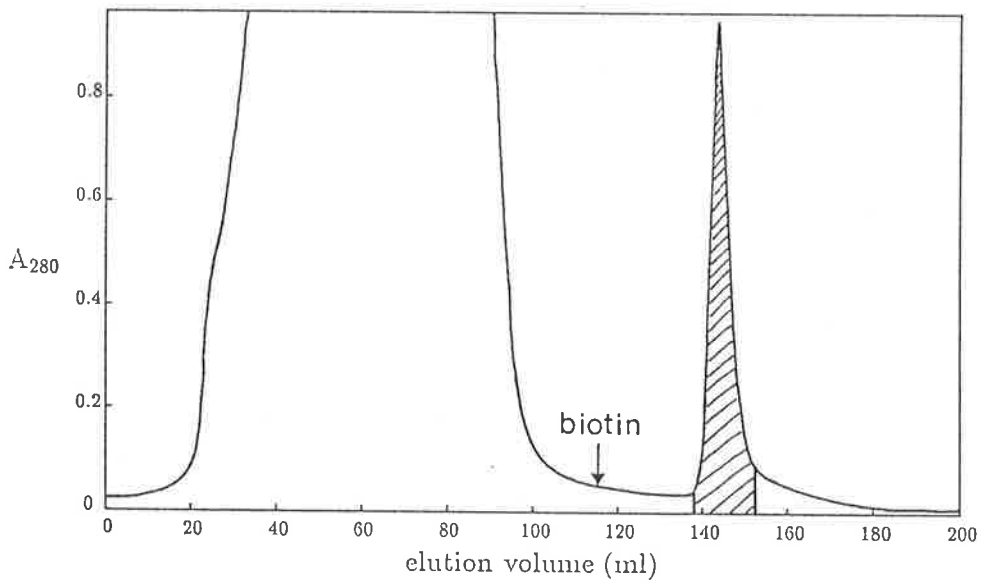
A280
biotin
elution volume (ml)

STEP	ACTIVITY (U)	PROTEIN (mg)	RECOVERY (%)	SPEC. AC. (U/mg)
LYSATE	3456	20160*	100	0.17
PROT SO_4	3525	16500*	102	0.21
$(NH_4)_2SO_4$	2308	2646*	67	0.87
PEG 8000	1983	1365	57	1.45
DEAE-SEPHACEL	1380	161	40	8.54
AVIDIN-SEPHAROSE	898	33	26	27

Table 3.2 **Results from a typical preparation of pyruvate carboxylase from yeast (500 g).** Enzyme activity was measured by the spectrophotometric method and the protein content estimated by the A_{260}/A_{280} method or the biuret method (*). PEG = polyethylene glycol. PROT = protamine.

Layne (1957) required a correction factor of 1.1. The Bradford method (using bovine serum albumin as the standard) required a correction factor of 0.87.

Using commercially available protein molecular weight standards, the relative molecular mass of yeast pyruvate carboxylase subunits estimated from SDS-polyacrylamide gel electrophoresis (Figure 3.3) was 123 000, in close agreement with previous estimates obtained by others (Barden *et al.* 1975; Cohen *et al*, 1979). However the calculated relative molecular mass derived from DNA sequencing of the yeast pyruvate carboxylase gene (Section 5.2.2) is 130 100. On close inspection this discrepancy appears to be due to the anomalous electrophoretic migration of one of the markers, β-galactosidase. The molecular weight of this protein was originally estimated to be 130 000 (Klotz and Darnell, 1969) but sequencing studies have since shown the correct value to be 116 351 (Kalnins *et al*, 1983). Nevertheless, when the nonlinear regression routine of Duggleby *et al* (1981) was used to compute best fit parabolic curves for values of relative mobility versus log molecular weight, the curve obtained using yeast pyruvate carboxylase (M_r 130 100) yielded a lower standard error of fit (0.035, Figure 3.3 solid line) than that obtained using β-galactosidase (M_r 116 351) (standard error of fit = 0.038, Figure 3.3 dotted line). It would appear that the electrophoretic characteristics of yeast pyruvate carboxylase are more similar to those of the other protein markers than are those of

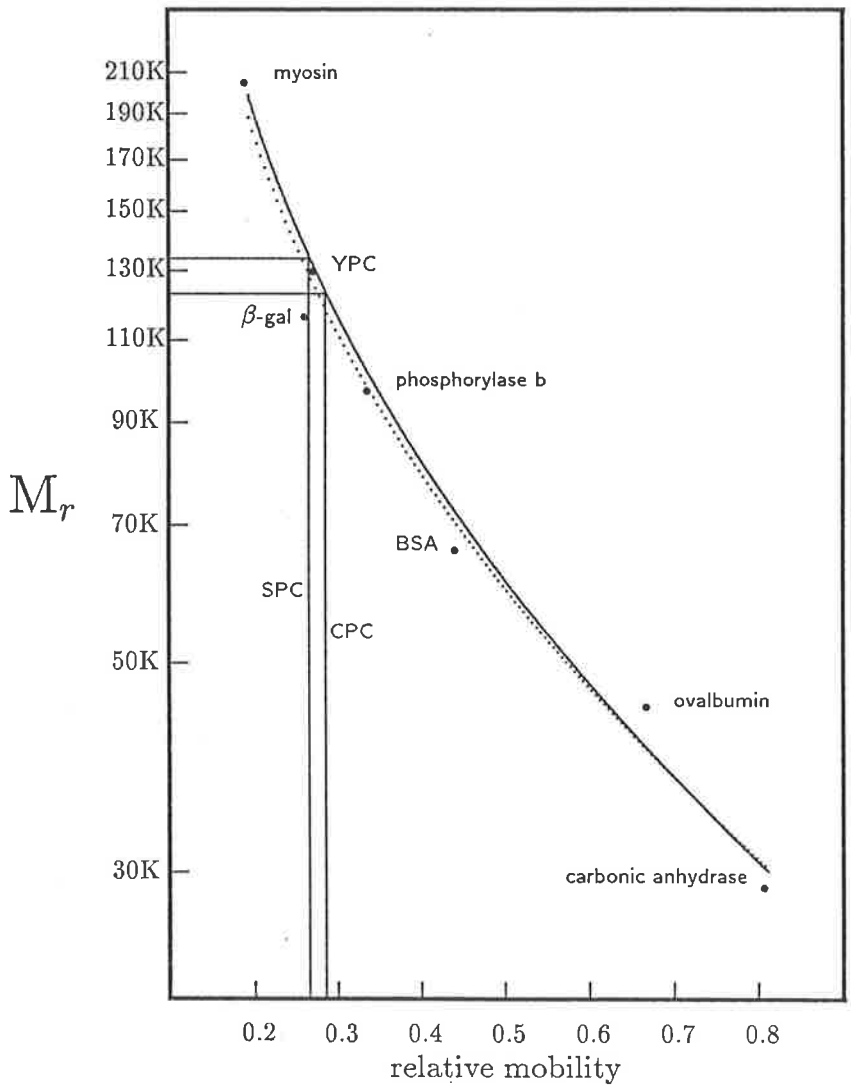

Figure 3.3: **Relationship between the relative molecular mass (M_r) and the relative electrophoretic mobility of yeast pyruvate carboxylase and six marker proteins on a 10% SDS polyacrylamide gel.** The relative molecular masses of the proteins were 205 000 (myosin), 130 100 (YPC = yeast pyruvate carboxylase), 116 351 (β-gal = β-galactosidase), 97 400 (phosphorylase b), 66 000 (BSA = bovine serum albumin), 45 000 (ovalbumin) and 29 000 (carbonic anhydrase). The parabolic curves were fitted to the data by a programme described by Duggleby *et al* (1981). Using β-galactosidase as a standard (dotted line) the standard error of fit was 0.038 whereas when yeast pyruvate carboxylase was substituted as the second marker (solid line) the standard error of fit was 0.035. The apparent molecular weights of chicken and sheep pyruvate carboxylases (CPC and SPC) estimated from the solid curve were 123 000 and 134 000 respectively.

β-galactosidase. The apparent molecular weights of chicken and sheep pyruvate carboxylases estimated from the curve using the yeast enzyme were 123 000 and 134 000 respectively (Figure 3.3).

Using a relative molecular mass of 130 100, the biotin content of yeast pyruvate carboxylase was measured to be 0.89 $\pm$ 0.1 mol/mol subunit. Measurements performed on enzyme preparations where biotin was not added to the cell lysate yielded lower values (0.4 – 0.7 mol/mol subunit), indicating that the increase in enzymatic activity observed with this treatment is probably due to biotinylation of apoenzyme. Under standard assay conditions yeast pyruvate carboxylase retained $\sim$ 30% of its activity in the absence of acetyl-CoA but when $KHCO_3$ (10 mM) was used in place of $NaHCO_3$ (10 mM) in the assay mix (see Section 2.2.3) the acetyl-CoA independent activity was as high as 60%.

3.2.3 Screening of Crystallisation Conditions

A vapour diffusion method which required relatively small quantities of protein ($\sim$ 50 μg per sample) was used to test a number of conditions for crystallisation of pyruvate carboxylase. In this method enzyme in a low concentration of precipitant is placed as a droplet (10 μl) on a coverslip which is then inverted and sealed over a reservoir of precipitant at a higher concentration. The slow equilibration of vapour pressure, the rate and endpoint of which depends on the relative volumes and the salt concentrations of the reservoir and the droplet, results in a gradual increase in the precipitant concentration of the droplet (see Section 2.2.6).

The parameters varied were precipitant type (and precipitant concentration), temperature, buffer system and pH. Initially conditions were chosen according to what was known about the stability optima of pyruvate carboxylases of other species, but some of these parameters for the yeast enzyme were later examined more thoroughly. Figure 3.4 shows the variation of the stability of yeast pyruvate carboxylase (1 mg/ml)

Figure 3.4: **Inactivation of yeast pyruvate carboxylase at different pH values.** Enzyme at 1 mg/ml was incubated at 30°C in 100 mM Tris-chloride at the indicated pH values.

A At the indicated times samples were withdrawn and assayed for activity by the spectrophotometric method. The data was fitted to an exponential decay function by nonlinear regression (Duggleby, 1980) which yielded an estimate of the inactivation rate constants at each pH.

B Secondary plot of the inactivation rate constants (k) obtained at different pH values. The lowest rate of enzyme inactivation was observed at pH 7.2.

A

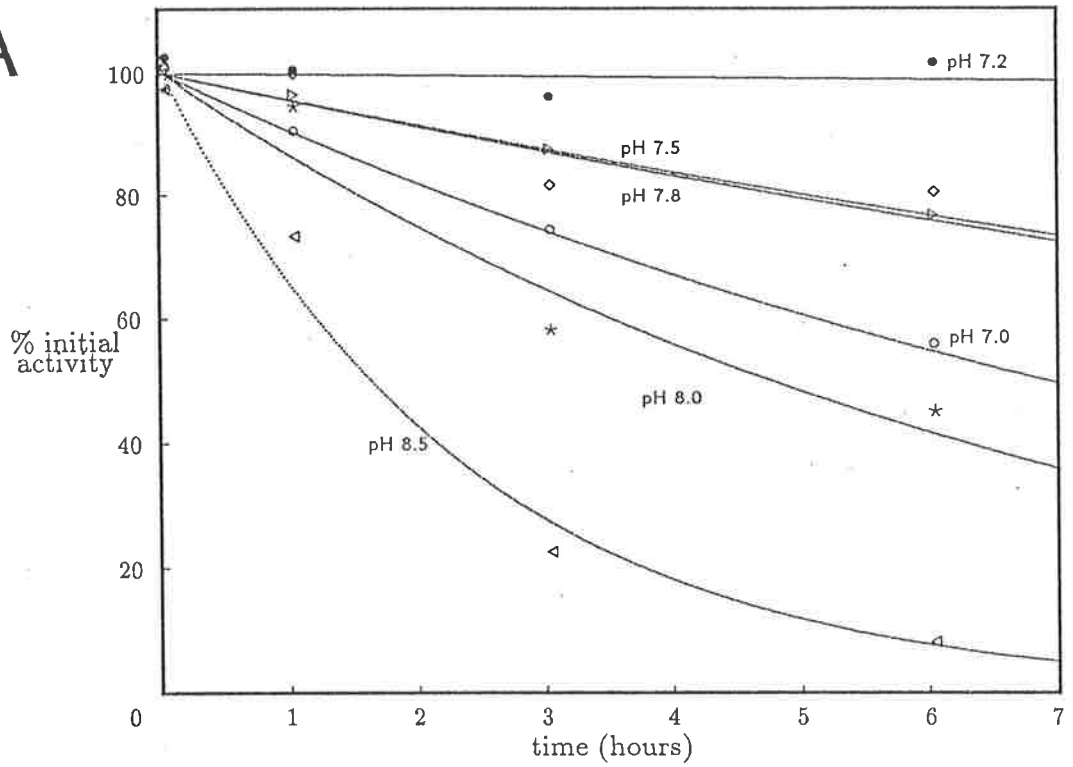
pH 7.2
pH 7.5
pH 7.8
pH 7.0
pH 8.0
pH 8.5
% initial activity
100
80
60
40
20
0
1
2
3
4
5
6
7
time (hours)

B

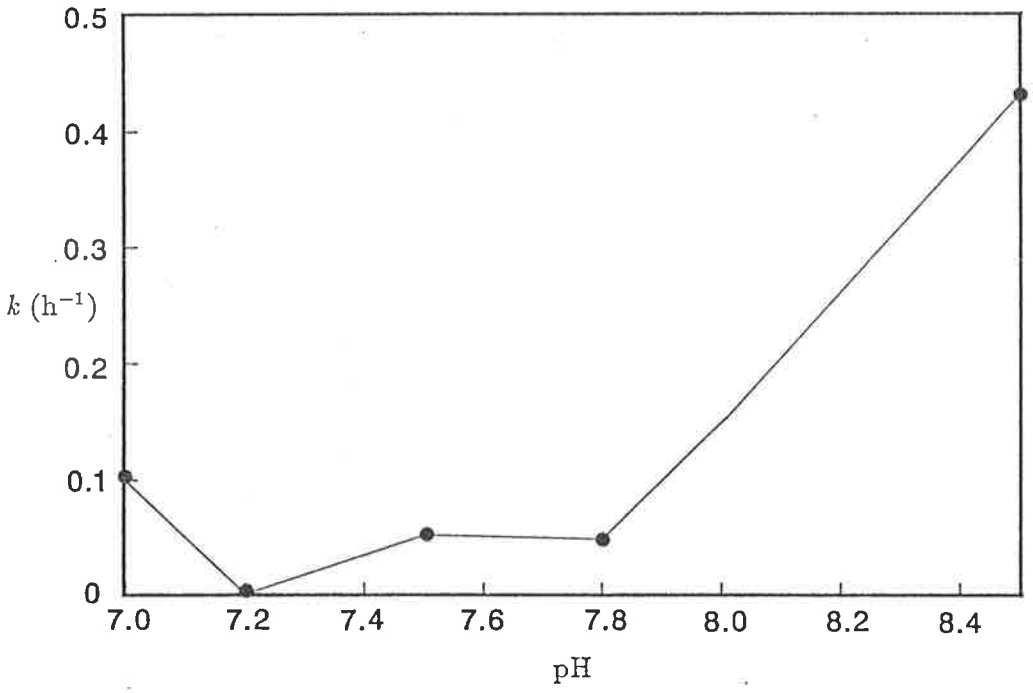
0.5
0.4
0.3
0.2
0.1
0
k (h⁻¹)
7.0
7.2
7.4
7.6
7.8
8.0
8.2
8.4
pH

with pH. The primary plot (Figure 3.4A) shows the decay curves obtained by fitting the data to the equation

$$A_t = A_0.e^{-kt}$$

where A_t is the enzyme activity at time t, A_0 is the initial enzyme activity and k is the inactivation rate constant. The parameters A_0 and k were estimated by the nonlinear regression programme of Duggleby (1980). From the secondary plot of the inactivation rate constants obtained at different pH values (Figure 3.4B), it is apparent that the pH stability optimum of yeast pyruvate carboxylase is in the region of 7.2, as has been found for pyruvate carboxylases of other species (Goss, 1978).

A similar procedure was followed to examine the stability of yeast pyruvate carboxylase at different ionic strengths (Tris-chloride) and temperatures. In Figure 3.5 the secondary plots for these experiments are shown. The enzyme appeared to be most stable in 50 mM Tris-chloride and at low temperatures. The latter observation is significant in view of the fact that the avian pyruvate carboxylases exhibit higher inactivation rates at temperatures between 0 and 5°C (Scrutton and Utter, 1965; Irias *et al*, 1969). It appears that at the protein concentration used (1 mg/ml) yeast pyruvate carboxylase does not display this phenomenon of cold inactivation.

Table 3.3 summarises the conditions screened using the hanging drop vapour diffusion method. The enzyme concentration was kept as high as possible and varied between 5 – 8 mg/ml. In some cases acetyl-CoA was added to stabilise the enzyme. The use of hexylene glycol as a secondary precipitant was also tested in some samples. The samples were monitored by examination with a light microscope; in all of the conditions tested the enzyme failed to crystallise.

3.2.4 Structure of Native Yeast Pyruvate Carboxylase

When yeast pyruvate carboxylase (8–80 μg/ml) was mounted for electron microscopy immediately after dilution with Tris-acetate or Tris-chloride, tetramers with four clearly

Figure 3.5: **Secondary plots for the inactivation of yeast pyruvate carboxylase at different ionic strengths (A) and temperatures (B).** Enzyme (1 mg/ml) was incubated in Tris-chloride pH 7.2 and five time points taken over 24 hours. In (A) the temperature was 30°C and in (B) the ionic strength was 50 mM. Enzyme activity was assayed by the spectrophotometric method and the data fitted to exponential decay functions. The estimated inactivation rate constants (k) are shown plotted against ionic strength (A) or temperature (B).

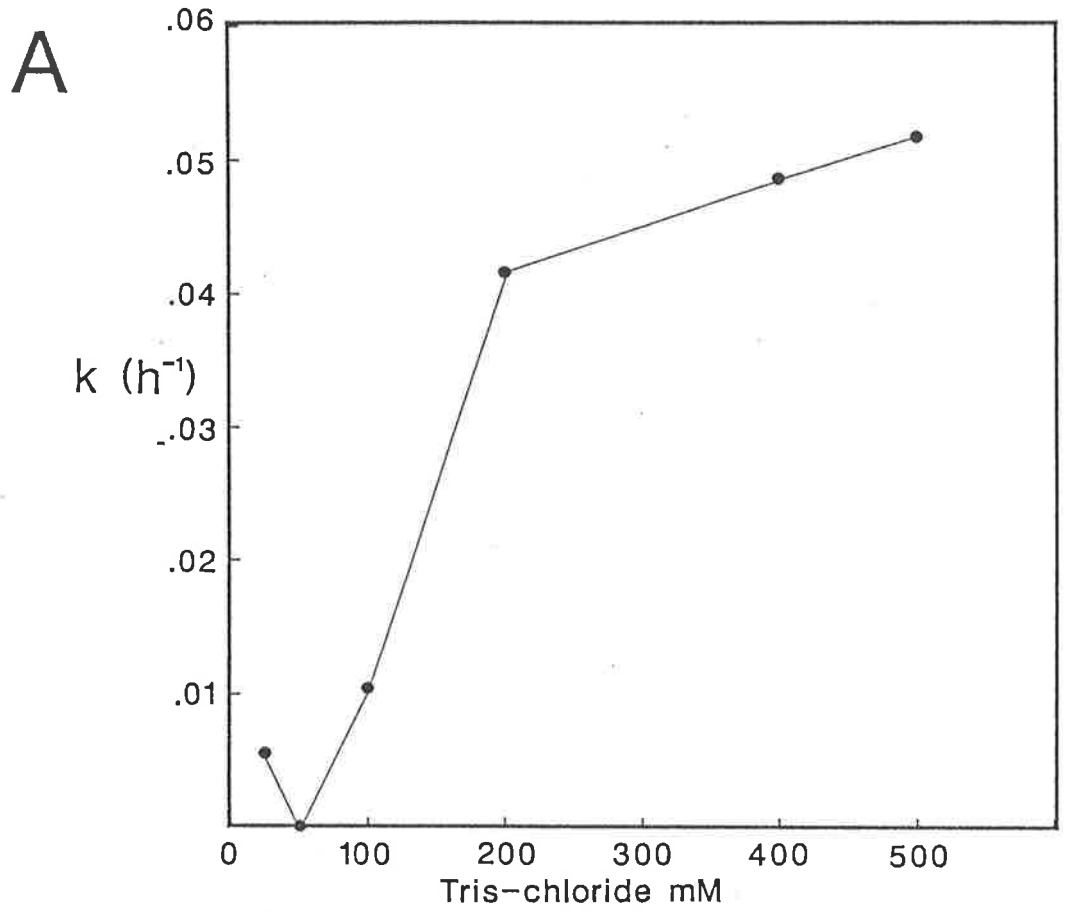
A
.06
.05
.04
k (h⁻¹)
.03
.02
.01
0
100
200
300
400
500
Tris-chloride mM

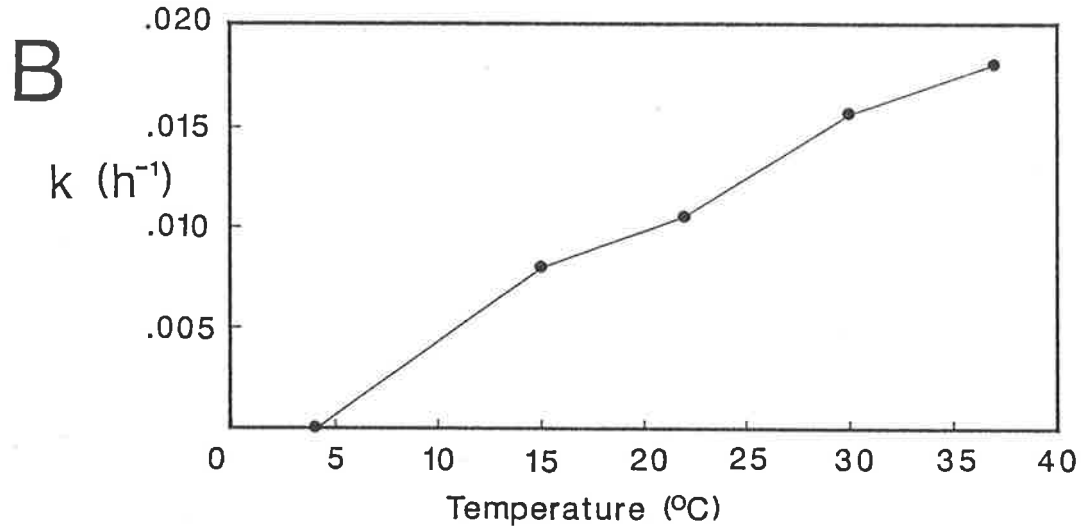
B
.020
.015
k (h⁻¹)
.010
.005
0
5
10
15
20
25
30
35
40
Temperature (°C)

P	Conc Range	T°C	Buffer System	pH	Other
$(NH_4)_2SO_4$	3.2 M – 1.4 M	22	100 mM Tris-acetate	7.2	—
	1.6 M – 0.6 M	22	25 mM Tris-acetate	7.2	—
	1.6 M – 0.6 M	22	25 mM Tris-acetate	8.0	—
	1.6 M – 0.6 M	22	25 mM Potassium phosphate	7.2	—
	1.6 M – 0.6 M	22	25 mM Potassium phosphate	8.0	—
	1.0 M – 0.5 M	22	25 mM Potassium phosphate	8.0	—
	1.0 M – 0.5 M	22	25 mM Tris-acetate	8.0	—
	3.2 M – 1.4 M	4	100 mM Tris-acetate	7.2	—
	1.6 M – 0.2 M	4	25 mM Tris-acetate	7.2	—
	1.6 M – 0.2 M	4	25 mM Tris-acetate	7.2	240 μM acetyl-CoA
$MgCl_2$	2.0 M – 0.8 M	22	100 mM Tris-acetate	7.2	—
	2.0 M – 0.8 M	4	100 mM Tris-acetate	7.2	—
PEG 6000	26% – 2%	22	100 mM Tris-acetate	7.2	—
	2% – 0.2%	22	25 mM Tris-acetate	7.2	—
	2% – 0.2%	22	25 mM Tris-acetate	8.0	—
	2% – 0.2%	22	25 mM Potassium phosphate	7.2	—
	0.6% – 0.2%	22	25 mM Tris-acetate	8.0	—
	0.2% – 0.1%	22	25 mM Tris-acetate	7.2	—
	26% – 2%	4	100 mM Tris-acetate	7.2	—
	1.6% – 0.2%	4	25 mM Tris-acetate	7.2	—
	1.6% – 0.2%	4	25 mM Tris-acetate	7.2	240 μM acetyl-CoA
	0.008% – 0.001%	4	25 mM Tris-acetate	7.2	—
	0.008% – 0.001%	4	25 mM Tris-acetate	7.2	.0025% hexylene glycol
	0.004% – 0.0005%	4	25 mM Tris-acetate	7.2	—
	0.004% – 0.0005%	4	25 mM Tris-acetate	7.2	.0025% hexylene glycol
PEG 8000	0.008% – 0.001%	4	25 mM Tris-acetate	7.2	—
	0.008% – 0.001%	4	25 mM Tris-acetate	7.2	.0025% hexylene glycol
	0.004% – 0.0005%	4	25 mM Tris-acetate	7.2	—
	0.004% – 0.0005%	4	25 mM Tris-acetate	7.2	.0025% hexylene glycol

Table 3.3 **Conditions for the crystallisation of yeast pyruvate carboxylase screened using the hanging drop vapour diffusion method.** Six wells with decreasing amounts of precipitant were set up within each of the concentration ranges indicated. The figures given are the starting concentrations within the hanging drop. The starting concentration of precipitant in the reservoir was always twice that in the drop. P = precipitant. T = temperature.

Figure 3.6: **Electron micrographs of yeast pyruvate carboxylase negatively stained with uranyl acetate** The bar represents 50 nm in the low-magnification micrographs and 25 nm in the high-magnification micrographs in the galleries. (a, b) Dilution in Tris-chloride (a) and dilution in Tris-acetate (b). Broken molecules are circled in (a) and (b). Arrows indicate tetramers exhibiting an area of negative stain at the centre. (c, d) Dilution in Tris-acetate containing 250 μM acetyl-CoA using deep stain (c) and shallow stain (d). The galleries beside (a) and (c) show examples of rhombic (1), square (2), triangular (3) and dual-intensity projections (4) found in the absence and presence of 250 μM acetyl-CoA respectively. Arrowheads indicate the longitudinal clefts often seen in enzyme subunits. Further examples of molecules in which clefts are clearly visible are shown in c5–8.

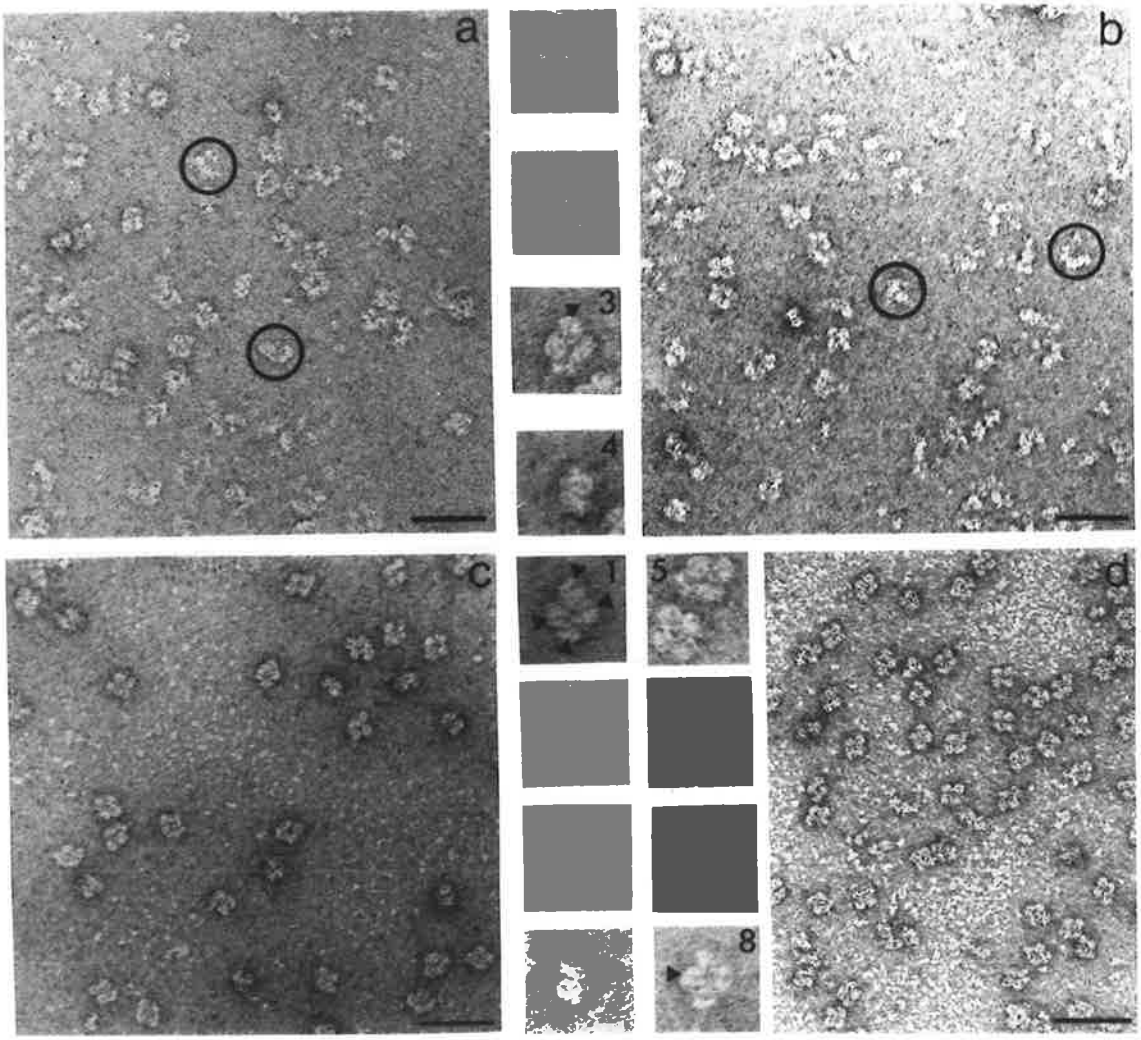
a
b
c
d
1
3
4
5
8

visible subunits were detected. However, many (~55%, see Table 3.4) of the enzyme molecules were broken (Figure 3.6a and 3.6b) and exhibited a diffuse or irregular appearance. Dilution in the presence of 250μM acetyl-CoA markedly increased the frequency of intact tetramers in the electron micrographs (Figure 3.6c and 3.6d). The majority of the molecules yielded images with four intensity maxima placed at the corners of a rhombus (Figure 3.6, a1 and c1) although some had a more square-like appearance (Figure 3.6, a2 and c2). Triangular forms with three intensity maxima (Figure 3.6, a3 and c3) and projections containing two intensity maxima (Figure 3.6, a4 and c4) were also found but at a very low frequency (less than 1%). In the absence of acetyl-CoA the tetramers appeared to be more diffuse and a sharply defined, dark spot was often (~40%, compared with <3% in samples containing acetyl-CoA) found at the centres of the rhombic and square projections (see arrows in field view of Figure 3.6a and micrographs a1 and a2 in the gallery of Figure 3.6). Molecules mounted in the presence of acetyl-CoA had a well-defined appearance and clearly showed the presence of protein at their centres (Figure 3.6, c1 and c2).

Measurements made of the dimensions of 25 well-preserved tetramers in the absence of acetyl-CoA yielded 19.9 ± 0.5 nm (standard error of the mean) and 18.0 ± 0.5 nm for the axial lengths of the rhombic projections and 17.5 ± 0.5 nm and 14.0 ± 0.5 nm in the presence of 250 μM acetyl-CoA. These differences in dimensions may be due to a change in the conformation induced by acetyl-CoA from a near planar molecule to a more compact tetrahedron-like structure, as has been noted previously for pyruvate carboxylase purified from *Aspergillus nidulans* (Osmani *et al*, 1984) and chicken liver (Mayer *et al*, 1980). These observations indicate that acetyl-CoA also has a stabilising effect on the structure of yeast pyruvate carboxylase.

No difference in the preservation of structure was discerned when either deep or shallow stain conditions were employed (Figure 3.6 c and d), suggesting that at least

in the presence of acetyl-CoA the yeast enzyme is more stable than other pyruvate carboxylases investigated (Mayer *et al*, 1980; Osmani *et al*, 1984). In many of the projections a cleft along the longitudinal axes of the subunits could be seen (arrowheads in the gallery micrographs of Figure 3.6). This cleft was apparent both in the presence and absence of acetyl-CoA.

Figure 3.7 shows the images obtained when samples of the enzyme mounted in the presence of acetyl-CoA were tilted in both directions with respect to the electron beam. Interconversion between all observed forms was obtained, showing that these projections are different views of the same molecule. These results indicate that like the enzyme from all other species so far studied (Libor *et al*, 1979; Mayer *et al*, 1980; Osmani *et al*, 1984), yeast pyruvate carboxylase has a tetrahedron-like structure.

3.2.5 Structural Effects of Ligand Binding

As previously reported (Myers *et al*, 1983) palmitoyl-CoA is an activator of yeast pyruvate carboxylase (Figure 3.8). The effect of this ligand at low concentrations (1 μM) on the structure of the enzyme was similar to that of acetyl-CoA and enhanced preservation of enzyme tetramers was obtained (Figure 3.9e). In these experiments, where the activity of samples prepared for electron microscopy was measured, the spectrophotometric assay was started by the addition of the concentrated reactants to an aliquot of the pre-diluted enzyme rather than the usual procedure of adding enzyme to pre-diluted reactants. Another aliquot was simultaneously mounted thus enabling the measurement of the activity of the enzyme at the same dilution and after the same incubation period (15 minutes) as mounted samples. Both in this case and in the presence of acetyl-CoA the catalytic activity of the enzyme was greatly increased (Table 3.4). At higher concentrations (10 – 25 μM), palmitoyl-CoA caused a further increase of activity (Table 3.4 and Figure 3.8) but electron microscopic examination revealed a decrease in tetramer frequency (Table 3.4 and Figure 3.9f), presumably

Figure 3.7: **Tilt series using yeast pyruvate carboxylase mounted in the presence of 250 μM acetyl-CoA.** The tilt angles and the tilt axis are indicated on the figure. The arrowheads indicate individual subunits seen in different projection forms.The bar represents 25 nm. Interconversion between rhombic (R), square (S), triangular (T) and dual-intensity (D) forms can be observed as follows: (a, b, c) D R D; (d, h) D R T D; (e, g) D S D; (f) D T D; (i) S R.

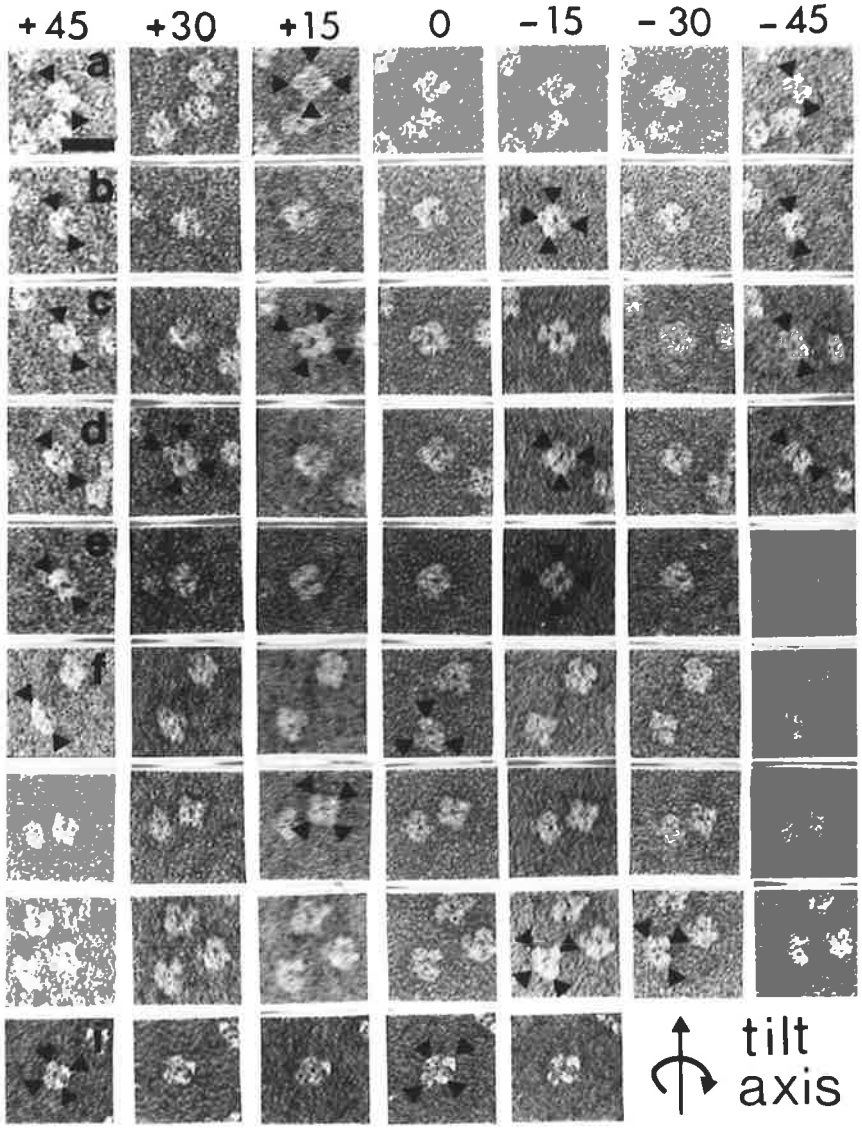
+45
+30
+15
0
-15
-30
-45
a
b
c
d
e
f
tilt
axis

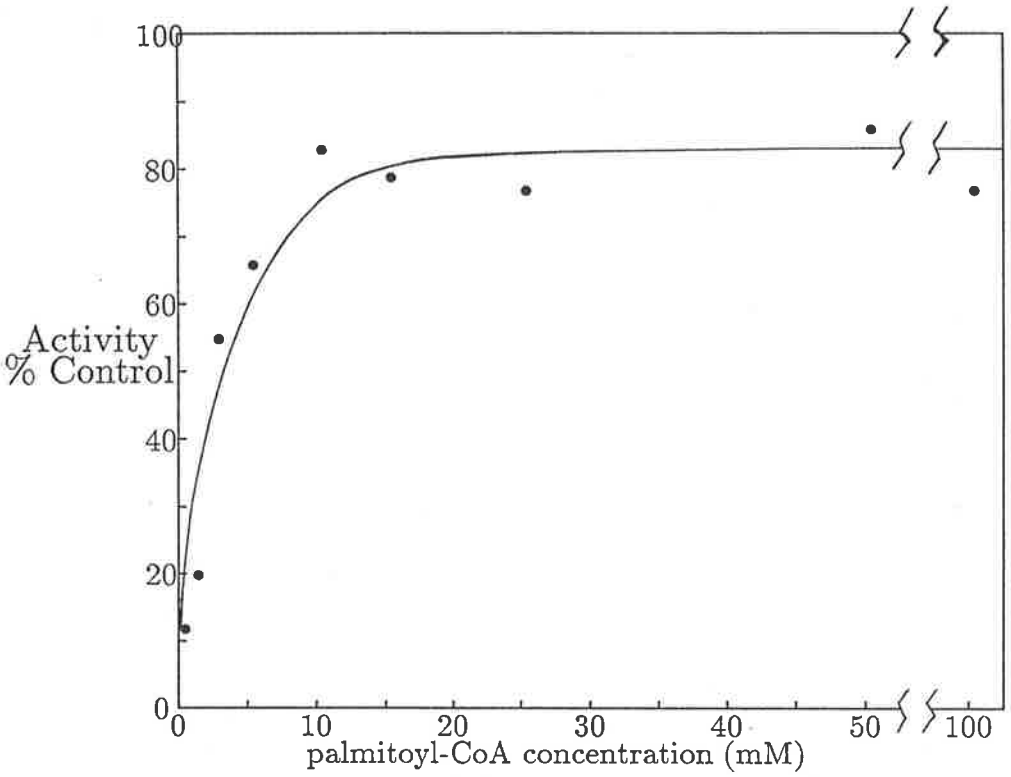

Figure 3.8: **Stimulation of pyruvate carboxylase activity by palmitoyl-CoA.** Yeast pyruvate carboxylase was incubated at 40 μg/ml for 15 minutes in Tris-chloride pH 8.0 containing various concentrations of palmitoyl-CoA as indicated on the abscissa. The samples were assayed for catalytic activity by the spectrophotometric method and the results expressed as a percentage of the activity found in an identical sample incubated with 250 μM acetyl-CoA.

Figure 3.9: **Electron micrographs of yeast pyruvate carboxylase mounted in the presence of activators and inhibitors.** The bar represents 50 nm.

(a) 10 mM aspartate	(b) 40 mM 2-oxo-glutarate
(c) 10 mM aspartate and 40 mM 2-oxo-glutarate	(d) 40 mM 2-oxo-glutarate and 250 μM acetyl-CoA
(e) 1 μM palmitoyl-CoA	(f) 25 μM palmitoyl-CoA
(g) 10 mM aspartate and 250 μM acetyl-CoA	(h) 10 mM aspartate and 1 μM palmitoyl-CoA

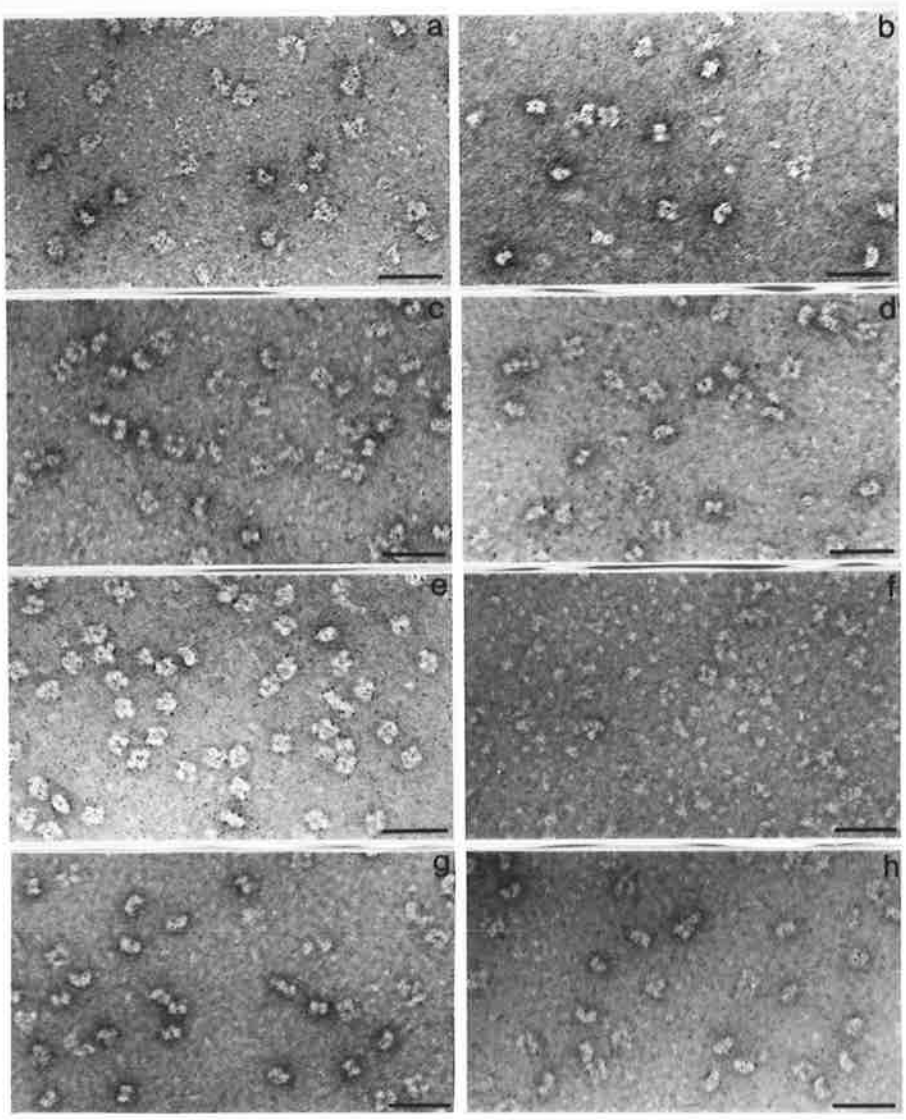
a
b
c
d
e
f
g
h

SAMPLE ADDITIONS	ENZYME ACTIVITY % OF CONTROL	% ENZYME FOUND AS TETRAMERS
none (Tris-chloride)	1	45
none (Tris-acetate)	1	47
250 μM acetyl-CoA	100	85
1 μM palmitoyl-CoA	20	86
2 μM palmitoyl-CoA	48	85
10 μM palmitoyl-CoA	86	39
10 mM L-aspartate	0	19
10 mM L-aspartate and 250 μM acetyl-CoA	1	33
10 mM L-aspartate and 1 μM palmitoyl-CoA	0	30
40 mM 2-oxo-glutarate	0	17
40 mM 2-oxo-glutarate and 250 μM acetyl-CoA	0	28
40 mM 2-oxo-glutarate and 250 μM palmitoyl-CoA	0	34
10 mM L-aspartate and 40 mM 2-oxo-glutarate	0	16

Table 3.4 **Effect of allosteric ligands on the quaternary structure and catalytic activity of yeast pyruvate carboxylase.** Pyruvate carboxylase activity was measured by the spectrophotometric method and expressed as a percentage of the activity found in the sample diluted with 250 μM acetyl-CoA. 100 mM Tris-acetate pH 7.2 containing 10 mM $MgCl_2$ was used as the dilution buffer for all samples except the first, which contained 100 mM Tris-chloride pH 7.2 and 10 mM $MgCl_2$. Particles of pyruvate carboxylase containing less than half the mass of well preserved tetramers were assessed as broken. Numbers of enzyme molecules were obtained from field electron micrographs containing at least 100 molecules.

due to the detergent effects of this activator (Myers *et al*, 1983). These observations indicate that the tetramer state of the enzyme may not be mandatory for catalytic activity.

The presence of the inhibitors L-aspartate and 2-oxo-glutarate separately (Figure 3.9 a and b) and together (Figure 3.9c) caused a marked reduction in the number of tetramers (Table 3.4). The dissociating effects of these two ligands was evident even in the presence of acetyl-CoA or 1 μM palmitoyl-CoA.(Table 3.4, Figure 3.9 g and h).

3.2.6 Binding of Avidin

Figure 3.10 shows the micrographs obtained with samples containing excess avidin (a), equimolar ratios of enzyme and avidin (d), and excess enzyme (b). In (c) avidin was incubated with excess biotin prior to addition of enzyme. Figure 3.11 depicts the percentage of enzyme found in chains at different stages of the titration and the catalytic activity of these samples. Increasing the avidin:enzyme ratio drastically reduced catalytic activity which was undetectable at ratios higher than 2:1. When the ratio of avidin to enzyme was between 1:2 and 2:1, linear unbranched chains were observed, with up to 31 tetramers being seen in the one structure. Tilting studies were attempted but these did not provide any further information about the structure of these enzyme:avidin complexes.

The concatenated tetramers appeared as dual-intensity projections with the exception of the terminal molecules, which sometimes exhibited three or four intensity maxima. These linear polymers exhibited considerable kinking and some completely circularised chains containing either 6 or 7 tetramers (Figure 3.10f) were noted in the samples where the avidin:enzyme ratio was 1:1.

3.2.7 Polyclonal Antibodies

Polyclonal antibodies against yeast pyruvate carboxylase were raised in a rabbit and purified as described in Section 2.2.8. When these antibodies were tested for their ability to inhibit the catalytic activity of pyruvate carboxylases from yeast, chicken and sheep, high specificity for the yeast enzyme was evident (Figure 3.12). Sheep pyruvate carboxylase activity was inhibited by anti-yeast pyruvate carboxylase antibodies weakly while chicken pyruvate carboxylase was almost unaffected by the antibodies.

Immunodiffusion analysis under non-denaturing conditions of yeast, chicken and sheep pyruvate carboxylases and transcarboxylase from *P. shermanii* (Figure 3.13A)

Figure 3.10: **Complexes of yeast pyruvate carboxylase with avidin at different ratios of avidin:enzyme.** The bar represents 25 nm in (e) and 50 nm in the other panels. (▲) Enzyme subunits; (△) avidin molecules.
(a) 4:1, single avidin:enzyme complexes and free avidin molecules are visible.
(b) 1:4, as in (a), only single avidin:enzyme complexes and free enzyme are detectable.
(c) 1:1, a control sample in which avidin was pre-incubated with an excess of *d*-biotin before the addition of enzyme. No avidin:enzyme complexes are visible but tetrameric enzyme molecules (circled) and free avidin can be seen.
(d–f) 1:1, unbranched, linear chain-like structures (d) appeared at this point of the titration. Circularised chains (f) were also detectable at a lower frequency. Avidin molecules in the concatemers (e) were usually bound to both subunits but sometimes only to one (–▷).

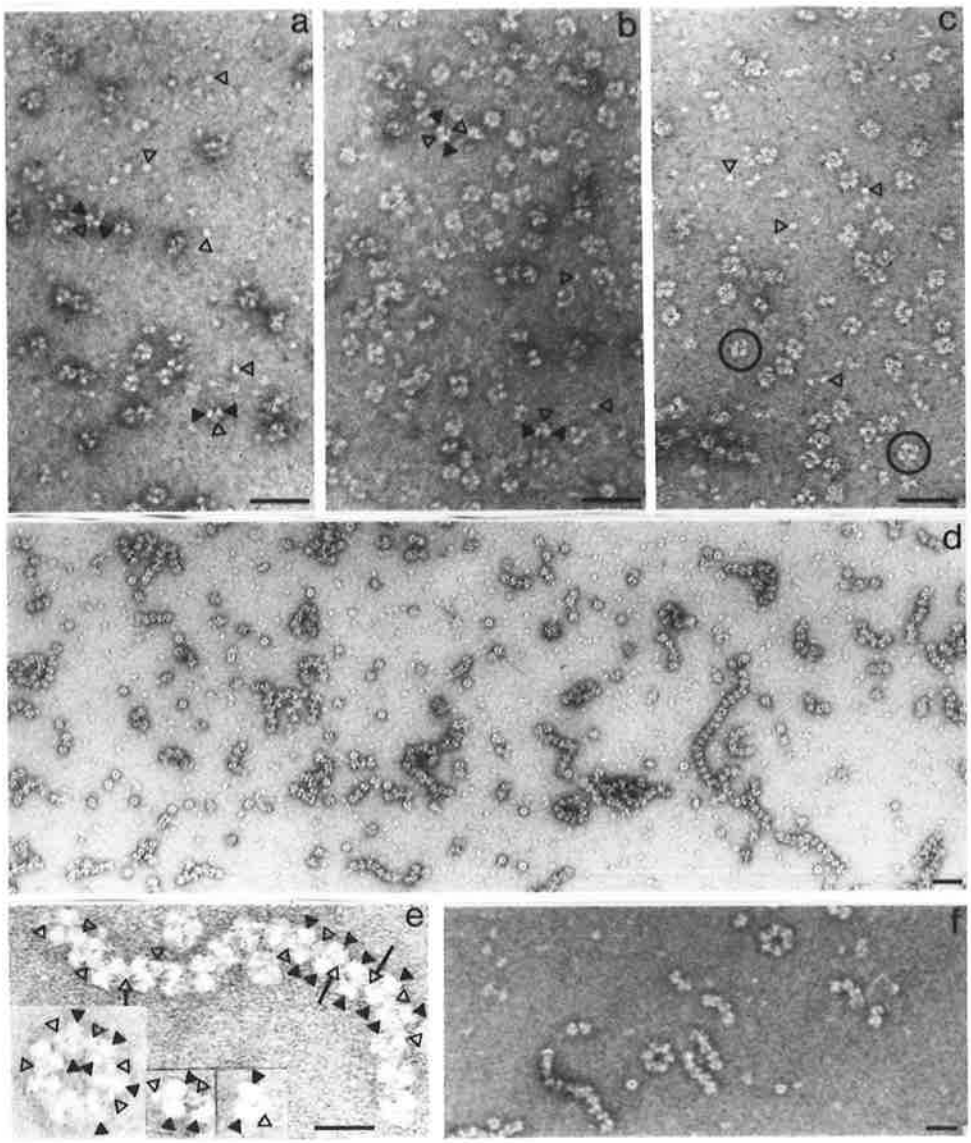
a
b
c
d
e
f

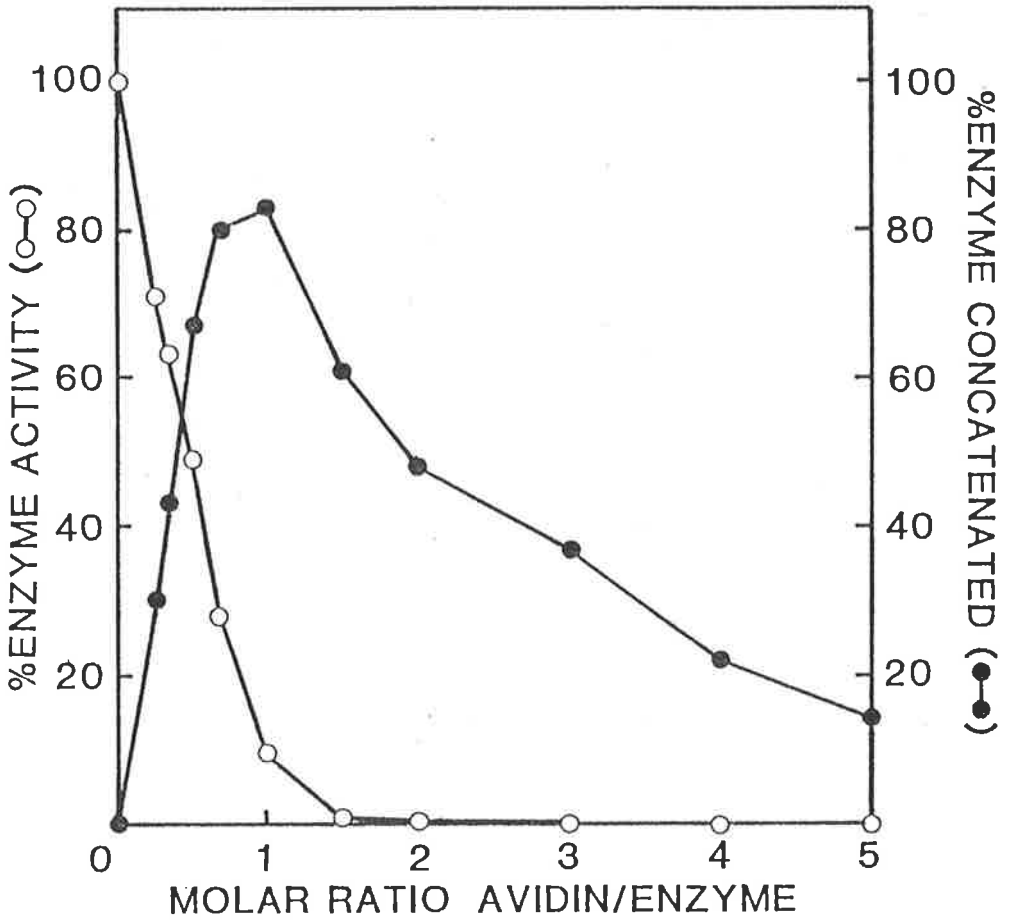

Figure 3.11: **Titration of yeast pyruvate carboxylase with avidin.** The concentration of biotinyl residues and biotin-binding sites was measured directly by the method of Rylatt *et al* (1977). Enzyme was incubated with avidin at the dilution used for electron microscopy (8–80 μg/ml) in the presence of 250 μM acetyl-CoA. After 1 hour aliquots of the samples were withdrawn for mounting and activity measurements. Micrographs of samples prepared after 8 hours and 24 hours yielded identical results.

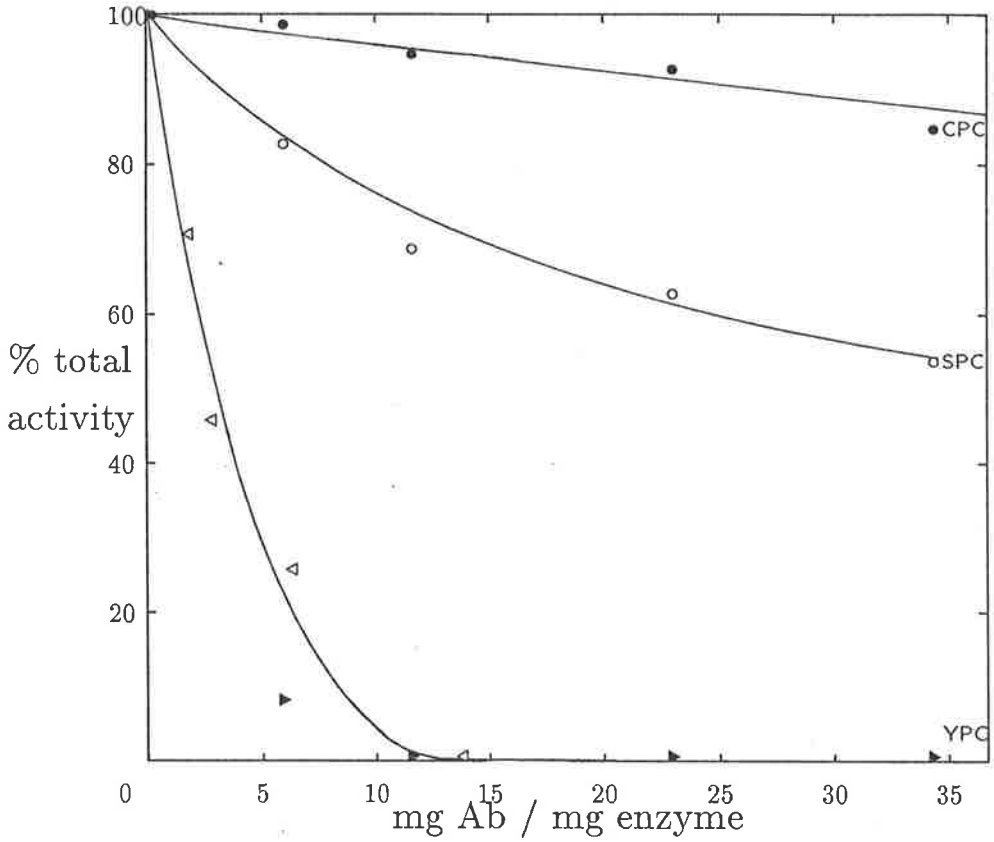

Figure 3.12: **Inhibition of catalytic activity by polyclonal anti-yeast pyruvate carboxylase antibodies.** The antibodies (Ab) were purified from the serum of an immunised rabbit by protein A-Sepharose chromatography and ammonium sulphate precipitation. Enzyme activity was assayed by the spectrophotometric method at pH 7.8 for chicken pyruvate carboxylase (CPC, •) and pH 8.4 for sheep pyruvate carboxylase (SPC, o). The results for yeast pyruvate carboxylase (YPC) at pH 8.0 were obtained from two separate experiments (◁ and ▶).

Figure 3.13: **Binding of polyclonal anti-yeast pyruvate carboxylase antibodies to transcarboxylase (TC) and pyruvate carboxylases from yeast (YPC), sheep (SPC) and chicken (CPC).**

A Ouchterlony double diffusion under non-denaturing conditions shows that in the native state, none of the other biotin carboxylases cross-react with the antibodies raised against yeast pyruvate carboxylase. Antibody was placed in the central well. The faint precipitin lines seen near the SPC and TC wells were not consistently reproducible, suggesting very weak reactivity. Bovine serum albumin (BSA) was used as a negative control.

B Western blot analysis revealed strong cross-reaction of denatured chicken pyruvate carboxylase and sheep pyruvate carboxylase with antibodies raised against the yeast enzyme. Transcarboxylase showed only very weak cross-reactivity which could only be observed after a long development time, after which various breakdown products of the 3 pyruvate carboxylases could be seen.
The nitrocellulose filters were visualised with rabbit anti-YPC antibodies followed by goat anti–rabbit/alkaline phosphatase ($\alpha\ YPC$), avidin–alkaline phosphatase (*avidin*)and Coomassie Brilliant Blue (*Coomassie*) as indicated. The protein molecular mass markers (M) consisted of myosin (205 kDa), β-galactosidase (116 kDa), phosphorylase b (97.4 kDa), bovine serum albumin (66 kDa), ovalbumin (45 kDa) and carbonic anhydrase (29 kDa).

A

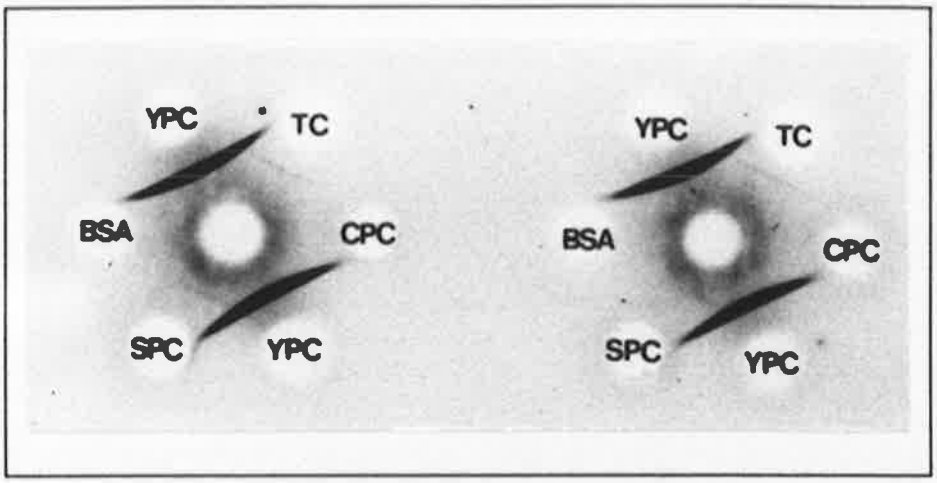
YPC
TC
BSA
CPC
SPC
YPC
YPC
TC
BSA
CPC
SPC
YPC

B

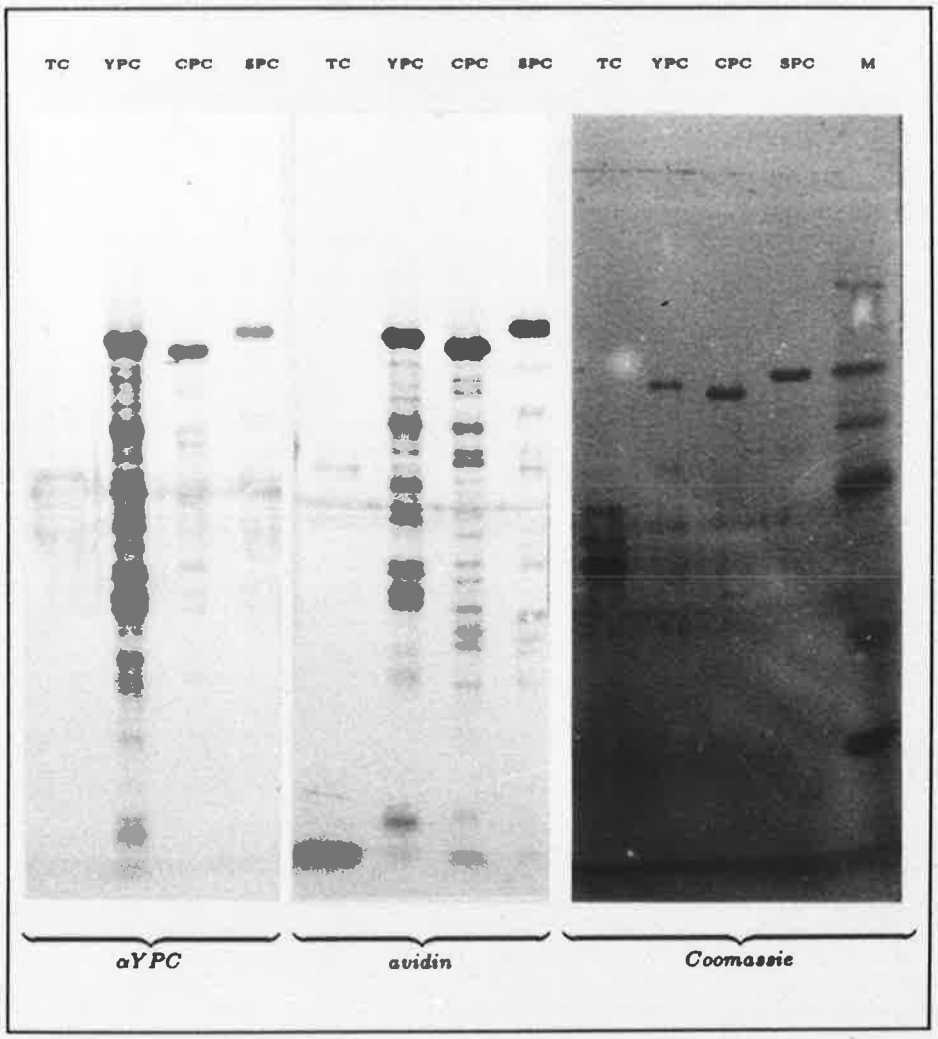
TC
YPC
CPC
SPC
TC
YPC
CPC
SPC
TC
YPC
CPC
SPC
M
αYPC
avidin
Coomassie

revealed that only yeast pyruvate carboxylase showed strong reactivity with anti-yeast pyruvate carboxylase antibodies. Faint precipitin lines were sometimes observed with transcarboxylase and sheep pyruvate carboxylase but these were not consistently reproducible, suggesting that the crossreactivity was very weak.

When Western blots of the above four enzymes denatured by SDS polyacrylamide gel electrophoresis were probed with the anti-yeast pyruvate carboxylase antibodies (Figure 3.13B), strong crossreactivity to chicken and sheep pyruvate carboxylase and a very weak reaction to transcarboxylase was observed. Replicate blots were stained for biotin and protein to give an indication of the relative quantities loaded.

3.3 DISCUSSION

A satisfactory purification procedure for isolating pyruvate carboxylase from baker's yeast was developed. Specific activity and biotin content measurements were consistent with previous reports and are similar to those obtained for pyruvate carboxylases from other species (Wallace, 1985). In contrast to vertebrate pyruvate carboxylases, the yeast enzyme shows a large amount of activity in the absence of acetyl-CoA, particularly in the presence of potassium ions, as previously reported (Ruiz-Amil *et al*, 1965).

Previous subunit molecular weight values (Wallace and Easterbrook-Smith, 1985) of the yeast enzyme obtained by SDS-polyacrylamide gel electrophoresis have been underestimates due to the use of β-galactosidase (M_r 116 351) as a marker. When compared with other commonly used markers, this protein lies further off the standard curve than does yeast pyruvate carboxylase (M_r 130 100, from sequencing studies - see Chapter 5). This suggests a use for yeast pyruvate carboxylase as a molecular weight standard, since few protein standards of this size range are available. This may be more significant once large amounts of the enzyme are produced by overexpression of

the gene.

Electron micrographs of negatively stained samples of pyruvate carboxylase from vertebrate sources (Mayer *et al*, 1980), a thermophilic *Bacillus* (Libor *et al*, 1979), *Aspergillus nidulans* (Osmani *et al*, 1984) and *Saccharomyces cerevisiae* (Cohen *et al*, 1979; Rohde *et al*, 1986) appear to be very similar. However the structural model proposed by Cohen *et al* (1979) for the yeast enzyme is fundamentally different from those of the other pyruvate carboxylases. These authors chose a model in which ellipsoid subunits are arranged with their centres located in the same plane at the corners of a rhombus, but with the diagonally opposite pairs of subunits aligned in perpendicular planes (Figure 3.14). This arrangement implies either that the subunits are of two different types or that each of the apparently identical subunits has four different binding domains (see Figure 3.14), two of which are unoccupied.

The tilting studies carried out on yeast pyruvate carboxylase in the present study clearly indicate that as for the vertebrate and *A.nidulans* enzymes, the various observed projection forms represent different rotational views of a tetrahedron-like molecule (Figure 3.15a). In most of the images where four intensity maxima are seen, these are arranged at the corners of a rhombus, rather than at the corners of a square, as would be expected from the model. However, this projection form can be easily explained by the collapse of one of the two pairs of opposing subunits during the mounting process, possibly due to interaction with the carbon support film (Figure 3.15b). The non-tetrahedral model (Figure 3.15c) previously proposed for yeast pyruvate carboxylase (Cohen *et al*, 1979) is inconsistent with experimental data:

- Since all available data indicates that the subunits of the enzyme are identical, the non-tetrahedral model predicts the presence of unoccupied binding sites. The presence of these unoccupied binding sites could lead to polymerisation of the tetramer to higher molecular weight forms, but there is no evidence for such an

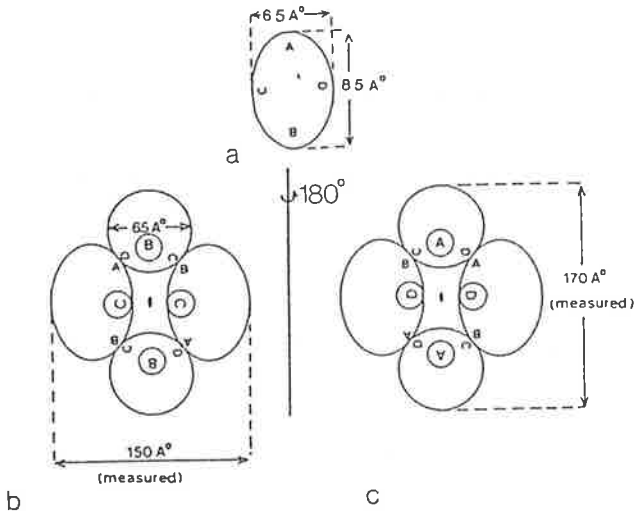

Figure 3.14 **Model for the quaternary structure of yeast pyruvate carboxylase proposed by Cohen *et al* (1979).** (a) The enzyme subunits are prolate ellipsoids 8.5 nm long by 6.5 nm wide, each containing four separate binding sites, A, B, C, D. (b, c) Two separate views of the tetramer as it is rotated 180° about the vertical axis. The two subunits on the left and right of each drawing lie with their long axes in the plane of the paper. The two subunits at the top and bottom of each tetramer lie with their long axes perpendicular to the plane of the paper. The circled letters show unoccupied binding sites. (Adapted from Cohen *et al*, 1979).

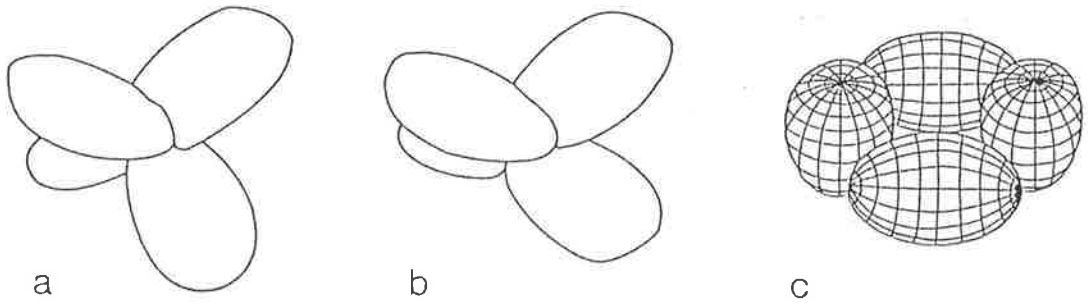

Figure 3.15 **Models for the quaternary structure of yeast pyuvate carboxylase.** (a) Tetrahedron-like structure based on model proposd for vertebrate pyruvate carboxylases (Mayer *et al*, 1980). (b) Collapse of one pair of opposing subunits during mounting for electron microscopy increases the length of its axis, thus producing a projection form with four intensity maxima arranged at the corners of a rhombus. (c) Model based on that previously proposed for yeast pyruvate carboxylase (Cohen *et al*, 1979).

occurrence.

- There was no evidence of many of the images predicted by computer-generated rotations (described by Cohen *et al*, 1979) of that model, nor can it account for those projection forms in which protein is clearly evident in the centre of the molecule.

- Yeast pyruvate carboxylase was observed to form linear *unbranched* concatemers with avidin. Using models of the non-tetrahedral structure it is not possible to construct these complexes whereas they are easily formed using the tetrahedron-like model (Figure 3.16 a – e).

The addition of the protective ligand acetyl-CoA to samples of pyruvate carboxylase has been used as a technique for stabilizing the structure of the enzyme for electron-microscopic examination. Like the enzyme from all other species so far examined, yeast pyruvate carboxylase becomes more compact in the presence of acetyl-CoA (Mayer *et al*, 1980; Osmani *et al*, 1984). Palmitoyl-CoA at low concentrations (<5 μM) enhances

Figure 3.16: **Models of the complexes between avidin and pyruvate carboxylase.** (Adapted from Johannssen *et al*, 1983.)

(a) Unbranched chain-like polymer composed of alternating pyruvate carboxylase tetramers and avidin tetramers. The enzyme is depicted by the white lobes while avidin molecules are represented as dark rectangular blocks.

(b) **and (c)** Single avidin-enzyme complexes in two different orientations.

(d) Diagrammatic side view of half of an enzyme tetramer with a bound avidin tetramer attached. The biotin-binding sites (▲) on avidin and the active sites of the enzyme (shaded) are indicated.

(e) Exploded face-view of the pyruvate carboxylase tetramer with an indication of the bound avidin molecule (shaded). The biotin-binding sites of the avidin attached to the upper pair of pyruvate carboxylase subunits (★) and of the avidin bound to the lower pair of pyruvate carboxylase subunits (☆) are indicated.

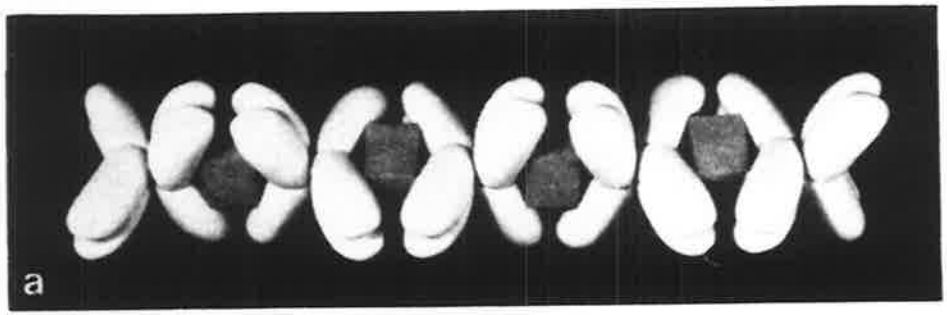

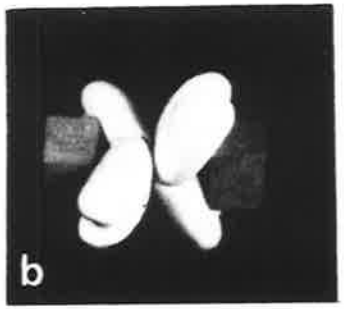

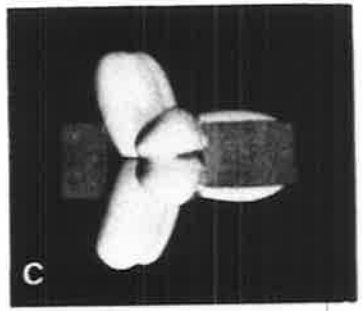

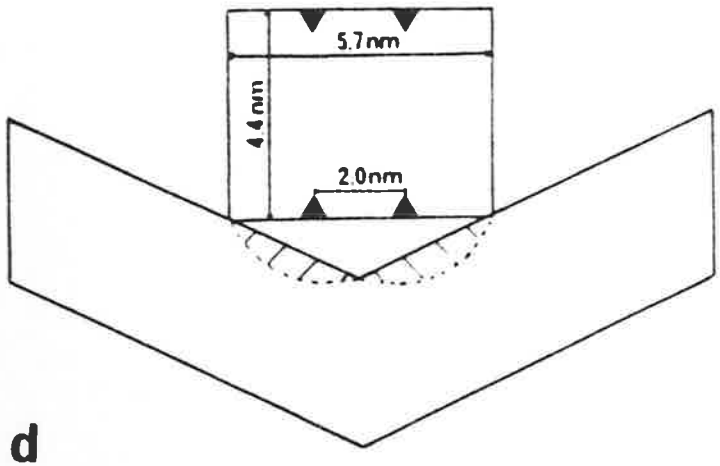

d

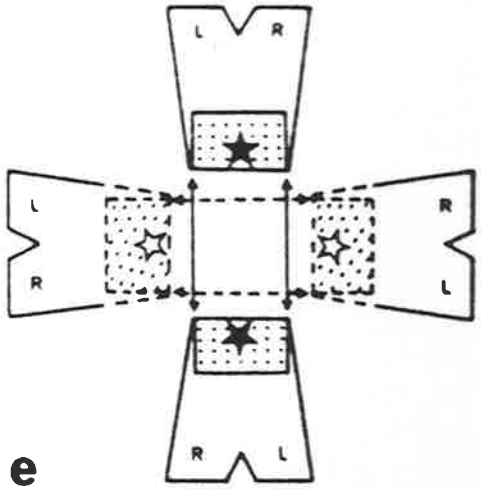

e

both the activity and the structural integrity of the yeast enzyme. At higher concentrations, the opposing effects of this ligand on the structure and function of the enzyme indicate that two factors are operating: disruption of intersubunit forces is caused presumably by the detergent property of the long chain acyl moiety while allosteric interactions stabilise the polypeptide chains in a conformation which is favourable for activity. Thus, in contrast to reacting enzyme sedimentation studies (Taylor *et al*, 1978), it appears that activity is not directly dependent on the tetrameric state of the enzyme.

Both of the inhibitors L-aspartate and 2-oxoglutarate caused dissociation of yeast pyruvate carboxylase tetramers when they were present either alone or in combination with activators. This is in contrast to *A.nidulans* pyruvate carboxylase where the dissociating effect of L-aspartate was evident only in the presence of acetyl-CoA and 2-oxo-glutarate actually appeared to enhance tetramer preservation (Osmani *et al*, 1984). It would seem that the effect of these inhibitors is to alter the conformational state of the enzyme protomers to decrease their catalytic activity. In the case of the yeast protein this structural change may then perturb the intersubunit forces sufficiently to cause tetramer dissociation whereas this effect is less pronounced in the enzyme from *A.nidulans*.

Polyclonal antibodies raised against yeast pyruvate carboxylase had little effect on the activity of chicken pyruvate carboxylase and inhibited sheep pyruvate carboxylase activity only at very high concentrations. In immunodiffusion analysis there was no evidence for precipitation of native chicken or sheep pyruvate carboxylases by the anti-yeast pyruvate carboxylase immunoglobulins whereas Western blotting showed appreciable reaction of these antibodies to the denatured proteins. These results indicate that the surface of pyruvate carboxylase has changed substantially during evolution. The antigenic determinants in chicken and sheep pyruvate carboxylases which cross-

react with anti-yeast pyruvate carboxylase antibodies on Western blots are normally buried within the enzymes and have probably been conserved due to their functional importance.

Chapter 4

Intracellular Localisation and Gene Isolation

4.1 INTRODUCTION

Isolation of the gene for yeast pyruvate carboxylase was attempted by two different approaches. In the first, we (Lim *et al*, 1987) had hoped to make use of a pyruvate carboxylase-deficient yeast *pyc* strain (Wills and Melham, 1985) to select plasmids harbouring the pyruvate carboxylase gene by genetic complementation. However, despite having an identical growth pattern on various media to that previously reported (Wills and Melham, 1985), this *pyc* mutant was found to contain levels of pyruvate carboxylase identical to those found in the wild type.

In explaining the growth characteristics of the yeast *pyc* mutant Wills and Melham (1985) postulated a model in which pyruvate carboxylase was located in the mitochondria of yeast. The majority of evidence favours an intramitochondrial localisation of pyruvate carboxylase in vertebrate tissues (Wallace, 1985), whereas in yeast it has been reported on the basis of cell fractionation studies to be cytosolic (Haarasilta and Taskinen, 1977), as it is in *Aspergillus nidulans* (Osmani and Scrutton, 1983) and *Rhizopus arrhizus* (Osmani and Scrutton, 1985). However, due to the inherent imprecision of cell fractionation techniques studies it has not been possible to be certain whether the small amounts of pyruvate carboxylase activity associated with yeast mitochondrial fractions represent the occurrence of this enzyme in the mitochondria or its presence merely as

an artifact of the fractionation procedure. Since it had been claimed that yeast pyruvate carboxylase was mitochondrial and that its absence from the mitochondria of the *pyc* mutant accounted for that mutant's growth characteristics (Wills and Melham, 1985) the localisation of this enzyme was reinvestigated using a completely alternative approach not previously applied to pyruvate carboxylase, viz. immunogold labelling. The electron microscopy in this section of work was performed by Dr. Manfred Rohde.

In the second approach to gene isolation, the highly conserved sequence around the biotin attachment site of biotin carboxylases was used to design an olignucleotide probe which was then used to screen a library of yeast genomic DNA fragments. This was carried out by Dr. Phillip Morris who obtained a small (1.4 kb) yeast DNA fragment containing the 3′-end of the pyruvate carboxylase gene. Since no protein sequence data existed at the time for yeast pyruvate carboxylase, my work in parallel to the DNA screening was to isolate and sequence peptides to confirm the identity of any putative yeast pyruvate carboxylase gene clones. To enable rapid identification of the clones isolated with the biotin attachment site oligomer, the biotin-containing tryptic peptide of yeast pyruvate carboxylase was purified and sequenced. The methodology developed for this was also used to sequence the biotin-containing peptides from sheep and chicken propionyl-CoA carboxylases (in collaboration with Ms. Alison Whittle as part of her B.Sc. Honours project).

4.2 RESULTS

4.2.1 Determination of Activity in the *pyc* Mutant

The cell yields from 500 ml cultures of the control and *pyc* yeasts in rich medium were 10.9 g and 10.5 g respectively. Samples of the control strain grew on minimal + glucose, minimal + ethanol and minimal + pyruvate whereas the *pyc* cells grew only on minimal + glucose as reported previously (Wills and Melham, 1985). This indicated

ASSAY SYSTEM	CONTROL	*pyc* MUTANT
Avidin-sensitive units (spec. assay)	9.8 ± 0.5	10.8 ± 0.5
Pyruvate-dependent units (spec. assay)	4.3 ± 0.4	4.6 ± 0.4
Pyruvate-dependent units (isotopic assay)	5.0 ± 0.5	4.5 ± 0.5

Table 4.1 **Pyruvate carboxylase activity in wild type and *pyc* cell extracts.** Enzyme units in three different crude extracts made from 5 g pellets of yeast were measured in three separate experiments: using the enzyme-linked spectrophotometric assay in the presence and absence of avidin; using the enzyme-linked spectrophotometric assay in the presence and absence of pyruvate; using the ^{14}C incorporation assay in the presence and absence of pyruvate. Figures given are the mean of three measurements ± the standard error of the mean.

that revertants had not been generated during the culture in rich medium.

Crude extracts obtained from the cells after passage through a French pressure cell were assayed for pyruvate carboxylase (Young *et al*, 1969) by three different procedures: 1) measuring the incorporation of $[^{14}CO_2]$ into oxaloacetate in the presence and absence of pyruvate; 2) using the enzyme-linked spectrophotometric assay in the presence and absence of pyruvate; 3) using the enzyme-linked spectrophotometric assay in the presence and absence of avidin (500 μg/ml). Since several NADH-utilising systems present in the crude extracts can interfere with the spectrophotometric method, the use of avidin allowed calculation of biotin-dependent activity. The results from three separate experiments shown in Table 4.1 reveal no significant difference between the levels of activity found in the *pyc* mutant and the control cell extracts.

Further purification of the cell extracts resulted in similar yields of pyruvate carboxylase from the control and *pyc* strains. The elution time of activity upon Superose 6 gel filtration in both cases was the same as that of purified pyruvate carboxylase, indicating that the native form of the enzyme in the mutant was of the same size as that of the wild type.

Figure 4.1: **Western analysis of yeast cell extracts.** Molecular weight markers (M) were carbonic anhydrase (29K), ovalbumin (45K), bovine serum albumin (66K), phosphorylase b (97.4K), β-galactosidase (116K) and myosin (205K). Crude extracts from the *pyc* mutant (pyc) and the control strain (con) and purified yeast pyruvate carboxylase (YPC) were electrophoresed and:
1) stained with Coomassie Blue;
2) transferred to nitrocellulose and probed with anti-YPC antibody followed by goat anti-rabbit alkaline phosphatase;
3) transferred to nitrocellulose and probed with avidin-alkaline phosphatase.

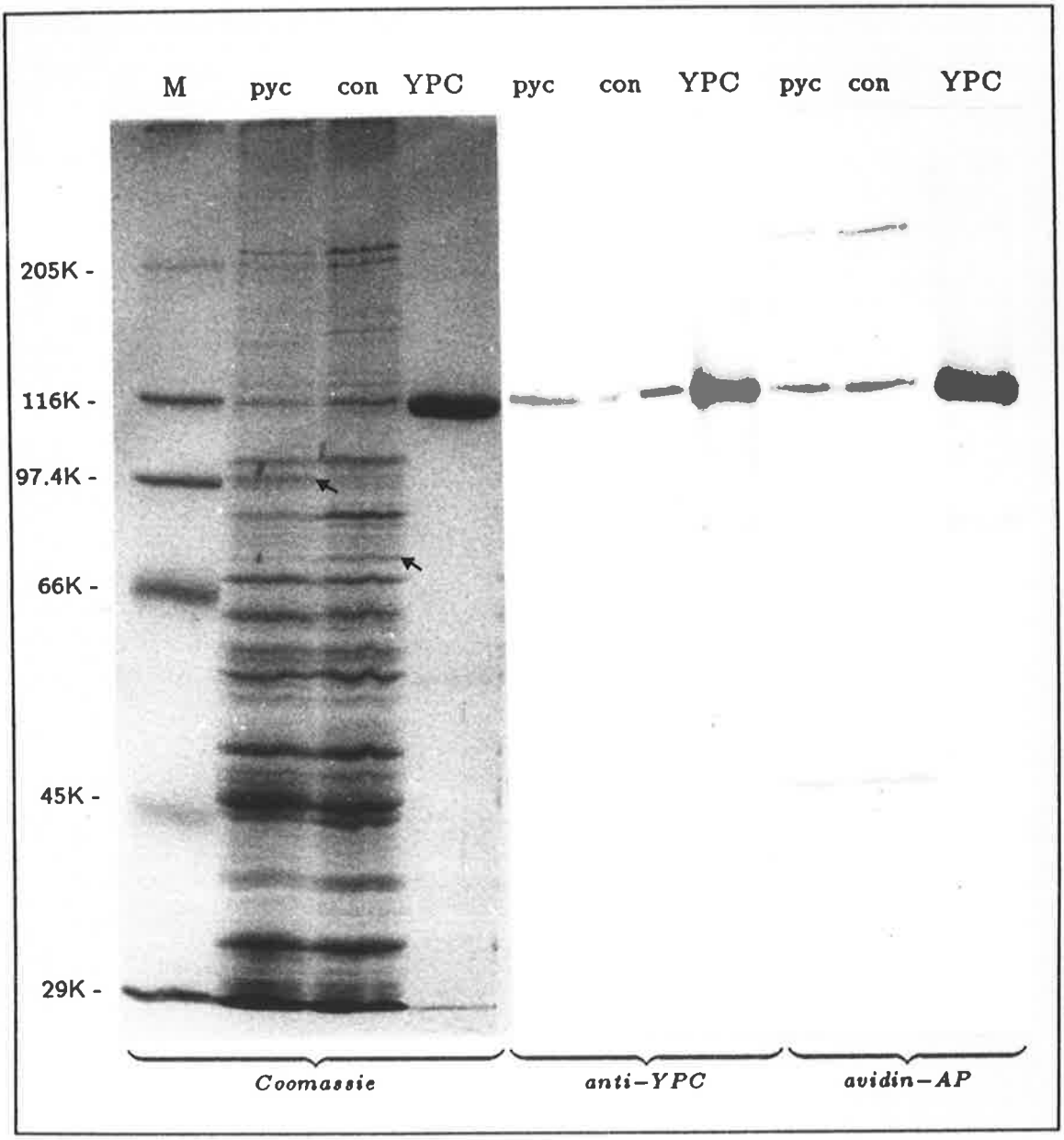
M
pyc
con
YPC
pyc
con
YPC
pyc
con
YPC
205K -
116K -
97.4K -
66K -
45K -
29K -
Coomassie
anti-YPC
avidin-AP

4.2.2 Western Analysis

When crude extracts of the *pyc* mutant and wild type yeast were electrophoresed in the presence of SDS the resulting patterns of Coomassie stained protein bands (Figure 4.1) were, with the exception of several unidentified bands of $M_r \sim 74\,000$ and $\sim 98\,000$, essentially identical. In particular, both the *pyc* mutant and wild type yeast extracts revealed protein bands having the same mobility as purified yeast pyruvate carboxylase. The identity of these bands as pyruvate carboxylase was confirmed by probing Western blots of replicate gels with anti-yeast pyruvate carboxylase antibodies (Figure 4.1). Similarly, when another Western blot of a replicate gel was probed with avidin-alkaline phosphatase conjugate, both the *pyc* mutant and the wild type cell extracts revealed a biotin-containing protein band having the same mobility as purified yeast pyruvate carboxylase. In addition, both extracts also revealed a biotin-containing band of $M_r \sim 205\,000$ which is probably attributable to the presence of acetyl-CoA carboxylase. A third biotin containing protein band of $M_r \sim 47\,000$ was also detected in both extracts. It is apparently not a breakdown product of pyruvate carboxylase since it was not detected by the anti-yeast pyruvate carboxylase antibodies. Its identity is unknown at this stage.

4.2.3 Intracellular Localisation

When the immunogold technique using polyclonal anti-yeast pyruvate carboxylase antibodies was applied to yeast protoplasts made from mutant and control cells (Figure 4.2) it could be seen that the mitochondria, nucleus and vacuole of the protoplasts were devoid of any labelling. A comparison of Figure 4.2 a, b, c, d and e shows that the *pyc* strain exhibits approximately the same amount of pyruvate carboxylase as the control, and in both cases the enzyme is clearly cytosolic. The few gold particles observed at the periphery of some of the mitochondria can be attributed to the fact that the gold

Figure 4.2: **Localisation of yeast pyruvate carboxylase using the antibody-gold method.** Ultrathin sections of yeast protoplasts were treated with anti-yeast PC antibody (a, c, d 100 μg/ml, b and e 64 μg/ml) followed by GARG ($\frac{1}{25}$ dilution) and poststained with uranyl acetate. Panels a and b: wild type strain, c, d, e and f: *pyc* strain. In f the section was incubated with nonspecific antibody (115 μg/ml) followed by GARG ($\frac{1}{25}$ dilution). The scale bar represents 250 nm. M = mitochondria, N = nucleus, V = vacuole, G = gold particle.

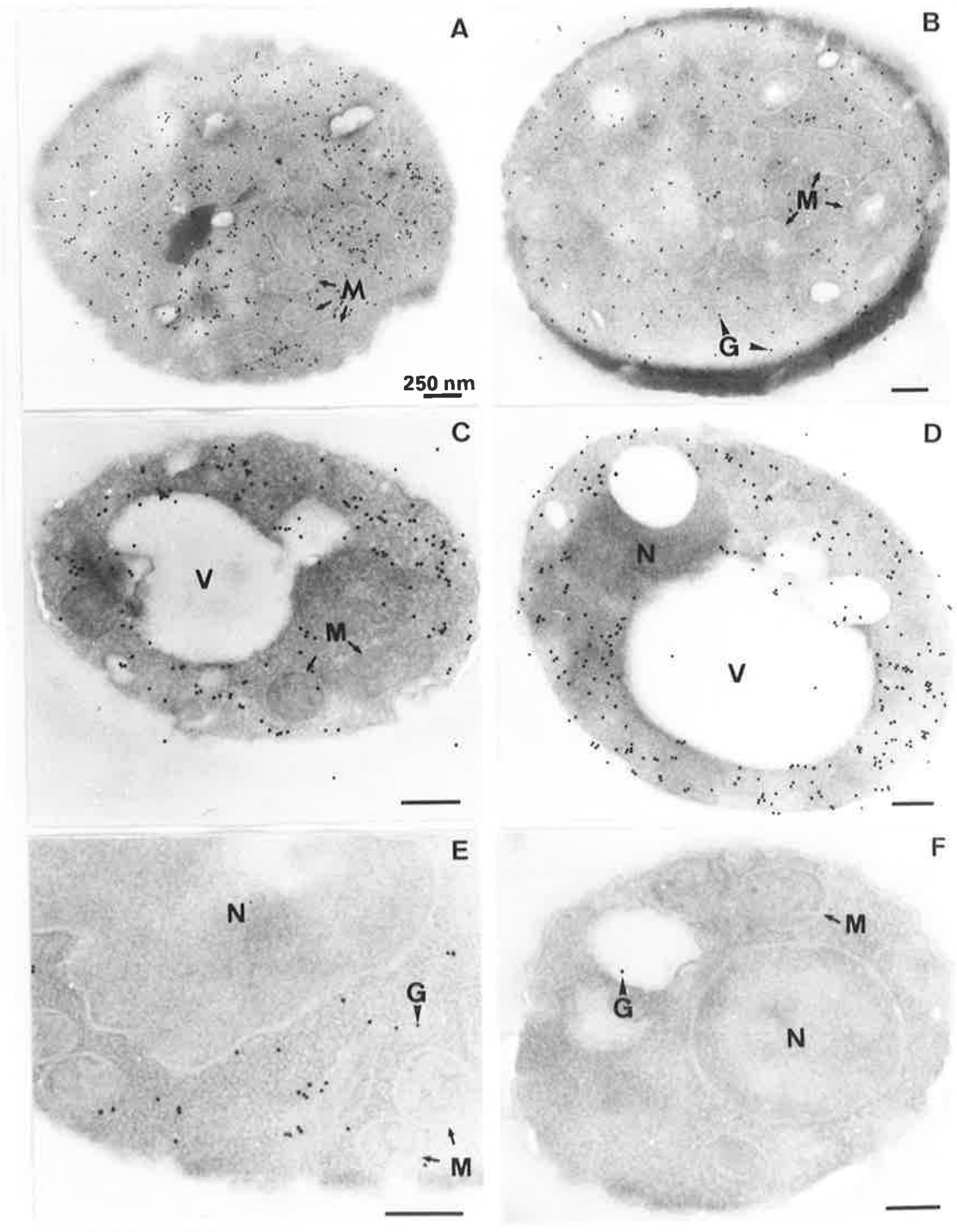
A
M
250 nm
B
M
G
C
V
M
D
N
V
E
N
G
M
F
M
G
N

particles are separated from the enzyme by an immunoglobulin bridge of about 20 nm. No labelling is detectable when nonspecific antibodies are used (Figure 4.2 f).

4.2.4 Sequencing of Tryptic Peptides

When 1 nmol of intact purified yeast pyruvate carboxylase was subjected to automated Edman degradation sequencing, no PTH-derivatives were detected. This indicated that the enzyme from yeast is N-terminally blocked, as is pyruvate carboxylase from other species (Wallace and Easterbrook-Smith, 1985).

Peptides were generated by digestion of purified yeast pyruvate carboxylase with trypsin under denaturing conditions. Figure 4.3A shows the absorbance profiles obtained by C_8 reverse phase HPLC of the peptides from a digest of 5 nmol of yeast pyruvate carboxylase. Well separated peaks (numbered) were collected and sequenced by automated Edman degradation (Figure 4.3B). This peptide data confirmed the amino acid sequence predicted by DNA sequencing (see Chapter 5).

4.2.5 Isolation and Sequencing of the Biotin-containing Peptide

The twenty-six amino acid sequence of the biotin-containing tryptic peptide of yeast pyruvate carboxylase was deduced from overlaps obtained by sequencing several peptides isolated by gel filtration (Figure 4.4) and by avidin-Sepharose chromatography (Figure 4.5). In the first attempt at peptide isolation a tryptic digest of 126 nmol of yeast pyruvate carboxylase was incubated with avidin and subjected to gel filtration chromatography. Acid dissociation released 86 nmol of biotin-containing material from the avidin (Figure 4.4A, solid squares) and this was then further purified by a second gel filtration step. The biotin-containing material (41 nmol) was recovered in this second step (Figure 4.4A, open squares) and when the 3 peak fractions (31 nmol) were purified by C_{18} reverse phase HPLC, the absorbance profile shown in Figure 4.4B

Figure 4.3: **Sequencing of tryptic peptides of yeast pyruvate carboxylase.** A complete tryptic digest of 5 nmol of enzyme was chromatographed on an Aquapore RP300 C_8 column (panel A). The column was eluted at 1 ml/min using a gradient of 0–60% acetonitrile in 0.1% aqueous TFA over 60 minutes. Well separated peaks (numbered) were collected and sequenced by automated Edman degradation (panel B). Peak 1 appeared to contain two peptides and major (1a) and minor (1b) sequences were read. The amino acid sequence data shown here was later confirmed by DNA sequencing of the yeast pyruvate carboxylase gene (Chapter 5).

A

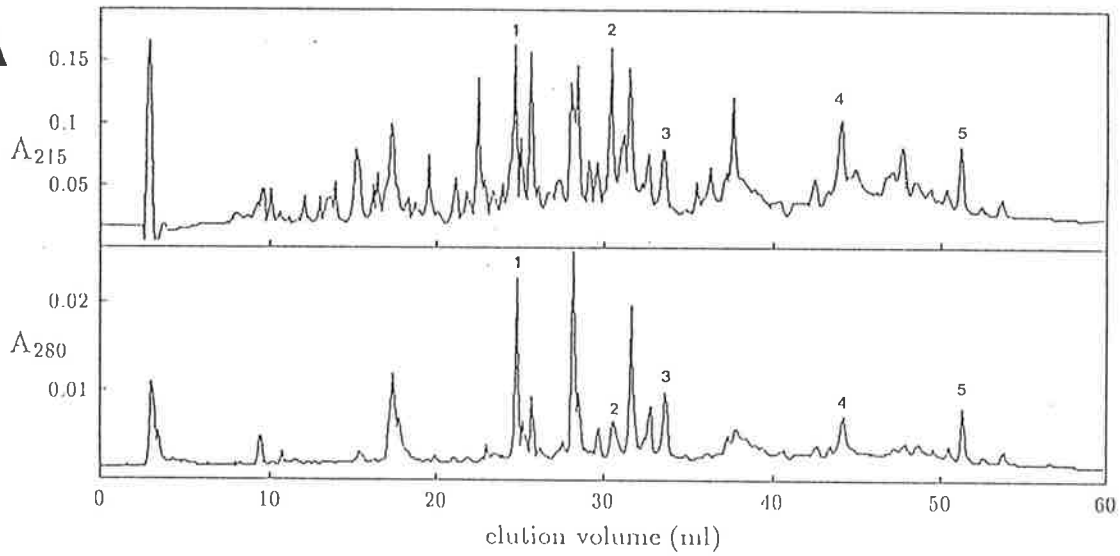

B

1a	PHE-LEU-HIS-GLU-ASP-PRO-TRP-GLN-ARG
1b	ASP-ASN-SER-VAL-ASP-ILE-PHE-ARG
2	HIS-GLN-VAL-ASP-PHE-ILE-HIS-PRO-GLY-TYR-GLY-PHE-LEU-SER-GLU-ASN-SER-GLU-PHE-ALA-ASP-LYS
3	ALA-GLY-ILE-THR-TRP-ILE-GLY-PRO-PRO-ALA-GLU-VAL-ILE-ASP-SER-VAL-GLY-ASP-LYS
4	ALA-ASN-VAL-PRO-THR-VAL-PRO-GLY-THR-PRO-GLY-PRO-ILE-GLU-THR-VAL-GLU-GLU-ALA-LEU-ASP-PHE--VAL-ASN-GLU-TYR-GLY-
5	THR-ASN-ILE-PRO-PHE-LEU-LEU-THR-LEU-LEU-THR-ASN-PRO-VAL-PHE-ILE-GLU-GLY-THR-TYR-TRP-

Figure 4.4: **Gel filtration isolation of the biotin-containing peptide of yeast pyruvate carboxylase.**

A Sephadex G-50 purification of a tryptic digest of yeast pyruvate carboxylase. Fractions were assayed for biotin using ^{14}C-biotin/avidin. ■ In the presence of avidin the biotin-containing peptide eluted in the void volume. □ Elution profile after acid dissociation of the peptide from avidin.

B C_{18} reverse phase HPLC of the acid dissociated material from (A). The three major peaks (numbered) were found to contain biotin. Peaks G2 and G3 were sequenced by automated Edman degradation (see Figure 4.6).

A

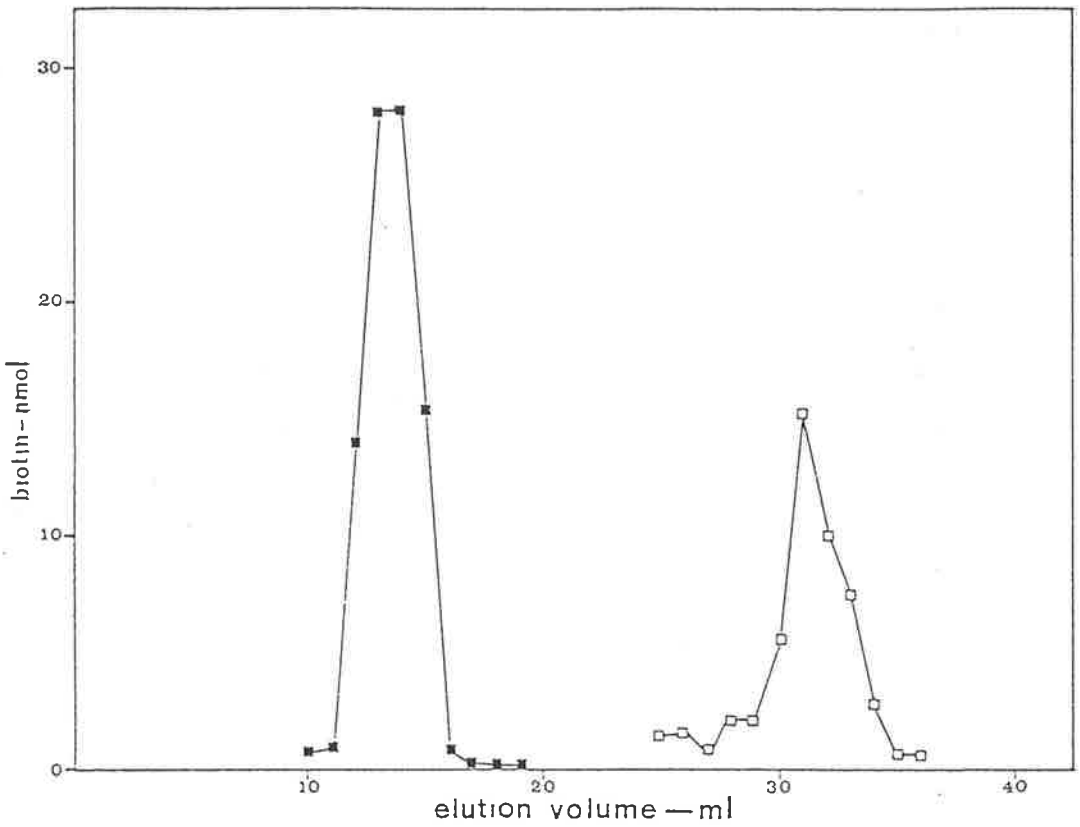
30
20
10
0
biotin - nmol
10
20
30
40
elution volume — ml

B

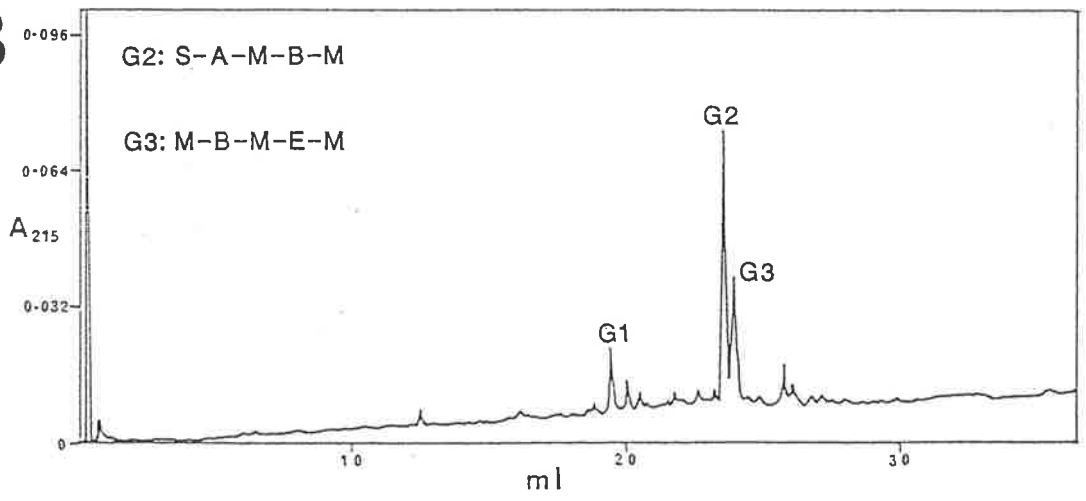
0·096
0·064
0·032
0
A 215
G2: S-A-M-B-M
G3: M-B-M-E-M
G1
G2
G3
10
20
30
ml

was obtained. Peaks G1, G2 and G3 were found to contain 1.4, 9.2 and 1.2 nmol of biotin respectively. Sequencing of peaks G2 and G3 (Figure 4.4B) indicated that the trypsin contained some contaminant proteolytic activity, since cleavage occurred on the C-terminal side of methionine residues. Nonspecific cleavage by tryptic digestion of oxaloacetate decarboxylase from *Klebsiella pneumoniae* under similar conditions has also been observed (D. Oesterhelt, personal communication) and this was at first attributed to contaminating chymotryptic activity. However, this problem is thought to be due to alteration of cleavage specificity caused by the formation of ψ-trypsin (Allen, 1981) by autolysis, since it was later eliminated by using fresh trypsin. The elution time of biocytin on the sequencer was determined by placing a sample of authentic biocytin in the sequencing cartridge.

Isolation of the biotin-containing peptide was later simplified by the use of avidin-Sepharose chromatography. When 31 nmol of yeast pyruvate carboxylase was digested with trypsin and chromatographed on monomeric avidin-Sepharose, 6 nmol of biotin-containing material was eluted from the column (Figure 4.5A). Half of this was purified by C_8 reverse phase HPLC and the absorbance profile shown in Figure 4.5B was obtained. The major peak (A1) contained 400 pmol of biotin and sequencing yielded the first 20 residues of the peptide (Figure 4.5B) before the signal became too low to read. In one previous attempt nonspecific cleavage gave rise to a shorter peptide and the C-terminal 15 residues were obtained (Figure 4.5B). Using this approach the biotin-containing peptides of sheep and chicken propionyl-CoA carboxylases were also isolated and sequenced. These sequences are compared to other biotin enzymes in Figure 5.6.

Figure 4.5: **Purification of the biotin-containing tryptic peptide of yeast pyruvate carboxylase by avidin-Sepharose chromatography.** The enzyme was digested to completion with trypsin and passed through an avidin-Sepharose column at neutral pH (panel A). After elution with acid and high salt, the biotin-containing material was further purified by C_8 reverse phase HPLC (panel B). The three major peaks were found to contain biotin and the largest (A1) was sequenced by automated Edman degradation. The first 20 amino acids of this 26-residue peptide were read before the signal level became too low. The C-terminal 15 residues were obtained on one previous attempt at peptide isolation when nonspecific cleavage by trypsin autolysis products gave rise to a shorter peptide (A2).

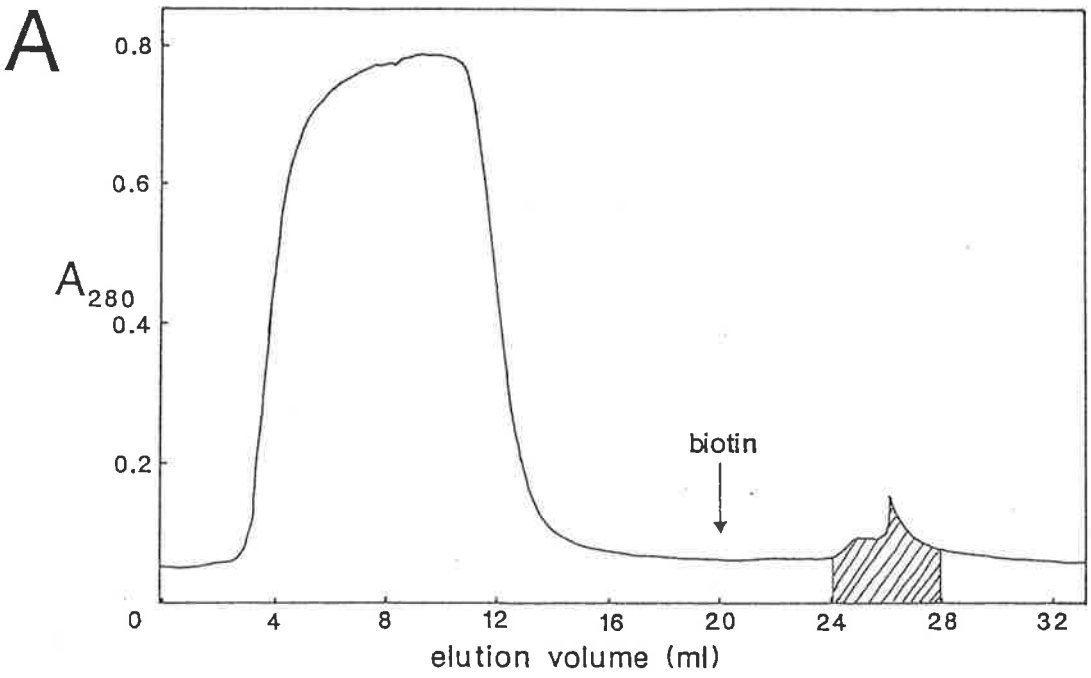
A
0.8
0.6
A_{280}
0.4
0.2
biotin
0
4
8
12
16
20
24
28
32
elution volume (ml)

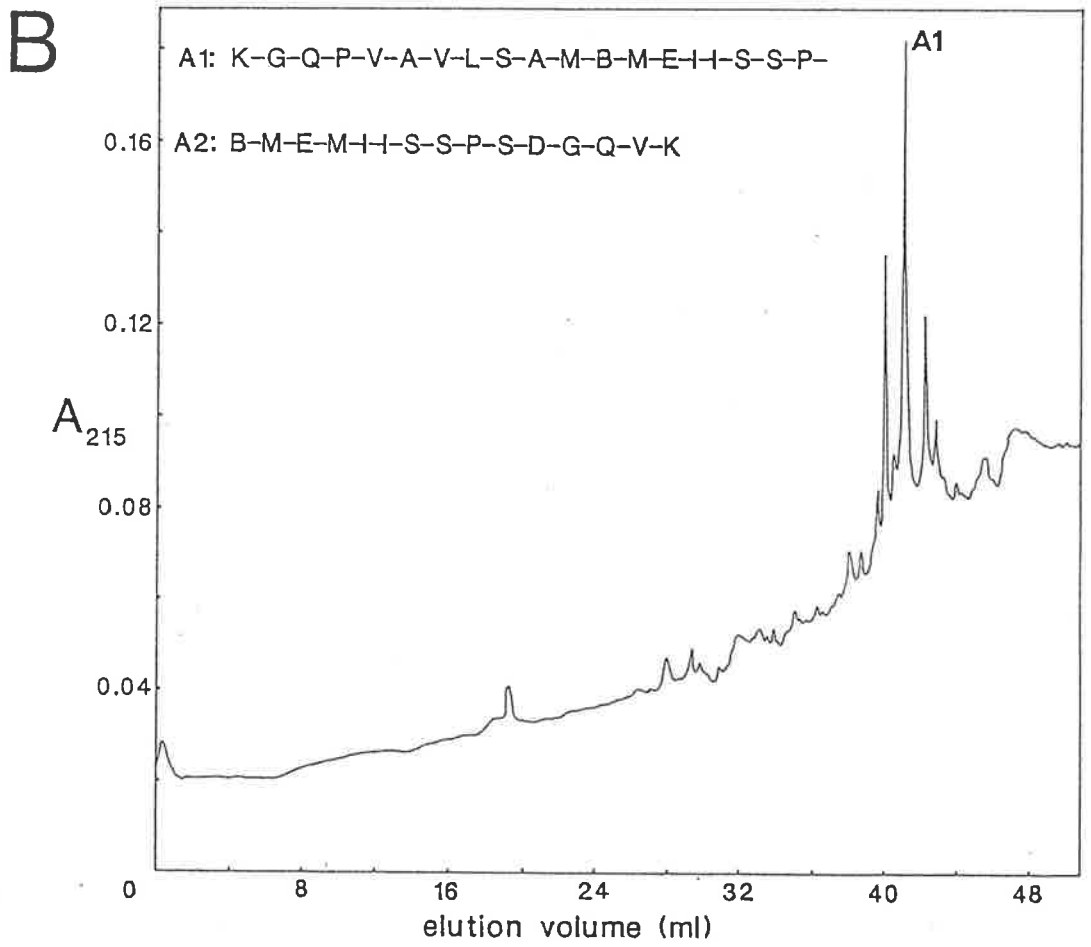
B
A1: K-G-Q-P-V-A-V-L-S-A-M-B-M-E-I-I-S-S-P-
A2: B-M-E-M-I-I-S-S-P-S-D-G-Q-V-K
A1
0.16
0.12
A_{215}
0.08
0.04
0
8
16
24
32
40
48
elution volume (ml)

4.2.6 Isolation of a Yeast Pyruvate Carboxylase Gene Fragment

A biotin carboxylase specific 14-mer probe (Freytag and Collier, 1984) was used to screen a library of genomic fragments in the vector YEp24 (Morris *et al*, 1987). Five positive clones with inserts ranging in size from 1.4 kb to 11 kb were obtained by screening 5 000 recombinants. Restriction mapping and 14-mer probed Southerns revealed that three of the clones contained inserts derived from the same region of the yeast genome (Morris *et al*, 1987). Probe-positive Eco RI fragments of these clones were then subcloned into pUC19. When these three subclones were used in Northern analysis of yeast poly(A)$^+$ mRNA only one subclone hybridised to a single mRNA species of about the right size to encode pyruvate carboxylase and comparable with the 4.2 kb mRNA species detected in rat liver extracts by a human pyruvate carboxylase cDNA clone.

The nucleotide sequence of this clone was determined by subcloning appropriate restriction fragments into M13mp19 followed by sequencing using the dideoxynucleotide chain termination method (Sanger *et al*, 1977). Figure 4.6 shows the identical match between the amino acid sequence obtained by peptide sequencing and the inferred protein sequence of the yeast genomic DNA clone isolated using the biotin carboxylase-specific oligomer (Morris *et al.* 1987).

4.3 DISCUSSION

The growth pattern of the *pyc* mutant on minimal medium supplemented by various carbon sources differed from that of the wild type yeast in a way consistent with a lack of pyruvate carboxylase activity (Wills and Melham, 1985). However, the results presented here clearly demonstrated a normal level of activity of this enzyme in the *pyc* mutant. Furthermore, the results from Western analysis and gel filtration indicated

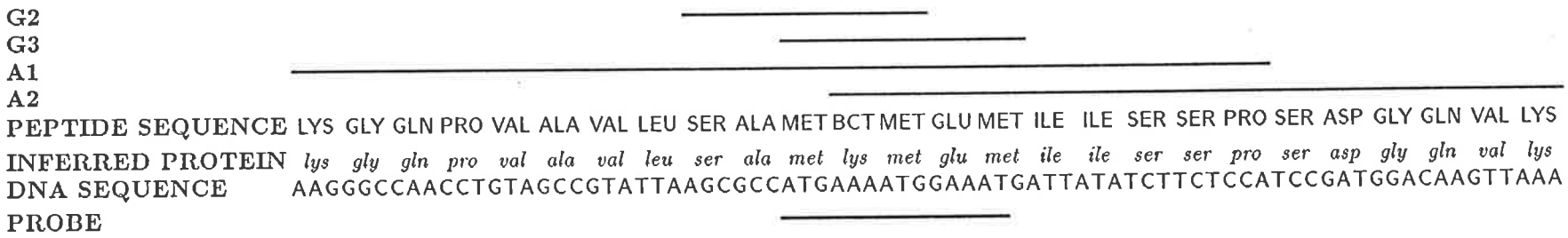

Figure 4.6 **Matching of the biotin-containing tryptic peptide sequence with the yeast pyruvate carboxylase DNA clone.** The full peptide sequence was deduced from overlaps obtained by gel filtration (G2 and G3) and avidin-Sepharose chromatography (A1 and A2). The DNA clone was isolated by screening a yeast genomic DNA library with a biotin carboxylase-specific probe (indicated). The last base of the probe did not match the clone. BCT = biocytin (ϵ-*N*-biotinyl-lysine).

that the size of denatured pyruvate carboxylase subunits as well as native complexes was unaltered in the *pyc* mutant. The most likely reason for the previously reported absence of pyruvate carboxylase (Wills and Melham, 1985; Osmani and Scrutton, 1983) is that enzyme activity was probably limited by the low levels of substrate (1 μM HCO_3^-) and activator (4 μM acetyl-CoA) used. Under these conditions I was unable to detect activity even in the wild type control strain whereas under optimum assay conditions (10 mM HCO_3^- and 250 μM acetyl-CoA) (Rohde *et al*, 1986) I have detected pyruvate carboxylase activity at levels similar to those previously reported (Wallace, 1985; Rohde *et al*, 1986; Haarasilta and Taskinen, 1977) for yeast.

The interpretation of the physiological effect of the *pyc* mutant published previously (Wills and Melham, 1985) depended on an intramitochondrial location for pyruvate carboxylase in *Saccharomyces cerevisiae*. However, we have found that the localisation of pyruvate carboxylase in the *pyc* mutant is identical to that of the wild type and is exclusively cytosolic. In support of this, the results from the Western analysis of the yeast cell extracts did not reveal any precursor or processed forms of the enzyme, which would be expected if pyruvate carboxylase were transported into the mitochondria as is the case with chicken pyruvate carboxylase (Srivastava *et al*, 1983). Thus the results show that the biochemical defect in the *pyc* mutant is neither a deficiency in pyruvate carboxylase nor a difference in compartmentation of this enzyme. However, the aberrant growth characteristics of this mutant may be consistent with a lesion in one of the mitochondrial metabolite transport systems.

In the absence of a *bona fide* pyruvate carboxylase-deficient yeast mutant it was not possible to use genetic complementation to isolate the yeast pyruvate carboxylase gene. However, using the oligonucleotide approach we (Morris *et al*, 1987) were able to isolate and sequence a yeast genomic DNA fragment encoding pyruvate carboxylase. The identity of the cloned gene was confirmed by comparing the encoded protein

with the 26 amino acid sequence of the biotin-containing tryptic peptide isolated from purified yeast pyruvate carboxylase. In addition the purification and sequencing of several other tryptic peptides provided data for checking the DNA sequence obtained later for the full coding region (see Chapter 5).

Chapter 5

Sequence and Domain Structure

5.1 INTRODUCTION

The biotin carboxylases all appear to exhibit considerable sequence similarity around the biotin attachment point (Wood and Barden, 1977) and this is consistent with the hypothesis that they share a common evolutionary origin (Lynen, 1975). Several of these enzymes have substrates and regulators in common, and it has been postulated that these multi-ligand binding proteins arose by fusion events within a pool of ancestral genes (Lynen, 1975). However, until now this hypothesis has not been amenable to testing because of the lack of sequence data.

In the preceding chapter I described the isolation of a small (1.4 kb) yeast pyruvate carboxylase DNA clone by Dr. Phillip Morris and confirmation of its identity by comparison with my peptide sequence data. During the last few months of his time in this laboratory Dr. Morris generated a library of large (13–20 kb) yeast genomic DNA fragments in the vector λEMBL3. From this he was able to isolate a clone containing the entire yeast pyruvate carboxylase gene. He then subcloned a 4 kb Hind III restriction fragment of this yeast DNA insert into the vector M13mp19 for subsequent sequence analysis. This Hind III fragment overlapped the previously sequenced 3′ part of the yeast pyruvate carboxylase gene by 70 bases and extended in the 5′ direction to cover the remaining 3 kb of the coding region. At this point I used the sequential subcloning/sequencing procedure of Dale *et al* (1985) to determine the nucleotide se-

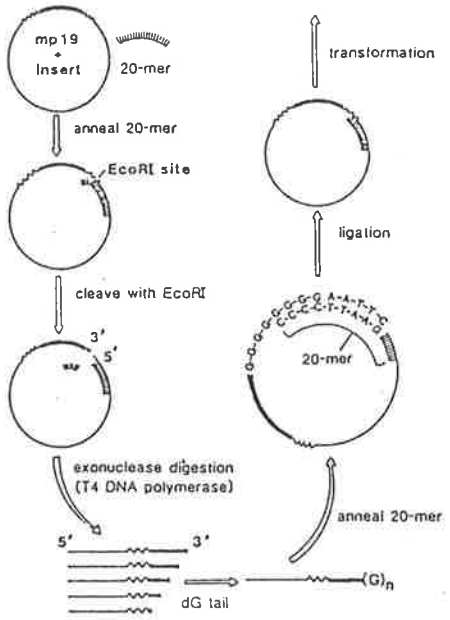

Figure 5.1: **Outline of the single-stranded sequential subcloning procedure for M13mp19 (adapted from Dale *et al*, 1985).** The solid bar represents the insert and the sawtooth line the polylinker region of M13.

quence of the 4 kb Hind III fragment. Briefly, in this method (Figure 5.1) a circular single-stranded M13 recombinant plasmid bearing the insert to be sequenced is cut open specifically at the 3′ end of the insert. The 3′ → 5′ exonuclease activity of T4 DNA polymerase is then used to shorten the insert from the 3′ end. After recircularisation the modified M13/insert construct is amplified by transfection into host bacteria. By the suitable selection of time points during the 3′ → 5′ exonuclease reaction it is possible to obtain a series of subclones differing in insert length such that sequencing by the dideoxynucleotide chain termination method yields overlapping readings. This procedure was applied to both orientations of the 4 kb Hind III yeast pyruvate carboxylase DNA fragment in M13mp19 and the complete nucleotide sequence of the gene determined.

In this chapter the entire primary structure of yeast pyruvate carboxylase is presented. I have used computer-aided sequence analysis to examine areas of similarity with other enzymes to locate potential ligand binding sites and to infer evolutionary relationships among these proteins. This approach is based on the assumption that

sequence conservation reflects some selective pressure to maintain a structural or functional component of a protein. From this it follows that if divergent evolution of a protein has given rise to two proteins which still share a common function such as binding of the same substrate, then conservation of sequence at the binding site would be expected to be higher than in other areas of the polypeptide chain. To complement this approach limited proteolysis was used to define structural domains within the enzyme. This technique has arisen from the observation that regions of polypeptide chain which link different structural domains are often particularly susceptible to proteolysis under native conditions whereas the more tightly folded polypeptide regions within the domains are resistant to cleavage (Hardie and Coggins, 1986). In the absence of crystallographic data limited proteolysis appears to be the most suitable technique for demonstrating the existence of structural domains. Porter (1959) was able to show the existence of the F_{ab} and F_c domains in immunoglobulin G by papain cleavage. Other examples where this approach has been used in the study of domain structure include the works of Perham and Wilkie (1980), Potter and Taylor (1980), Rabinowitz *et al* (1982), Mornet *et al* (1984) and Powers-Lee and Corina (1986).

To further relate function to structure, two analogues of ATP (Figure 5.2) were investigated as possible affinity labels of the ATP-binding site of yeast pyruvate carboxylase. The first of these analogues, oATP, contains a modified ribose moiety, and is the 2′, 3′ dialdehyde derivative obtained by periodate oxidation of ATP. Easterbrook-Smith *et al* (1976) showed that the magnesium complex of this derivative (Mg-oATP) was a competitive inhibitor of sheep pyruvate carboxylase with respect to Mg-ATP. These workers also showed that Mg-oATP could be covalently attached to sheep pyruvate carboxylase by reduction using sodium borohydride with concurrent irreversible inactivation of the enzyme. The second ATP analogue investigated, 8-azido-ATP, contains a modification at the adenine moiety. Ultraviolet irradiation of 8-azido-nucleotide

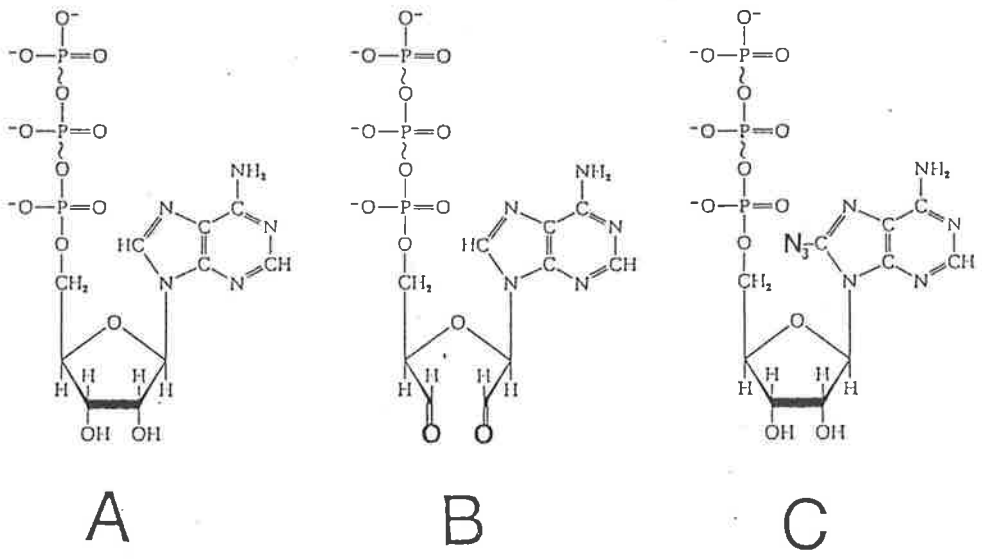

Figure 5.2: **Structures of ATP and the two analogues used to modify yeast pyruvate carboxylase.** A: ATP, B: oATP, C: 8-azido-ATP.

analogues has been used to covalently crosslink these derivatives to proteins and thus identify the ATP-binding sites of a number of enzymes, including *E. coli* recA (Knight and McEntee, 1986), *E. coli* recBCD (Julin and Lehman, 1987) and rabbit muscle fructose-1,6-biphosphate aldolase (Palczewski and Kochman, 1987). In this chapter I have characterised the inactivation of yeast pyruvate carboxylase by oATP and 8-azido-ATP and investigated the use of these analogues to isolate covalently labelled peptides.

Parts of the partial proteolysis and 8-azido-ATP affinity labelling studies were carried out in collaboration with Ms Filomena Occhiodoro during her B.Sc. Honours year and I have attempted to indicate where possible those sections of work in which I had minimal involvement. The data for rat and sheep pyruvate carboxylases shown and discussed for comparison with the yeast enzyme is entirely due to the work of Mr. Grant Booker.

5.2 RESULTS AND DISCUSSION

5.2.1 Isolation of the Yeast Pyruvate Carboxylase Gene

The fragment from the 3′-end of the yeast pyruvate carboxylase gene (Section 4.2.5; Morris *et al*, 1987) was used to screen a λEMBL3 library of yeast genomic fragments derived from a partial Sau 3A digest, as described in Section 2.2.16. Out of 13000 recombinant phage screened (about 15 genome equivalents), 20 positive hybridisation signals were obtained. These clones were mapped with respect to their restriction sites and fragments positive to the existing yeast pyruvate carboxylase probe were identified by Southern analysis (C.P. Morris, personal communication). The orientation of each of the yeast pyruvate carboxylase gene clones was determined by using probes derived from the 5′- and 3′-ends of the existing pyruvate carboxylase clone. This approach identified one λEMBL3 recombinant which contained a centrally located 4kb Hind III fragment (Figure 5.3) which extended from within the previously determined yeast pyruvate carboxylase DNA sequence to beyond the 5′-end of the gene. This fragment was excised from the λ clone and ligated into Hind III-cleaved M13mp19.

5.2.2 Sequencing of the Yeast Pyruvate Carboxylase Gene

The nucleotide sequence of both orientations of the 4kb Hind III yeast DNA insert was determined by the sequential deletion method of Dale *et al* (1985). The sequencing strategy shown in Figure 5.3 indicates the position of the 4kb Hind III fragment relative to the coding region and previously published sequence (Morris *et al*, 1987). The overlapping gel readings obtained by sequencing of the deletion subclones generated by the 5′ → 3′ exonuclease procedure (Dale *et al*, 1985) are shown by the arrowed lines. Figure 5.4 shows the complete nucleotide sequence of the yeast pyruvate carboxylase gene and flanking untranslated DNA. The deduced amino acid sequence obtained by translation of the largest continuous open reading frame was partially confirmed by

Figure 5.3: **Strategy for sequencing the yeast pyruvate carboxylase gene.** A 4kb Hind III fragment derived from a yeast genomic DNA insert in λEMBL3 (top) was cloned into M13mp19 in both orientations and sequenced by the method of Dale *et al* (1985). The probes used to select the 4kb Hind III fragment were derived from a previously sequenced clone (Morris *et al*, 1987). The positions of the restriction sites for Bam H1 (B), Eco R1 (E) and Hind III (H) are shown. The arrows indicate the start point, the direction and length of the sequence overlaps. The size of the sequenced region in nucleotides is indicated by the numbers and the position of the coding region is shown by the bar.

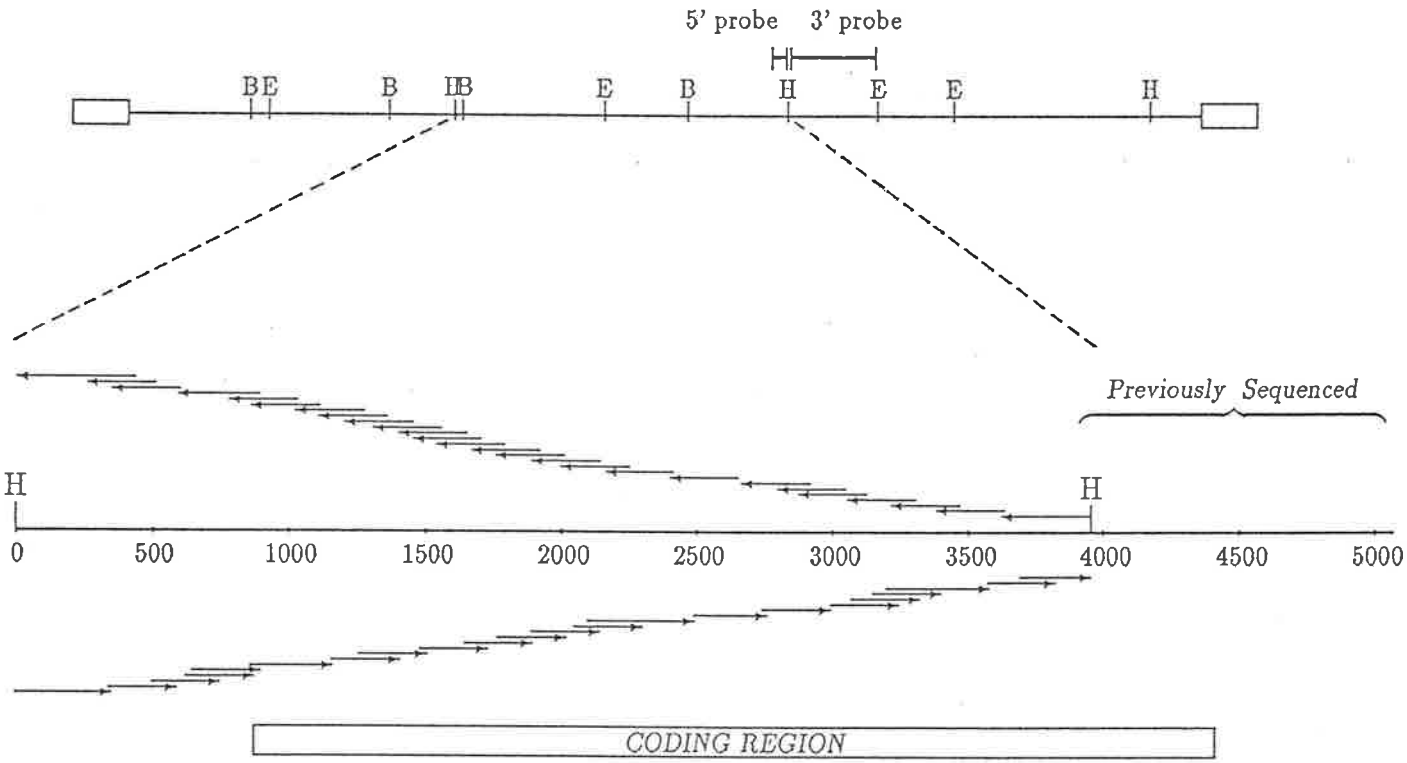
5' probe
3' probe
B E
B
B B
E
B
H
E
E
H
Previously Sequenced
H
H
0
500
1000
1500
2000
2500
3000
3500
4000
4500
5000
CODING REGION

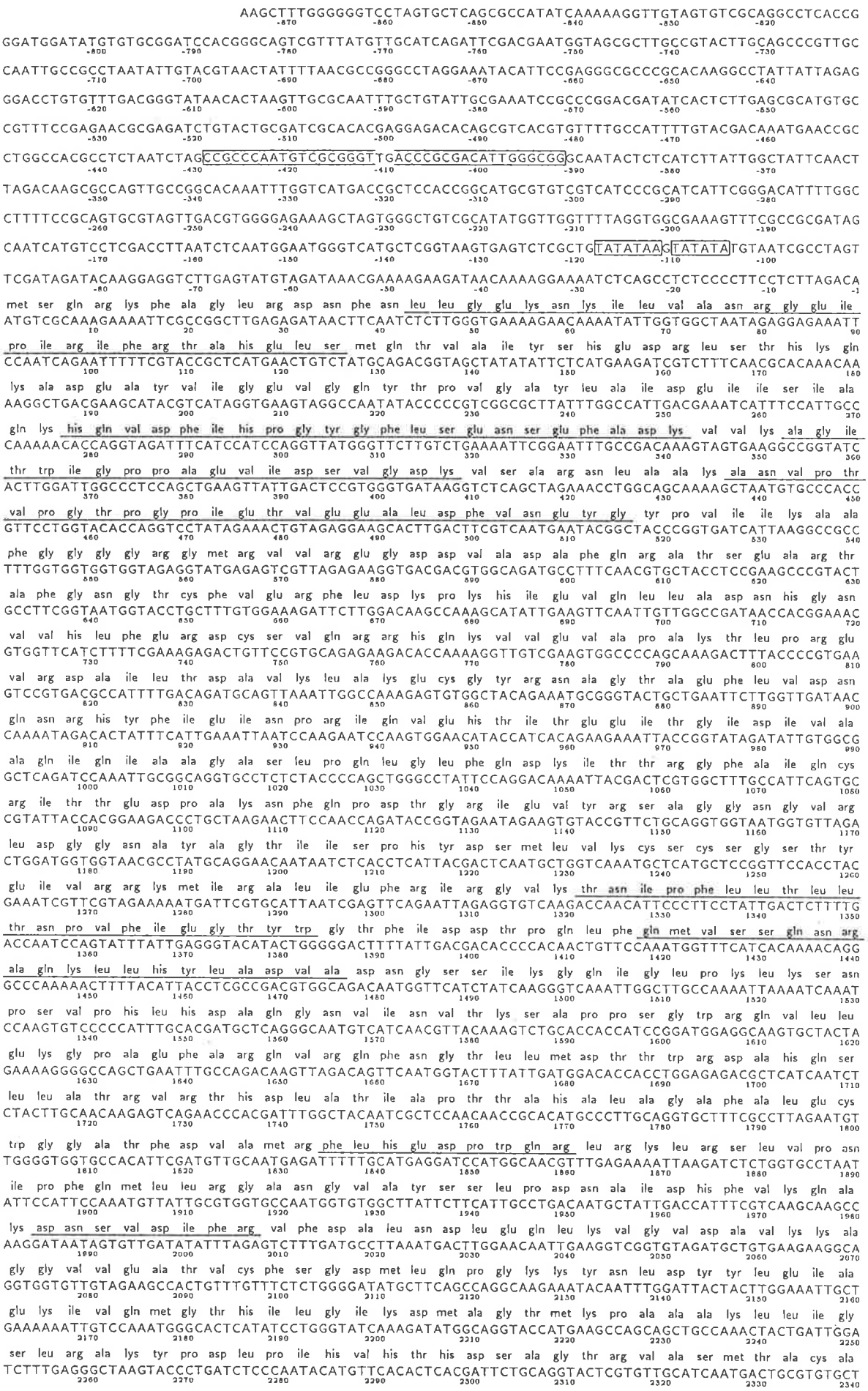

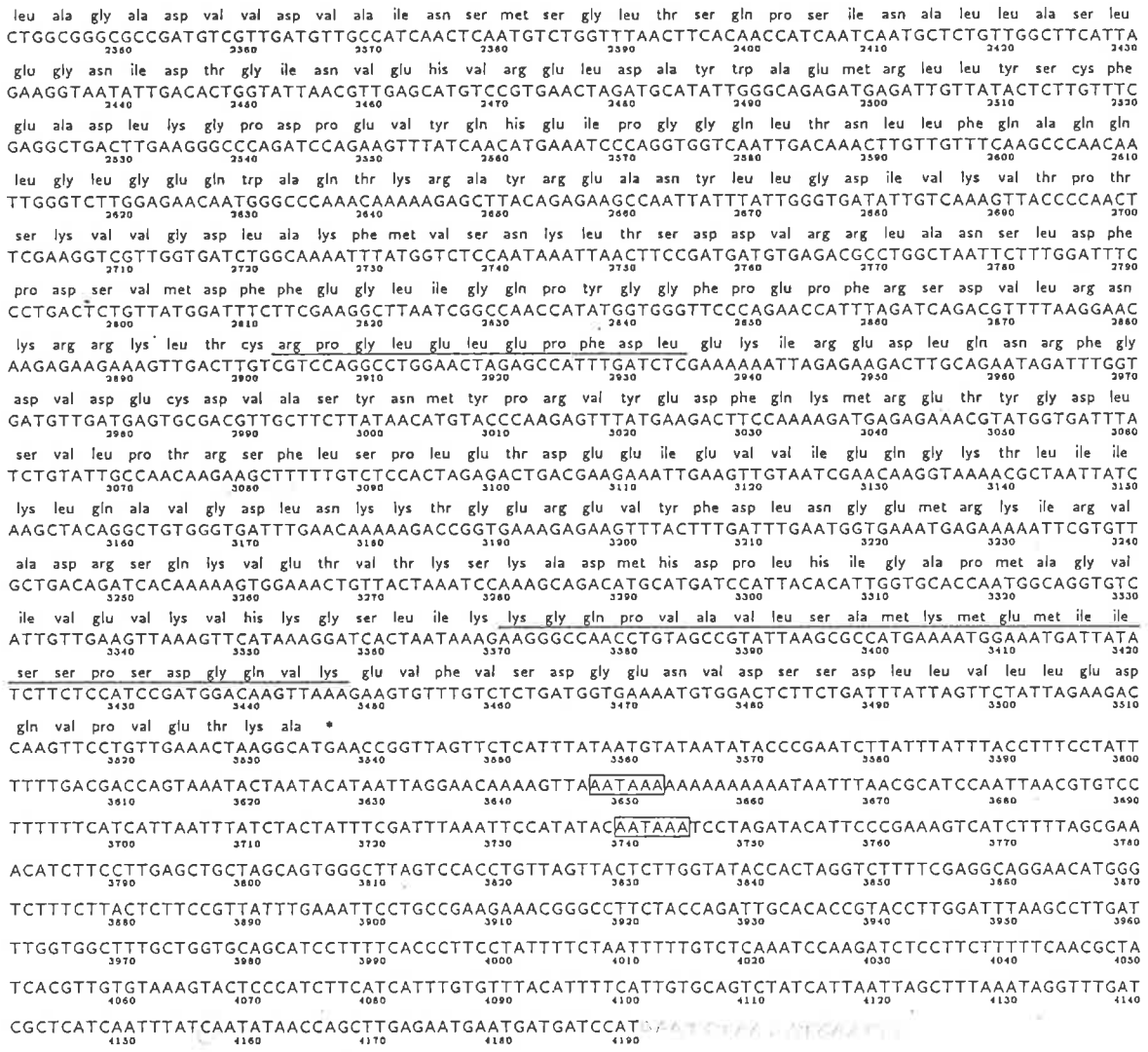

Figure 5.4: **Nucleotide sequence of the pyruvate carboxylase gene and the inferred amino acid sequence.** The sequence of the non-transcribed strand is shown with the inferred amino acid sequence above. Two potential TATA elements are indicated (*boxed*) about 110 bases before the coding region and two putative polyadenylation signals (*boxed*) 3′ to the gene are also shown. The large palindromic sequence at nucleotide -431 (*boxed*) may be involved in gene regulation. Matches of the inferred amino acids with data obtained by peptide sequencing are underlined. The bases are numbered relative to the start codon ATG (A = +1).

peptide sequencing (underlined amino acids in Figure 5.4). The amino-terminus of yeast pyruvate carboxylase is blocked and thus it was not possible to determine directly the start site by Edman degradation sequencing. However, the most N-terminal peptide sequenced corresponded to bases 43-126 and since an in-frame stop codon is present at base -6, the ATG at base 1 was deduced to be the start codon. This assignment is supported by the trinucleotide deviation plot obtained using the programme ANALYSEQ (Staden, 1984). This "local deviation" routine was designed to indicate unusual or similar regions of trinucleotide composition within a nucleotide sequence. "Unusual" is defined to indicate deviation from the composition of a selected section of the sequence (the standard). A common example of the use of this routine is to take a standard from the coding region of a gene and then to scan the rest of the sequence for regions of similar composition. Non-coding regions will often have a different composition, often being A.T rich and having a higher frequency of stop codons. The trinucleotide deviation plot shown in Figure 5.5 was obtained by using as the standard the section of the yeast pyruvate carboxylase gene spanning from base 43 (corresponding to the most N-terminal peptide sequenced) to the stop codon at base 3535. It can be seen from the plot that the coding/noncoding boundary is predicted to occur between bases -34 to +16. The only in-frame start codon within this section is the ATG at +1.

The inferred protein sequence of yeast pyruvate carboxylase codes for a polypeptide of 1178 amino acids with a calculated relative molecular mass of 130100. Table 5.1 shows the codon usage for this gene. Only the codons CGA (Arg) and CGG (Arg) are absent from the sequence. The frequency of optimal codon usage (Ikemura, 1982) was calculated to be 0.65, a value typical of a moderately expressed yeast gene (Nyunoya and Lusty, 1984). This is consistent with the fact that neither of the two potential TATA elements indicated in Figure 5.4 have the "perfect" TATAAA consensus sequence

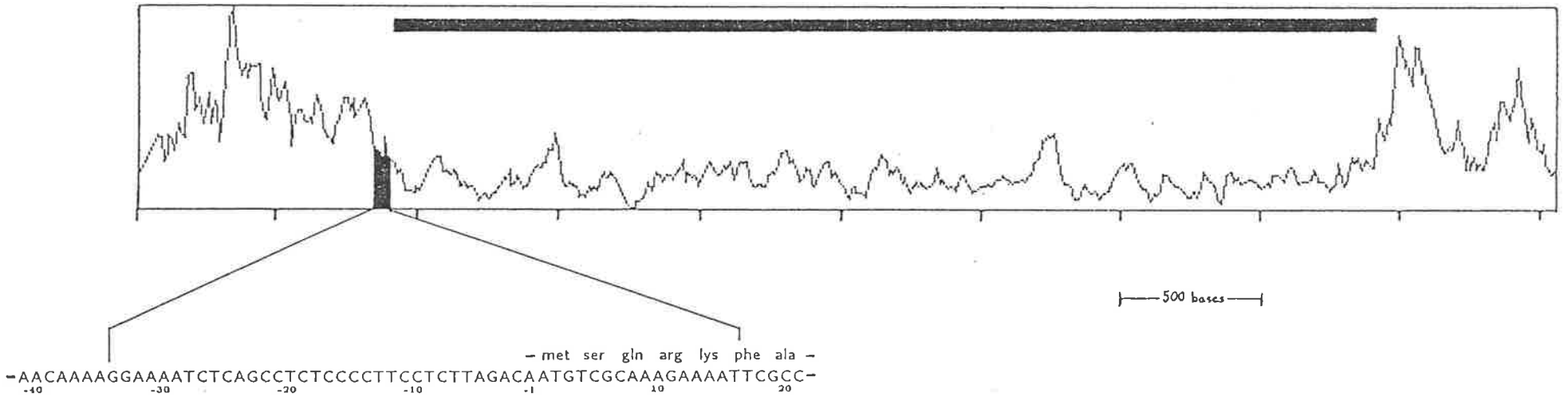

Figure 5.5: **Prediction of the translation start site of the yeast pyruvate carboxylase gene by trinucleotide deviation analysis.** The vertical axis indicates in arbitrary units the relative amount of deviation (increasing towards the top) of the trinucleotide composition of the nucleotide sequence compared to the standard. The standard was defined as that section of the yeast pyruvate carboxylase gene spanning from base 43 (corresponding to the most N-terminal peptide sequenced), to the stop codon at base 3535 (horizontal black bar). An abrupt increase in trinucleotide deviation is seen upstream of base -35 and the expansion of the region -40 to 20 shows that the only in-frame ATG in this area occurs at +1. The inferred amino acid sequence is shown above the nucleotide sequence in the expansion. The distance between vertical markings on the horizontal axis represents 500 bases.

Phe	TTT	20	Ser	TCT	25	Tyr	TAT	14	Cys	TGT	7
Phe	TTC	27	Ser	TCC	11	Tyr	TAC	17	Cys	TGC	5
Leu	TTA	22	Ser	TCA	18	Term[a]	TAA	0	Term	TGA	1
Leu	TTG	41	Ser	TCG	3	Term	TAG	0	Trp	TGG	8
Leu	CTT	9	Pro	CCT	11	His	CAT	19	Arg	CGT	17
Leu	CTC	4	Pro	CCC	6	His	CAC	10	Arg	CGC	1
Leu	CTA	14	Pro	CCA	37	Gln	CAA	39	Arg	CGA	0
Leu	CTG	14	Pro	CCG	1	Gln	CAG	12	Arg	CGG	0
Ile	ATT	39	Thr	ACT	23	Asn	AAT	29	Ser	AGT	2
Ile	ATC	22	Thr	ACC	20	Asn	AAC	17	Ser	AGC	2
Ile	ATA	11	Thr	ACA	13	Lys	AAA	34	Arg	AGA	44
Met	ATG	26	Thr	ACG	6	Lys	AAG	32	Arg	AGG	4
Val	GTT	41	Ala	GCT	33	Asp	GAT	44	Gly	GGT	59
Val	GTC	23	Ala	GCC	35	Asp	GAC	34	Gly	GGC	18
Val	GTA	12	Ala	GCA	29	Glu	GAA	62	Gly	GGA	8
Val	GTG	23	Ala	GCG	5	Glu	GAG	11	Gly	GGG	5

Table 5.1 **Codon usage in the yeast pyruvate carboxylase gene.** The figures denote the number of occurrences of the particular codon within the gene sequence (total of 1178 codons). [a]Term, termination codon.

(Struhl, 1987). A 38 base pair sequence with dyad symmetry is indicated at nucleotide -431. The function of this is unknown at this stage but upstream palindromic sequences often serve as recognition sites for the binding of regulatory proteins. Two possible polyadenylation signals are indicated at nucleotides 3647 and 3739. The predicted size of the messenger RNA assuming the above assignments is just under 4 kilobases, consistent with Northern blot results (Morris *et al*, 1987).

5.2.3 Amino Acid Homology

When several databases (GENBANK version 52, EMBL version 7, NBRF version 14, NEWAT) were searched for proteins showing sequence similarity to yeast pyruvate carboxylase, three groups of enzymes were obtained: biotin carboxylases; lipoamide transferases; carbamyl phosphate synthetases. The degree of similarity with each of these proteins was quantified by calculation of the following scores:

I - This is the percentage of amino acids which are *identical* in the given alignment. Inserted gaps were counted as nonidentical amino acids.

Z - This score, calculated by the programme SEQDP (Needleman and Wunsch, 1970), is based on the mutation rate data of Dayhoff *et al* (1978) and takes into account *conservative* changes. The Z score represents the number of standard deviations greater than random sequence homology between sequences using 20 random sequences of the same amino acid composition as the data. A value of $Z \geq 3$, corresponding to a probability of ≤ 0.001 that the aligned sequences are homologous by chance, is considered significant.

5.2.4 The Biotinyl Carrier

The extreme conservation of sequence among the biotin enzymes in the region surrounding the biocytin residue (Figure 5.6) has been extensively discussed in numerous reports (Rylatt *et al*, 1977; Wood and Barden, 1977; Lamhonwah *et al*, 1987; Cassady, 1987; Samols *et al*, 1988). The selective pressure to maintain this sequence homology has two origins: structural requirements imposed by the similar catalytic mechanisms of the biotin enzymes, and structural requirements of these proteins as substrates of the holoenzyme synthetases which catalyse the attachment of biotin.

All of the biotin enzymes contain the tetrapeptide Ala-Met-Bct[1]-Met except chicken acetyl-CoA carboxylase (Takai *et al*, 1987) which has a valine in place of the alanine. Using oligonucleotide-directed mutagenesis Paranjape *et al* (1988) have shown that the two methionine residues of this tetrapeptide are not essential for biotinylation but are necessary for the carboxylation reaction.

With the exception of yeast pyruvate carboxylase, the tomato biotin enzyme-like protein and chicken acetyl-CoA carboxylase, all of the biotin enzymes sequenced have the biocytin residue located 35 amino acids from the carboxyl terminus. Murtif and Samols (1987) have shown that this distance is not critical for biotinylation but that *E. coli* biotin holoenzyme synthetase requires a hydrophobic amino acid in its substrate

[1]Bct = biocytin

Figure 5.6: **Sequence similarities around the prosthetic group attachment point in the biotin enzymes and the lipoamide transferases.** Gaps inserted in the alignments are represented by dashes. The asterisks denote the carboxyl termini of proteins. The attachment points of biotin (△) and lipoic acid (▼) are indicated. Since it is obvious that the sequences are highly similar in this region as discussed for the biotin enzymes in numerous other reports (Rylatt *et al*, 1977; Wood and Barden, 1977; Lamhonwah *et al*, 1987; Cassady, 1987; Samols *et al*, 1988), only the major features have been indicated here (boxed):

1 Two glycine residues are conserved in all but one of the enzymes shown.

2 The conserved tetrapeptide in the biotin enzymes.

3 All of the enzymes except chicken acetyl-CoA carboxylase contain a hydrophobic amino acid 34 residues C-terminal to the prosthetic group attachment point. In the biotin enzymes this residue has been shown to be critical for biotinylation (Murtif and Samols, 1987).

Yeast PDH - yeast pyruvate dehydrogenase (R. Perham, personal communication).
Bs PDH - *Bacillus stearothermophilus* pyruvate dehydrogenase (R. Perham, personal communication).
Ec ODH - *E. coli* 2-oxo-glutarate dehydrogenase (R. Perham, personal communication).
Ec PDH1–3 - *E.coli* pyruvate dehydrogenase lipoyl segments 1 to 3 (Guest *et al*, 1985).
Yeast PC - yeast pyruvate carboxylase.
Rat PC - rat pyruvate carboxylase (Cassady, 1988).
Human PC - human pyruvate carboxylase (Freytag and Collier, 1984).
Chick PC and sheep PC - chicken and sheep pyruvate carboxylases (Rylatt *et al*, 1977).
Human PCC - human propionyl-CoA carboxylase (Lamhonwah *et al*, 1987).
Chick PCC and sheep PCC - chicken and sheep propionyl-CoA carboxylases (author's work in collaboration with Ms Alison Whittle, see Section 4.2.5).
Ps TC - *Propionibacterium shermanii* transcarboxylase (Maloy *et al*, 1979).
Kp OD - *Klebsiella pneumoniae* oxaloacetate decarboxylase (Oesterhelt, personal communication).
EACC - *E. coli* acetyl-CoA carboxylase (Sutton *et al*, 1977).
CACC - chicken acetyl-CoA carboxylase (Takai *et al*, 1987).
Tom BC - putative biotin carboxylase from tomato (Hoffman *et al*, 1987).

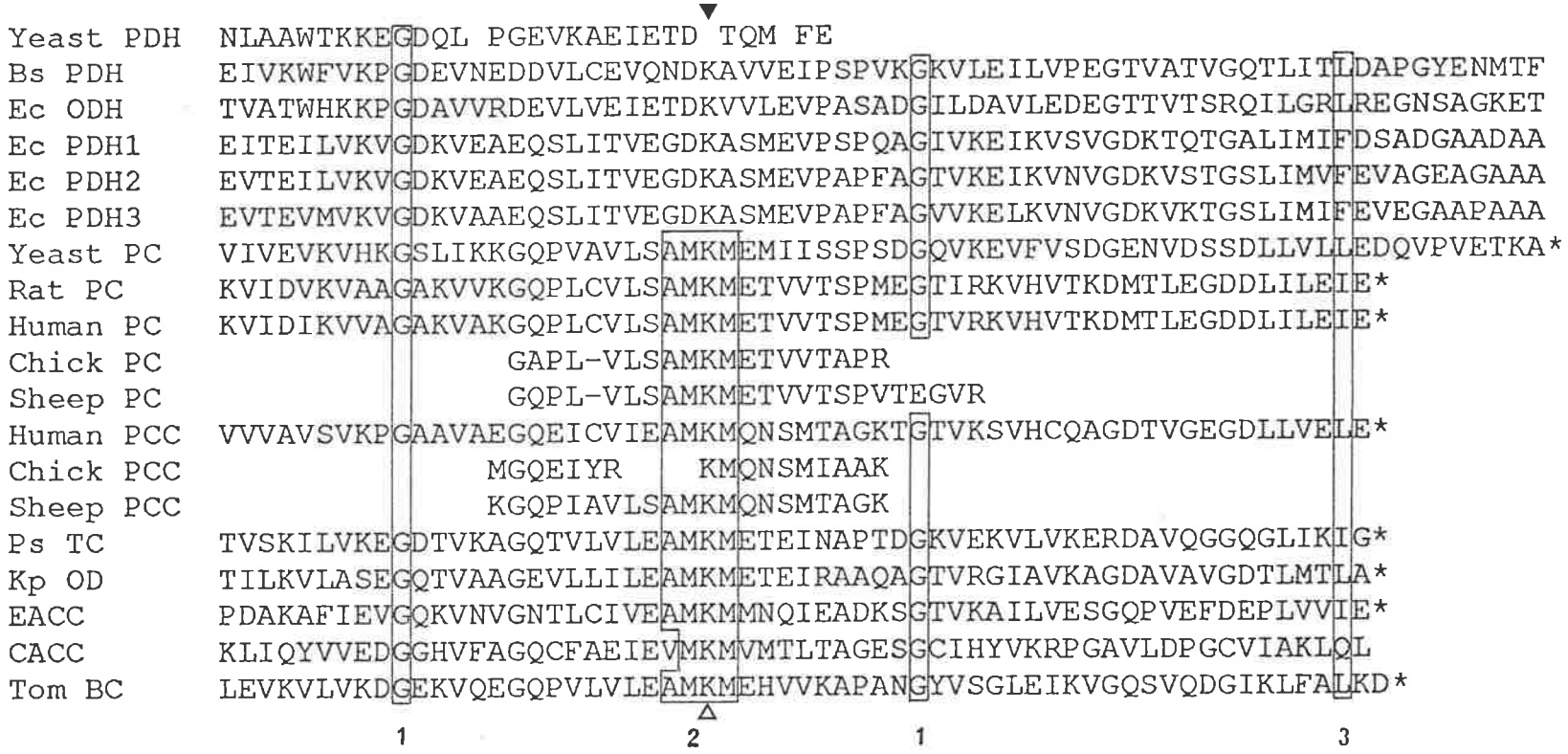
Yeast PDH NLAAWTKKEGDQL PGEVKAEIETD TQM FE
Bs PDH EIVKWFVKPGDEVNEDDVLCEVQNDKAVVEIPSPVKGKVLEILVPEGTVATVGQTLITLDAPGYENMTF
Ec ODH TVATWHKKPGDAVVRDEVLVEIETDKVVLEVPASADGILDAVLEDEGTTVTSRQILGRLREGNSAGKET
Ec PDH1 EITEILVKVGDKVEAEQSLITVEGDKASMEVPSPQAGIVKEIKVSVGDKTQTGALIMIFDSADGAADAA
Ec PDH2 EVTEILVKVGDKVEAEQSLITVEGDKASMEVPAPFAGTVKEIKVNVGDKVSTGSLIMVFEVAGEAGAAA
Ec PDH3 EVTEVMVKVGDKVAAEQSLITVEGDKASMEVPAPFAGVVKELKVNVGDKVKTGSLIMIFEVEGAAPAAA
Yeast PC VIVEVKVHKGSLIKKGQPVAVLSAMKMEMIISSPSDGQVKEVFVSDGENVDSSDLLVLLEDQVPVETKA*
Rat PC KVIDVKVAAGAKVVKGQPLCVLSAMKMETVVTSPMEGTIRKVHVTKDMTLEGDDLILEIE*
Human PC KVIDIKVVAGAKVAKGQPLCVLSAMKMETVVTSPMEGTVRKVHVTKDMTLEGDDLILEIE*
Chick PC GAPL-VLSAMKMETVVTAPR
Sheep PC GQPL-VLSAMKMETVVTSPVTEGVR
Human PCC VVVAVSVKPGAAVAEGQEICVIEAMKMQNSMTAGKTGTVKSVHCQAGDTVGEGDLLVELE*
Chick PCC MGQEIYR KMQNSMIAAK
Sheep PCC KGQPIAVLSAMKMQNSMTAGK
Ps TC TVSKILVKEGDTVKAGQTVLVLEAMKMETEINAPTDGKVEKVLVKERDAVQGGQGLIKIG*
Kp OD TILKVLASEGQTVAAGEVLLILEAMKMETEIRAAQAGTVRGIAVKAGDAVAVGDTLMTLA*
EACC PDAKAFIEVGQKVNVGNTLCIVEAMKMMNQIEADKSGTVKAILVESGQPVEFDEPLVVIE*
CACC KLIQYVVEDGGHVFAGQCFAEIEVMKMVMTLTAGESGCIHYVKRPGAVLDPGCVIAKLQL
Tom BC LEVKVLVKDGEKVQEGQPVLVLEAMKMEHVVKAPANGYVSGLEIKVGQSVQDGIKLFALKD*
1
2
1
3

polypeptide 34 residues C-terminal to the attachment point of the prosthetic group.

In addition to the conservation of sequence within the biotin enzyme family there is high sequence similarity of this C-terminal portion of yeast pyruvate carboxylase with the area surrounding the lipoyl-lysine of lipoamide transferases. For example, the acetyl-transferase (E2) subunit of the *E.coli* pyruvate dehydrogenase complex (Guest *et al*, 1985) contains three tandemly connected lipoylated segments at the N-terminus and residues 200–287 (Ec PDH3 of Figure 5.6) show 20% amino acid identity with the last 90 residues of yeast pyruvate carboxylase. The Z score for this alignment is 7.6, indicating a very high degree of homology. It is interesting to note that the biotinyl-lysine of pyruvate carboxylase is aligned with the lipoyl-lysine of dihydrolipoamide acetyltransferase. This conservation of sequence may reflect the similar functions of biotin and lipoic acid in acting as oscillating carriers between active sites. Alternatively the mechanisms of biotin addition and lipoic acid addition by the relevant holoenzyme synthetases may be sufficiently close to impose the same structural requirements near the attachment site. Particularly noteworthy in this respect is the conservation of two glycine residues, one 16 residues N-terminal to the prosthetic group, and the other 11 residues C-terminal to the prosthetic group, in all but one of the known sequences of the biotin and lipoic acid containing enzymes (Figure 5.6).

As in the case of biotinylation, a hydrophobic amino acid 34 residues C-terminal to the modified lysine may also play a critical role in lipoylation since all three lipoyl-binding regions of *E. coli* acetyltransferase contain a phenylalanine at this position and *E. coli* succinyltransferase (lipoyl subunit of 2-oxo-glutarate dehydrogenase) has a leucine at this site.

5.2.5 The Ketoacid Binding Site

It has been proposed on the basis of similarities in mechanism that the biotin enzymes share a common evolutionary origin (Lynen, 1975). It is not unreasonable to expect

therefore that functionally important residues such as common substrate binding sites would be conserved among them. This prediction appears to be supported by the fact that the N-terminal portion of the 5S subunit of transcarboxylase (D. Samols, personal communication) as well as the biotin-containing subunit of oxaloacetate decarboxylase (D. Oesterhelt, personal communication) show striking sequence similarity (I=32%, Z=39.3; I=37%, Z=41.6 respectively) to residues 550-900 of yeast pyruvate carboxylase (Figure 5.7). All three proteins are known to bind pyruvate and divalent metal ions.

5.2.6 The ATP/HCO_3 Binding Site

In Figure 5.8A extensive sequence homology can be noted between part of the α subunit of human propionyl-CoA carboxylase (Lamhonwah *et al*, 1987), a portion of chicken acetyl-CoA carboxylase (Takai *et al*, 1987) and residues 350-470 of yeast pyruvate carboxylase (34%, 18.0 and 28%, 11.5 respectively). These residues probably form part of the domain which catalyses the ATP-dependent carboxylation of biotin since all three of these polypeptides bind bicarbonate and ATP. Acetyl-CoA carboxylase and pyruvate carboxylase both bind acetyl-CoA but the work of Haase *et al* (1982) indicates that the CoA-ester binding site of propionyl-CoA carboxylase is located on the β subunit. This assignment is further supported by the high degree of sequence similarity between the β subunit of rat propionyl-CoA carboxylase (Kraus *et al*, 1986) and the 12S subunit of transcarboxylase (D. Samols, personal communication), which has been shown to be the CoA-ester binding subunit (Wood and Kumar, 1985). Neither the 12S subunit of transcarboxylase nor the β subunit of rat propionyl-CoA carboxylase show appreciable sequence similarity to yeast pyruvate carboxylase, but this may reflect the fact that the former two proteins bind CoA-esters as substrates whereas the latter binds acetyl-CoA as an allosteric ligand. Thus, at this stage it is not possible to assign the acetyl-CoA binding site to any particular region of the yeast pyruvate carboxylase sequence.

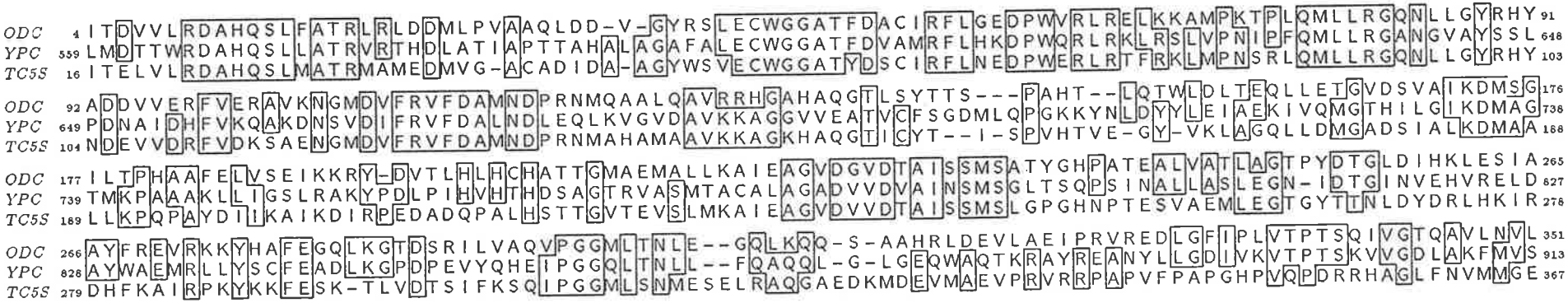

Figure 5.7: **Identification of the pyruvate-binding region of pyruvate carboxylase by sequence homology.** The amino acid sequences of the oxaloacetate decarboxylase α subunit (ODC) from *Klebsiella pneumoniae* (Oesterhelt, personal communication), yeast pyruvate carboxylase (YPC) and the transcarboxylase 5S subunit (TC5S) from *Propionibacterium shermanii* (Samols, personal communication) were aligned for maximum homology by the programme SEQHP. All of these proteins bind pyruvate and divalent metal ions. Identical residues are boxed and inserted gaps are represented by dashes.

Figure 5.8: **Identification of the ATP-binding regions of pyruvate carboxylase by sequence homology.** All of the compared proteins shown bind ATP. The sequences were aligned for maximum homology with the programme SEQHP. Identical residues are boxed and gaps inserted by the programme are represented by dashes. Amino acids are numbered relative to the amino-terminus (+1) of the protein where complete sequence data is available. Where only partial sequence data is available (acetyl-CoA carboxylase and propionyl-CoA carboxylase) the most N-terminal amino acid of the particular sequence fragment is numbered +1.

A Comparison of yeast pyruvate carboxylase (YPC) with chicken acetyl-CoA carboxylase (ACC) (Takai *et al*, 1987) and human propionyl-CoA carboxylase α subunit (PCC) (Lamhonwah *et al*, 1987).

B Comparison of yeast pyruvate carboxylase (YPC) with the N-terminal ATP-binding domains of rat carbamyl phosphate synthetase (RCPS) (Nyunoya *et al*, 1985) and yeast carbamyl phosphate synthetase (YCPS) (Lusty *et al*, 1983).

C Comparison of yeast pyruvate carboxylase (YPC) with the C-terminal ATP-binding domains of rat carbamyl phosphate synthetase (RCPS) and yeast carbamyl phosphate synthetase (YCPS).

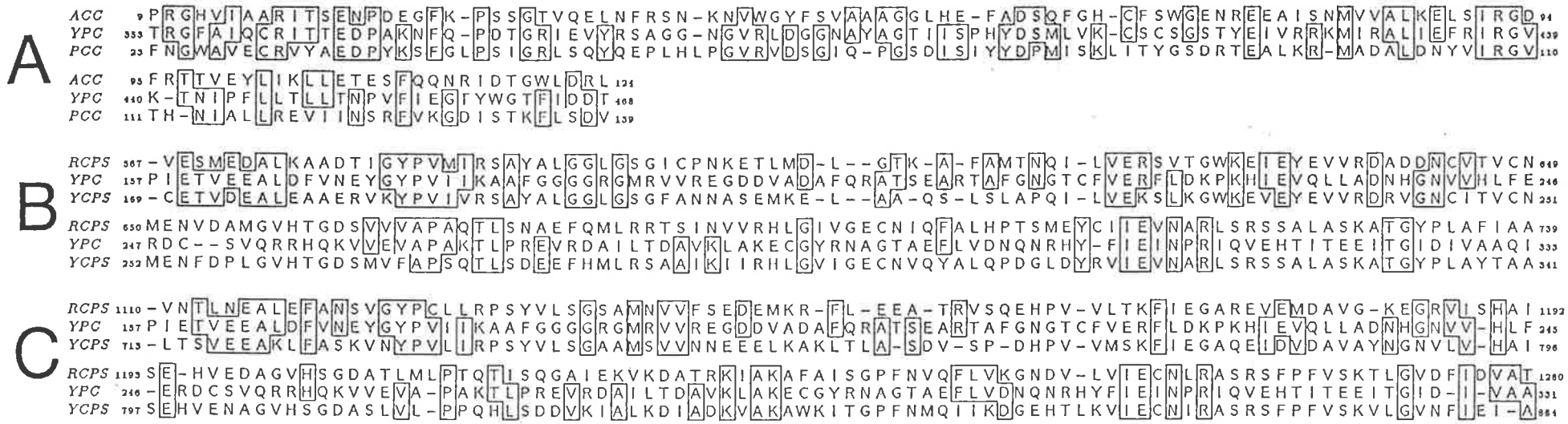
A
ACC 9 P R G H V I A A R I T S E N P D E G F K - P S S G T V Q E L N F R S N - K N V W G Y F S V A A A G G L H E - F A D S Q F G H - C F S W G E N R E E A I S N M V V A L K E L S I R G D 94
YPC 353 T R G F A I Q C R I T T E D P A K N F Q - P D T G R I E V Y R S A G G - N G V R L D G G N A Y A G T I I S P H Y D S M L V K - C S C S G S T Y E I V R R K M I R A L I E F R I R G V 439
PCC 23 F N G W A V E C R V Y A E D P Y K S F G L P S I G R L S Q Y Q E P L H L P G V R V D S G I Q - P G S D I S I Y Y D P M I S K L I T Y G S D R T E A L K R - M A D A L D N Y V I R G V 110
ACC 95 F R T T V E Y L I K L L E T E S F Q Q N R I D T G W L D R L 125
YPC 440 K - T N I P F L L T L L T N P V F I E G T Y W G T F I D D T 468
PCC 111 T H - N I A L L R E V I I N S R F V K G D I S T K F L S D V 139
B
RCPS 567 - V E S M E D A L K A A D T I G Y P V M I R S A Y A L G G L G S G I C P N K E T L M D - L - - G T K - A - F A M T N Q I - L V E R S V T G W K E I E Y E V V R D A D D N C V T V C N 649
YPC 157 P I E T V E E A L D F V N E Y G Y P V I I K A A F G G G G R G M R V V R E G D D V A D A F Q R A T S E A R T A F G N G T C F V E R F L D K P K H I E V Q L L A D N H G N V V H L F E 246
YCPS 169 - C E T V D E A L E A A E R V K Y P V I V R S A Y A L G G L G S G F A N N A S E M K E - L - - A A - Q S - L S L A P Q I - L V E K S L K G W K E V E Y E V V R D R V G N C I T V C N 251
RCPS 650 M E N V D A M G V H T G D S V V V A P A Q T L S N A E F Q M L R R T S I N V V R H L G I V G E C N I Q F A L H P T S M E Y C I I E V N A R L S R S S A L A S K A T G Y P L A F I A A 739
YPC 247 R D C - - S V Q R R H Q K V V E V A P A K T L P R E V R D A I L T D A V K L A K E C G Y R N A G T A E F L V D N Q N R H Y - F I E I N P R I Q V E H T I T E E I T G I D I V A A Q I 333
YCPS 252 M E N F D P L G V H T G D S M V F A P S Q T L S D E E F H M L R S A A I K I I R H L G V I G E C N V Q Y A L Q P D G L D Y R V I E V N A R L S R S S A L A S K A T G Y P L A Y T A A 341
C
RCPS 1110 - V N T L N E A L E F A N S V G Y P C L L R P S Y V L S G S A M N V V F S E D E M K R - F L - E E A - T R V S Q E H P V - V L T K F I E G A R E V E M D A V G - K E G R V I S H A I 1192
YPC 157 P I E T V E E A L D F V N E Y G Y P V I I K A A F G G G G R G M R V V R E G D D V A D A F Q R A T S E A R T A F G N G T C F V E R F L D K P K H I E V Q L L A D N H G N V V - H L F 245
YCPS 713 - L T S V E E A K L F A S K V N Y P V L I R P S Y V L S G A A M S V V N N E E E L K A K L T L A - S D V - S P - D H P V - V M S K F I E G A Q E I D V D A V A Y N G N V L V - H A I 796
RCPS 1193 S E - H V E D A G V H S G D A T L M L P T Q T I S Q G A I E K V K D A T R K I A K A F A F A I S G P F N V Q F L V K G N D V - L V I E C N L R A S R S F P F V S K T L G V D F I D V A T 1280
YPC 246 - E R D C S V Q R R H Q K V V E V A - P A K T L P R E V R D A I L T D A V K L A K E C G Y R N A G T A E F L V D N Q N R H Y F I E I N P R I Q V E H T I T E E I T G I D - I - V A A 331
YCPS 797 S E H V E N A G V H S G D A S L V L - P P Q H L S D D V K I A L K D I A D K V A K A W K I T G P F N M Q I I K D G E H T L K V I E C N I R A S R S F P F V S K V L G V N F I E I - A 884

Figure 5.8B shows the alignment of yeast pyruvate carboxylase sequence with another class of ATP-binding proteins. In yeast and vertebrates carbamyl phosphate is generated for pyrimidine and arginine synthesis by two separate enzymes. In *E. coli* a single carbamyl phosphate synthetase serves both biosynthetic pathways. The arginine-specific carbamyl phosphate synthetases of rat (Nyunoya *et al*, 1985) and yeast (Lusty *et al*, 1983) as well as the enzyme from *E. coli* (Nyunoya and Lusty, 1983) (not shown) contain two ATP-binding domains. Residues 160-330 of yeast pyruvate carboxylase exhibit striking sequence similarity to the N-terminal **halves** of each of these ATP-binding regions. The I and Z scores obtained for the four alignments shown in Figure 5.8B were: 43% and 12.4 for YPC/RCPS$_{567-739}$; 38% and 8.1 for YPC/YCPS$_{169-341}$; 39% and 14.3 for YPC/RCPS$_{1110-1280}$; 39% and 14.7 for YPC/YCPS$_{713-884}$. Part of this N-terminal "half domain" of carbamyl phosphate synthetase apparently corresponds (Lusty *et al*, 1983) to the glycine-rich loop of the ATP-binding site evident in the crystal structure of porcine adenylate kinase (Fry *et al*, 1986). The corresponding areas of acetyl-CoA carboxylase and propionyl-CoA carboxylase have not been sequenced but from the example of yeast pyruvate carboxylase it appears that the ATP/bicarbonate binding domain of the biotin carboxylases may be composed of two half-sites. Of these the N-terminal half-site appears to share common evolutionary origins with other enzymes, including carbamyl phosphate synthetase and adenylate kinase, whereas the C-terminal half-site appears to be conserved only among the biotin carboxylases. It is interesting to note that carbamyl phosphate has a structure similar to the proposed carboxyphosphate transition state intermediate of pyruvate carboxylase (Wallace *et al*, 1985). Indeed, it has been shown that acetyl-CoA carboxylase from *Escherichia coli* (Polakis *et al*, 1972) and sheep kidney pyruvate carboxylase (Ashman and Keech, 1975) will catalyse phosphoryl transfer from carbamyl phosphate to ADP to form ATP. The observed sequence similarities between pyruvate carboxylase and

carbamyl phosphate synthetase may well reflect mechanistic similarities between the two groups of enzymes.

5.2.7 Gene Fusion

Figure 5.9 shows the various blocks of sequence homology found in yeast pyruvate carboxylase and the proteins mentioned above. These results strongly support the proposal that some multifunctional polypeptides such as pyruvate carboxylase have resulted from gene fusion during evolution. The putative functional units, represented by the regions of homology indicated in Figure 5.9 are dispersed over a range of enzymes sharing some common binding or functional properties.

5.2.8 Structural Mapping by Partial Proteolysis

In an attempt to elucidate the domain structure of yeast pyruvate carboxylase, limited proteolysis of the protein with several different proteases under nondenaturing conditions was performed. The fragmentation patterns observed with yeast pyruvate carboxylase are similar to those of pyruvate carboxylases from sheep, rat and chicken (G. Booker, personal communication), indicating a close structural similarity across species for this enzyme. However the yeast enzyme appears to be more resistant to proteolysis since at the same substrate to protease mass ratio (100) as that used for cleavage of the vertebrate enzymes, little effect was observed on the yeast polypeptide.

Proteolysis time courses of yeast pyruvate carboxylase were conducted at 30°C using a substrate to protease mass ratio of 12.5 (chymotrypsin, thermolysin, proteinase K and endoproteinase Arg-C) and 30 (chymotrypsin, thermolysin, proteinase K and trypsin). Little cleavage was observed with endoproteinase Arg-C (F. Occhiodoro, personal communication) and the fragments obtained with tryptic digestion were degraded rapidly but the patterns obtained using chymotrypsin, thermolysin and proteinase K at either substrate to protease mass ratio were similar, the rate of fragment production

Figure 5.9: **Block diagram showing the relative positions of the homologous regions in the various enzymes compared in the previous figure.** The proteins have been drawn to scale (solid lines) or where only partial sequence is available the dashed boxes represent the sizes corresponding to molecular weight estimates. The left side of each box represents the amino terminus and subunit names are given under the relevant boxes. Homologous regions are represented by shading of the same kind. The areas delineated in the proteins are the biotinyl/lipoyl carrier domain (black), the putative pyruvate binding domain (stippled) and the putative ATP/bicarbonate binding domain (hatching and diagonal lines).
OD = oxaloacetate decarboxylase, α, β and γ subunits (Oesterhelt, personal communication)
ACC = acetyl-CoA carboxylase (Takai *et al*, 1987)
PC = pyruvate carboxylase
PCC = propionyl-CoA carboxylase, α and β subunits (Lamhonwah *et al*, 1987; Lamhonwah *et al*, 1986)
TC = transcarboxylase, 12S, 5S (Samols, personal communication) and 1.3S (Maloy *et al*, 1979) subunits
CPS = carbamyl phosphate synthetase, the small and the large subunits of the yeast enzyme (Nyunoya and Lusty, 1984; Lusty *et al*, 1983) and the rat enzyme (Nyunoya *et al*, 1985)
PDH = pyruvate dehydrogenase, the E1, E2 and E3 subunits (Guest *et al*, 1985).

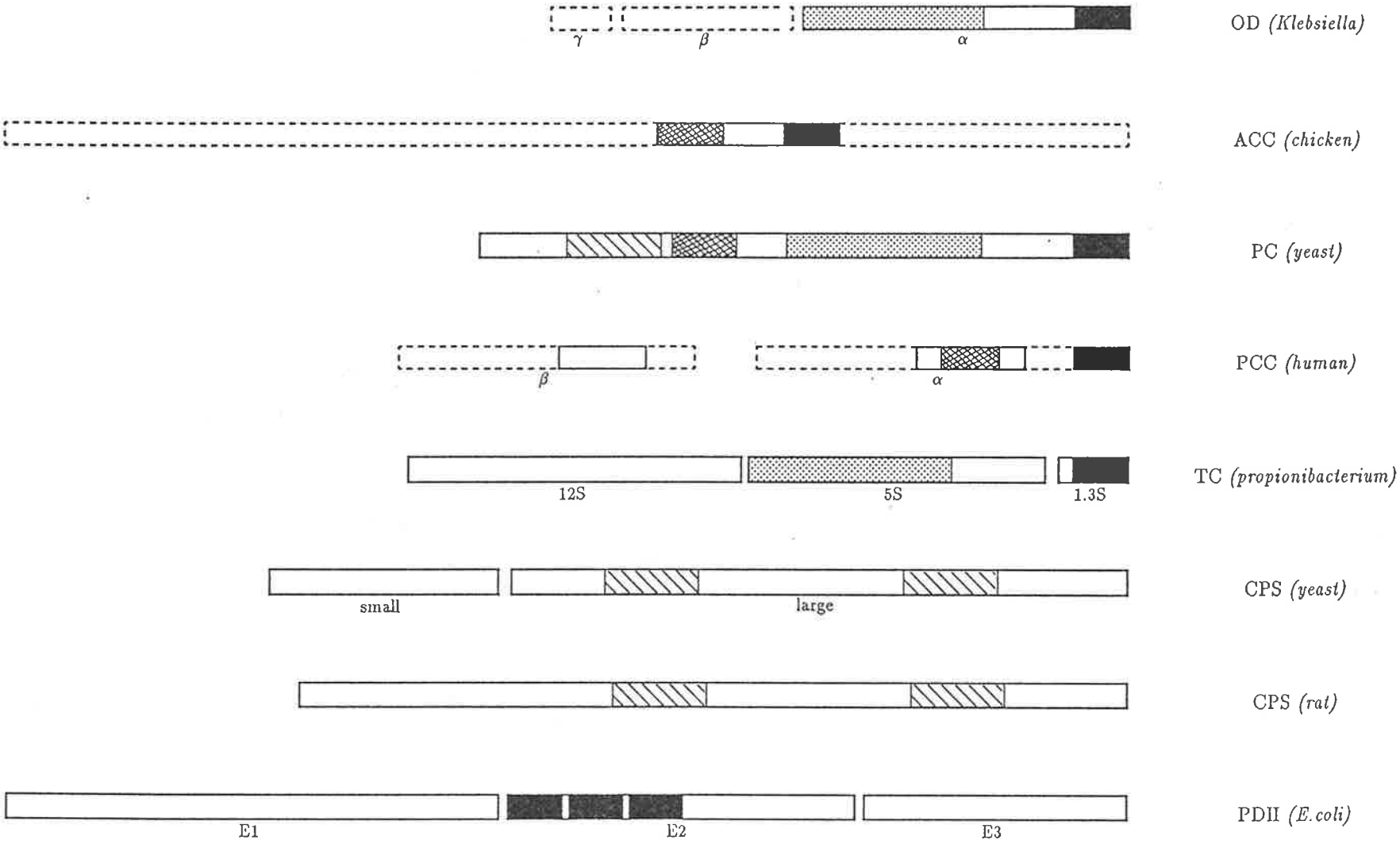
γ
β
α
OD (Klebsiella)
ACC (chicken)
PC (yeast)
β
α
PCC (human)
12S
5S
1.3S
TC (propionibacterium)
small
large
CPS (yeast)
CPS (rat)
E1
E2
E3
PDII (E.coli)

being slightly higher at the lower ratio. The time course of digestion of yeast pyruvate carboxylase with chymotrypsin is shown in Figure 5.10A. Figure 5.11 shows the isolation of the major chymotryptic fragment by Superose 12 gel filtration. An identical procedure was followed to isolate the fragments from thermolysin and proteinase K digestion (F. Occhiodoro, personal communication) except that gel filtration was performed on a TSK 3000 column instead of Superose 12. The N-terminal sequences of these fragments were then determined by automated Edman degradation. By performing a gel retardation assay with avidin (as described in the 2.2.17) it was possible to detect the presence or absence of biotin in fragments. Since the biotin moiety is positioned 39 residues from the carboxyl terminus of the intact protein (Section 5.2.4), this data enables the approximate localisation of the C-termini of the proteolytic fragments.

Chymotryptic cleavage was found to have occurred in the region between the putative pyruvate-binding domain and the putative ATP-binding domain to form a large C-terminal biotin-containing fragment (Figure 5.12). The remaining N-terminal portion of the enzyme was apparently degraded rapidly by the protease. Comparison of the N-terminal amino acid sequences of the large biotin-containing chymotryptic fragments of chicken (Khew-Goodall, 1985), sheep and rat (G. Booker, personal communication) pyruvate carboxylases reveals a high degree of sequence similarity near the cleavage point (Figure 5.11). Like the yeast enzyme, the N-terminal chymotryptic fragments of sheep and chicken pyruvate carboxylases show low stability to digestion after the initial cleavage, but in rat pyruvate carboxylase this N-terminal product appears to be stable and resistant to further degradation (G. Booker, personal communication). These results suggest that the chymotryptic cleavage site of pyruvate carboxylase (at residue 473 in the yeast enzyme) lies in an exposed and therefore proteolytically vulnerable region between more compact globular domains.

The N-terminus of yeast pyruvate carboxylase appears to be particularly suscepti-

Figure 5.10: **Time course of proteolysis of yeast pyruvate carboxylase with chymotrypsin (A) and proteinase K (B).** Aliquots of the digests were removed at the indicated times and proteolysis terminated by the appropriate inhibitor. The samples were then electrophoresed on a 12.5% SDS-polyacrylamide gel and stained with Coomassie Brilliant Blue R_{250} (top panels). Protein content of the major bands (arrowheads) was quantified by densitometry (100% defined as the protein content of the YPC band in the zero time point) and expressed as a function of time (bottom panels). YPC (•) = intact yeast pyruvate carboxylase. The three major proteinase K fragments are labelled I (○), II (◁) and III (◇). The positions of molecular weight standards (—) are indicated on the left of the zero time point track. These were (from top to bottom): β galactosidase (M_r 116000), phosphorylase b (M_r 97400), bovine serum albumin (M_r 66000), ovalbumin (M_r 45000) and carbonic anhydrase (M_r 29000).

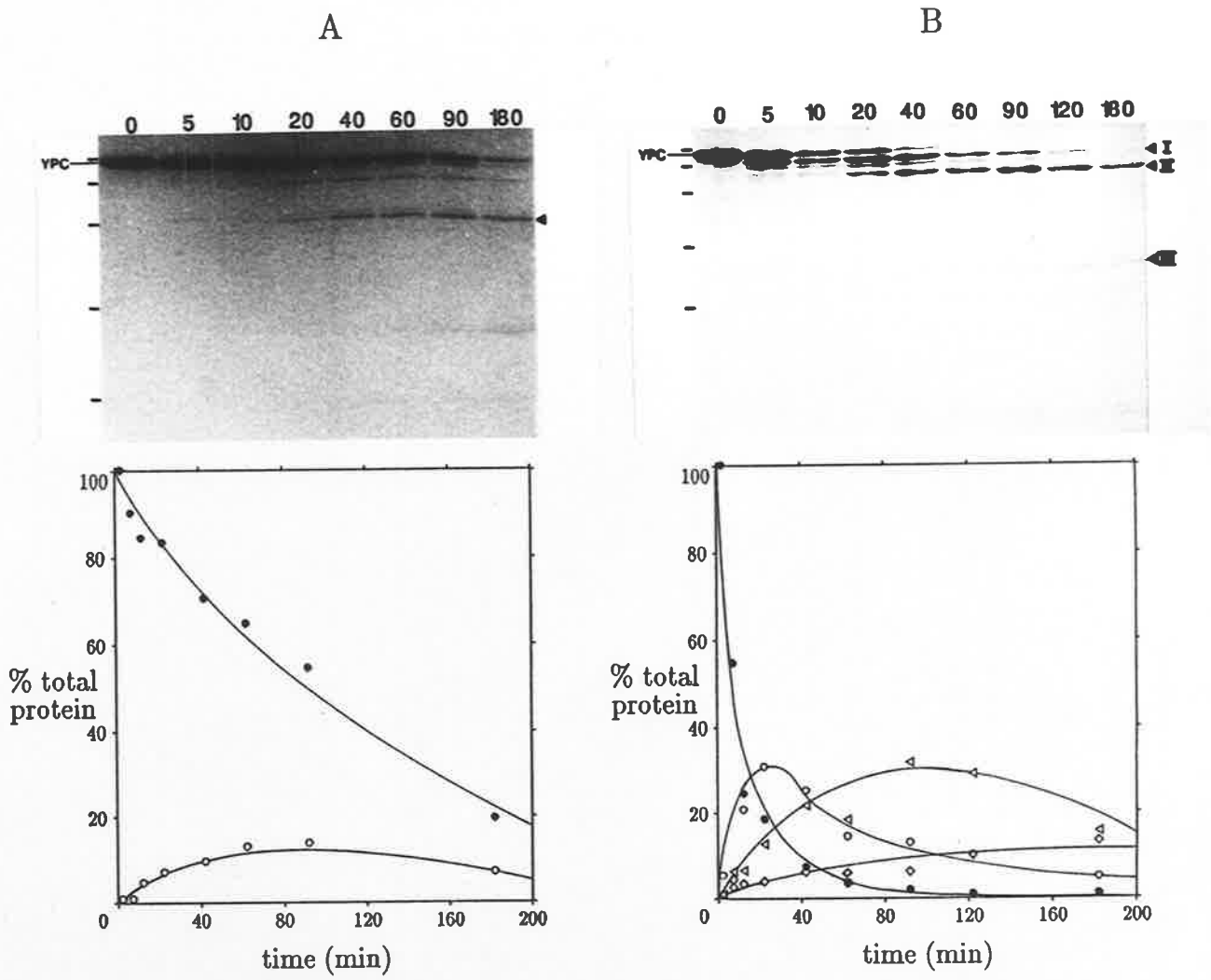
A
B
0 5 10 20 40 60 90 180
YPC
0 5 10 20 40 60 90 120 180
YPC
I
II
III
100
80
60
40
20
0
% total protein
40 80 120 160 200
time (min)
100
80
60
40
20
0
% total protein
40 80 120 160 200
time (min)

Figure 5.11: **Isolation and sequence of the chymotryptic fragment of yeast pyruvate carboxylase.**

A Yeast pyruvate carboxylase (1 mg) was digested with chymotrypsin at a substrate to protease mass ratio of 30 at 30°C for 120 minutes. Proteolysis was terminated with 5 mM PMSF and the digest chromatographed on Superose 12. The effluent was monitored at 280 nm and the fractions corresponding to the absorbance peaks (1 and 2) were collected. These were dried down and $\frac{1}{4}$ of each sample analysed by SDS gel electrophoresis on a 10% polyacrylamide gel (tracks above peaks 1 and 2). The two gel tracks on the left are intact yeast pyruvate carboxylase (YPC) and total chymotryptic digest of yeast pyruvate carboxylase (total).

B The N-terminal sequence of the isolated chymotryptic fragment of yeast pyruvate carboxylase (YPC) determined by automated Edman degradation is shown with the sequences of the chymotryptic fragments obtained from chicken liver pyruvate carboxylase (CLPC) (Khew-Goodall, 1985), sheep liver pyruvate carboxylase (SLPC) and rat liver pyruvate carboxylase (RLPC) (Booker, personal communication). The asterisks denote identical pairs of residues.

A

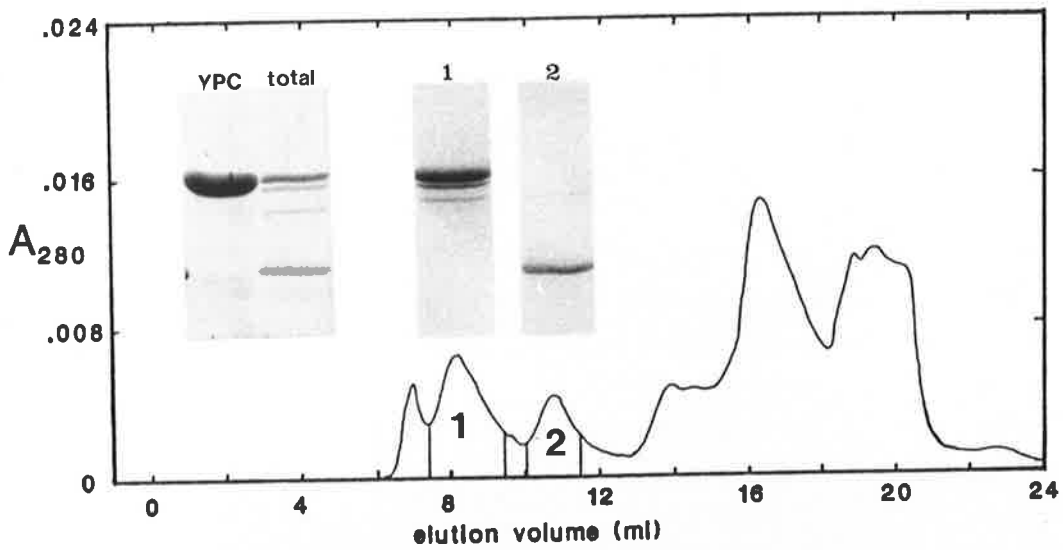

B

YPC	gln-met-val-ser-ser-gln-asn-arg-ala-gln-lys-leu-leu-his-tyr-leu-
SLPC	gln-leu-arg-pro-ala-gln-asn-arg-ala-gln-lys-leu-pro-his-tyr-leu-
RLPC	gln-leu-arg-pro-ala-gln-asn-arg-ala-gln-lys-leu- x - x -tyr-leu-
CLPC	ile-leu-arg-pro-ser-gln-asn-arg-ala-gln-lys-leu-leu-his-tyr-leu-

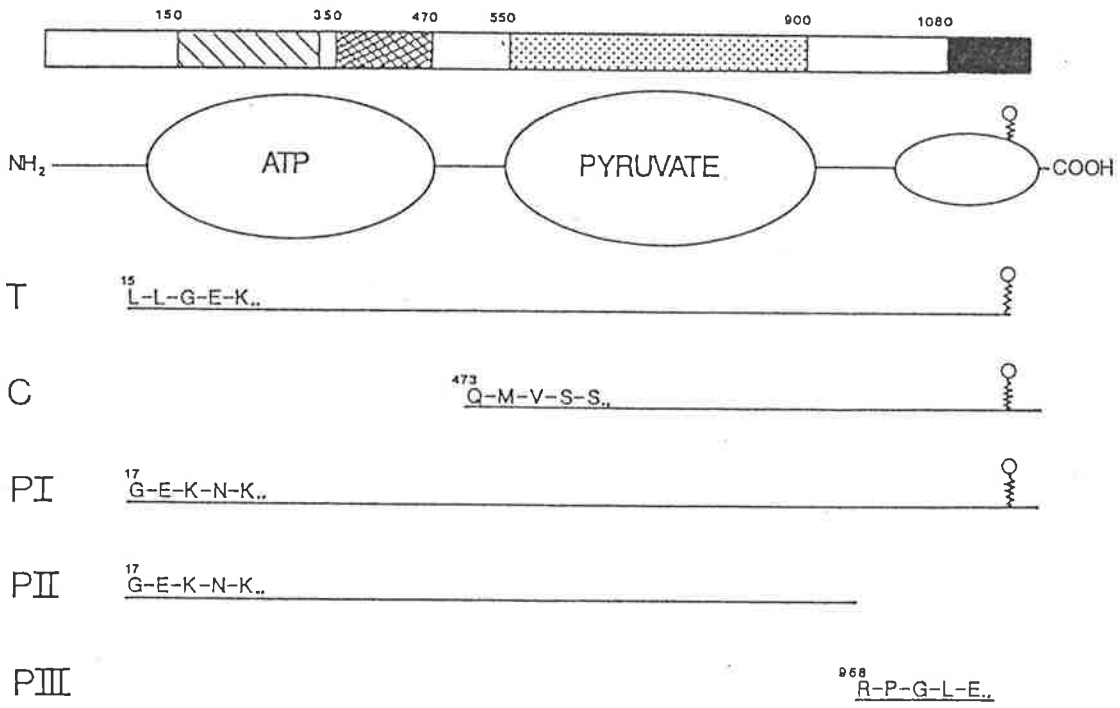

Figure 5.12: **Structural domain map of yeast pyruvate carboxylase.** The N-terminal sequences of the major polypeptides derived from limited proteolysis by thermolysin (T), chymotrypsin (C) and proteinase K (PI, PII, PIII) are aligned within the total protein sequence. The numbers given are relative to the amino-terminus and the block diagram from Figure 5.9 is shown for comparison. Biotin is represented by the circle and the putative binding sites for ATP and pyruvate are indicated.

ble to digestion with either thermolysin or proteinase K as exposure to either protease resulted in the rapid removal of the first 15-17 residues to produce initially a large biotin-containing fragment. The thermolysin fragment was resistant to further cleavage (F. Occhiodoro, personal communication) whereas the time course of proteinase K digestion (Figure 5.10B) indicated that the large fragment (I) is cleaved to form two non-biotin-containing fragments (II and III), and presumably a smaller biotin-containing peptide which is not visible on the gel.

When aligned within the total protein sequence (Figure 5.12), the sites susceptible to proteolysis identified by sequencing of the fragments indicate a linear distribution of the structural domains corresponding to the sections of sequence similarity shown in Figure 5.9. This further supports the model that pyruvate carboxylase is composed of several distinct functional domains. These domains appear to be common to pyruvate carboxylases from yeast, rat, sheep and chicken but presumably fine structural differences between these species result in different susceptibility to various proteases.

5.2.9 Effect of Partial Proteolysis on Enzyme Activity

Khew-Goodall (1985) reported that chymotryptic cleavage of sheep pyruvate carboxylase resulted in inactivation of the enzyme not by destruction of the catalytic site but rather by desensitising the enzyme to activation by acetyl-CoA. Thus in those experiments, proteolysis of sheep pyruvate carboxylase resulted in an increase in the ratio of the acetyl-CoA independent activity to the acetyl-CoA dependent activity. The effect of partial proteolysis of yeast pyruvate carboxylase by proteinase K, chymotrypsin and thermolysin on catalytic activity is shown in Figure 5.13. Enzyme activity was assayed both in the presence and absence of 250 μM acetyl-CoA. The assay mix contained 10 mM $KHCO_3$ instead of 10 mM $NaHCO_3$; in the presence of potassium ions the acetyl-CoA independent activity of yeast pyruvate carboxylase increases from ~30% to 50–60% of the total activity of the enzyme, thus facilitating measurement at low

Figure 5.13: **Effect of partial proteolysis on the activity of pyruvate carboxylase.** Yeast pyruvate carboxylase was digested under nondenaturing conditions with proteinase K (A), chymotrypsin (B) and thermolysin (C) at a substrate to protease mass ratio of 30 at 30°C. At the indicated times samples were withdrawn, proteolysis terminated by the addition of PMSF (proteinase K and chymotrypsin) or EDTA (thermolysin) and acetyl-CoA dependent activity (•–•) and acetyl-CoA independent activity (o–o) assayed by the spectrophotometric method. The results were expressed as a percentage of the total (acetyl-CoA dependent) activity of unproteolysed enzyme.

A

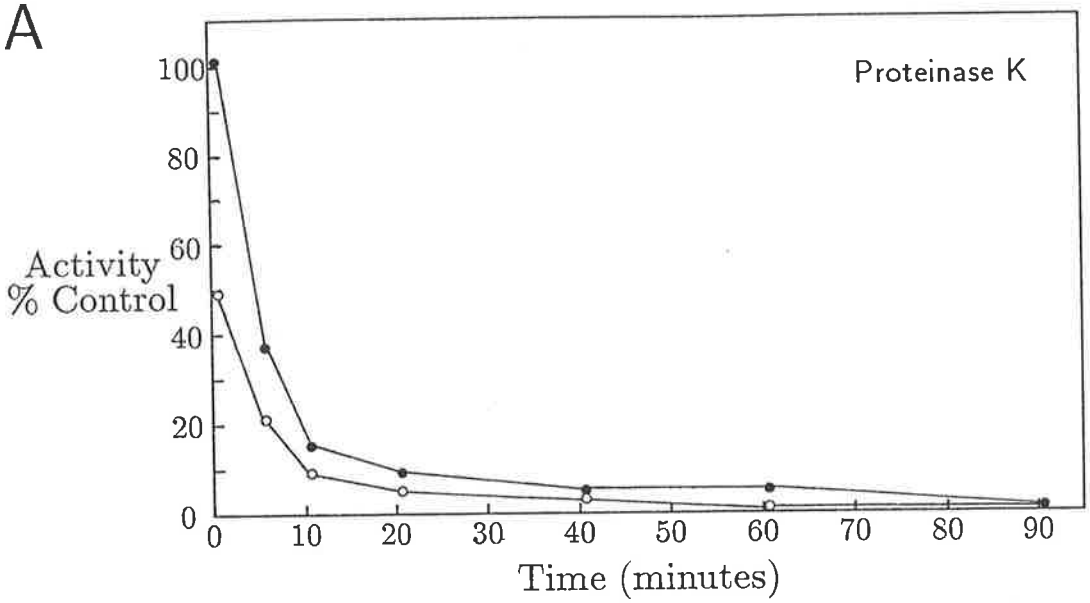
Proteinase K
Activity
% Control
100
80
60
40
20
0
0
10
20
30
40
50
60
70
80
90
Time (minutes)

B

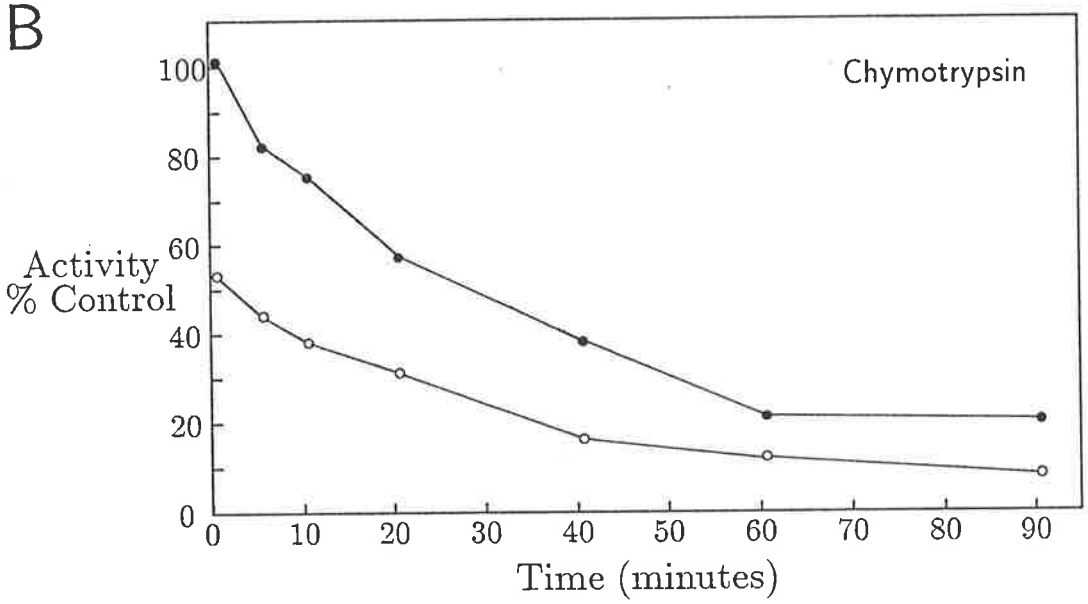
Chymotrypsin
Activity
% Control
100
80
60
40
20
0
0
10
20
30
40
50
60
70
80
90
Time (minutes)

C

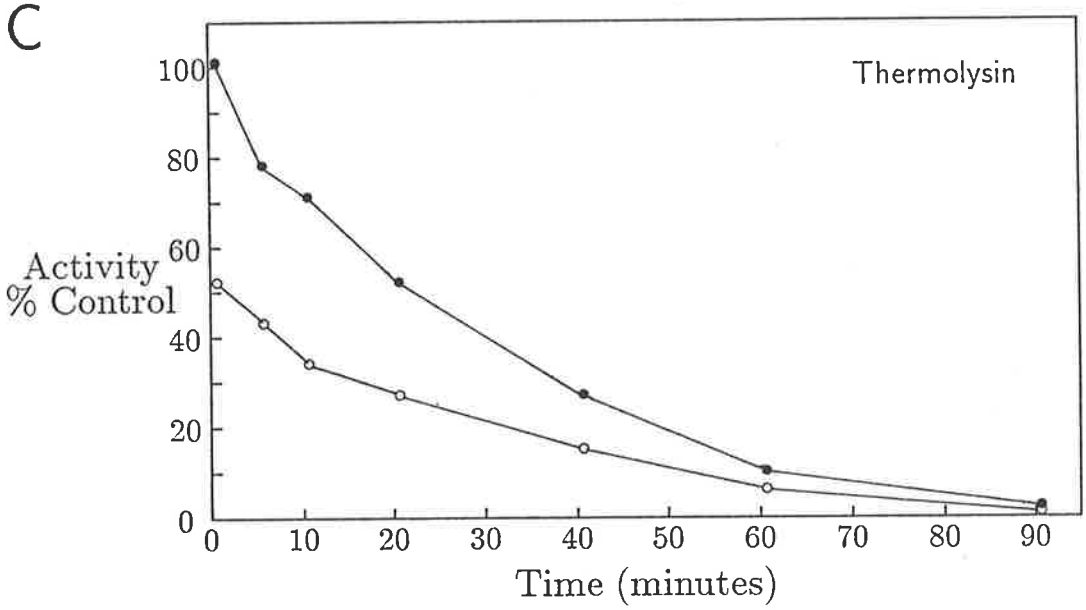
Thermolysin
Activity
% Control
100
80
60
40
20
0
0
10
20
30
40
50
60
70
80
90
Time (minutes)

values. It can be seen that both the acetyl-CoA dependent and independent activities of yeast pyruvate carboxylase decay exponentially with proteolysis and unlike the results obtained with sheep pyruvate carboxylase (Khew-Goodall, 1985), the acetyl-CoA independent activity to acetyl-CoA dependent activity ratio remained constant.

5.2.10 Modification of the ATP Binding Site

oATP

Figure 5.14 shows that under the conditions used for the oxidation reaction quantitative conversion of ATP to oATP was achieved. The magnesium complex of this derivative, Mg-oATP, behaved as a reversible inhibitor of yeast pyruvate carboxylase acting as a competitive inhibitor with respect to Mg-ATP (Figure 5.15) with an apparent K_i value of 4.3 mM. In Figure 5.16 it can be seen that reduction of the enzyme/Mg-oATP complex with sodium borohydride inactivated the enzyme. Using a reduction time of longer than 40 minutes did not result in a significant increase in inactivation. Sodium borohydride itself was not detrimental to enzymic activity since in a control sample where Mg-oATP was replaced by MgATP no loss of activity was observed. The observed inactivation was irreversible since after removal of small molecules from the reduced enzyme/Mg-oATP complex by buffer exchanges (centrifugation through a 30 kilodalton cut-off membrane repeated 3 times) there was no significant increase in enzyme activity.

To examine the stoichiometry of the inactivation process, yeast pyruvate carboxylase was modified using variable concentrations of [5′,8-^{3}H]oATP. After a 40 minute incubation with sodium borohydride enzyme activity was assayed by the spectrophotometric method and the remainder of the enzyme precipitated with 15% (w/v) trichloroacetic acid. The precipitate was collected by centrifugation and washed three times with 10% trichloroacetic acid. The protein pellet was then dissolved in formic acid and samples

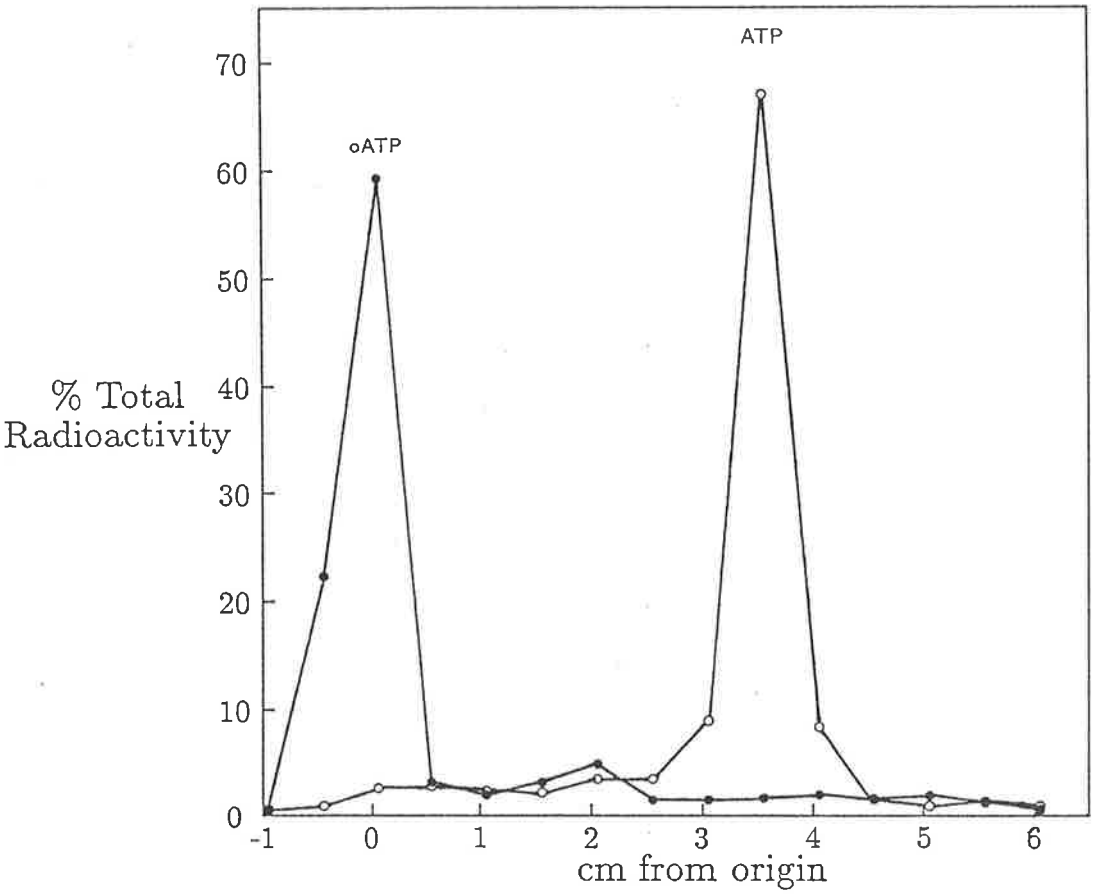

Figure 5.14: **Thin layer chromatography analysis of the synthesis of oATP.** To monitor the reaction [5′,8-^{3}H]ATP was added to the ATP to a final specific activity of 0.4 μCi/nmol. Two chromatography profiles are shown on the same axis. Samples of the reaction mix before (o–o) and after (•–•) oxidation with sodium periodate were subjected to polyethyleneimine thin layer chromatography in 0.8 M ammonium bicarbonate. After chromatography each of the two vertical tracks on the plate was cut into 0.5 cm horizontal strips and the radioactivity in each strip determined by scintillation counting.

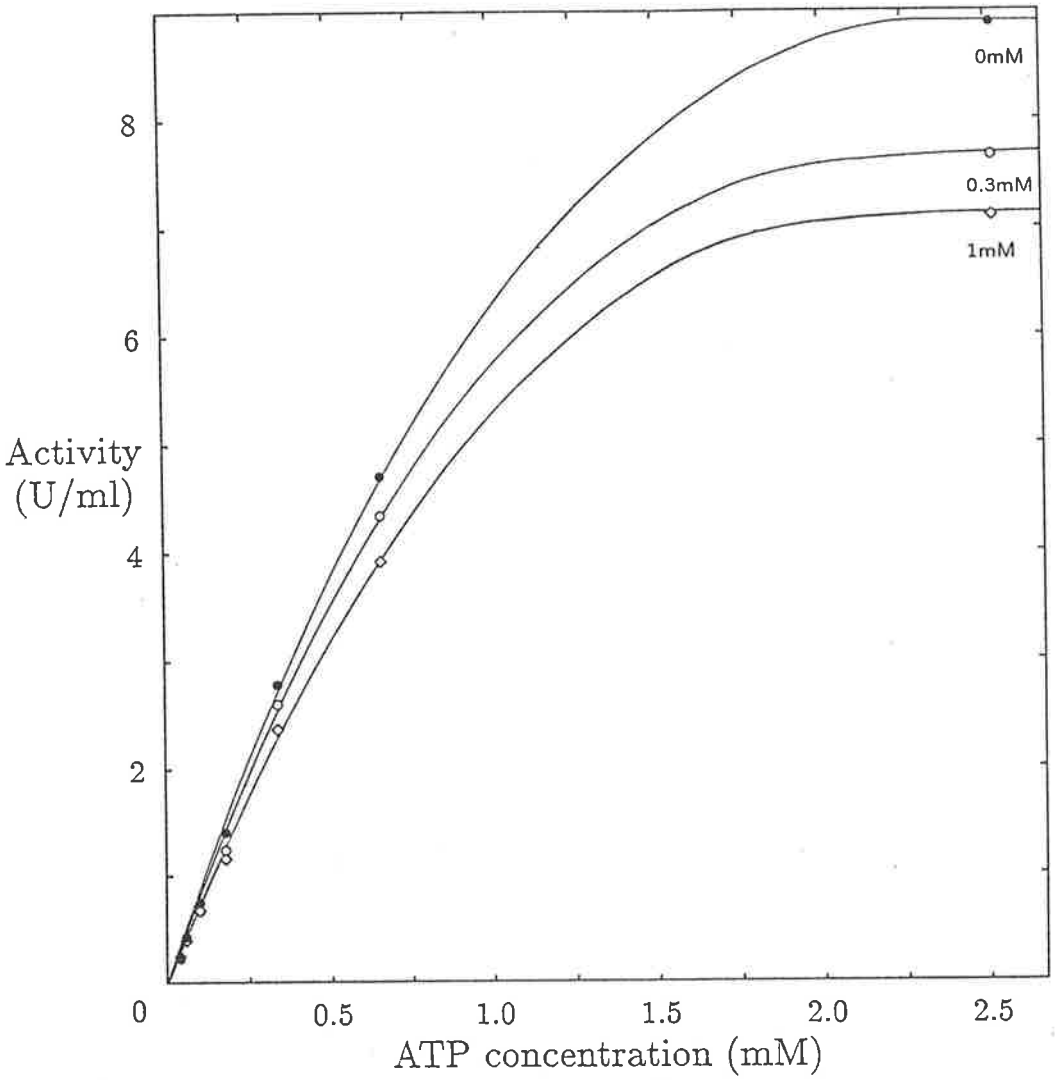

Figure 5.15: **Reversible inhibition of yeast pyruvate carboxylase by oATP.** Enzyme activity was assayed by the isotopic method in the presence of 250 μM acetyl-CoA. The ATP concentration was varied as indicated on the abscissa in samples with 1 mM oATP ($\diamond$), 0.3 mM oATP ($\circ$) and no added oATP ($\bullet$).

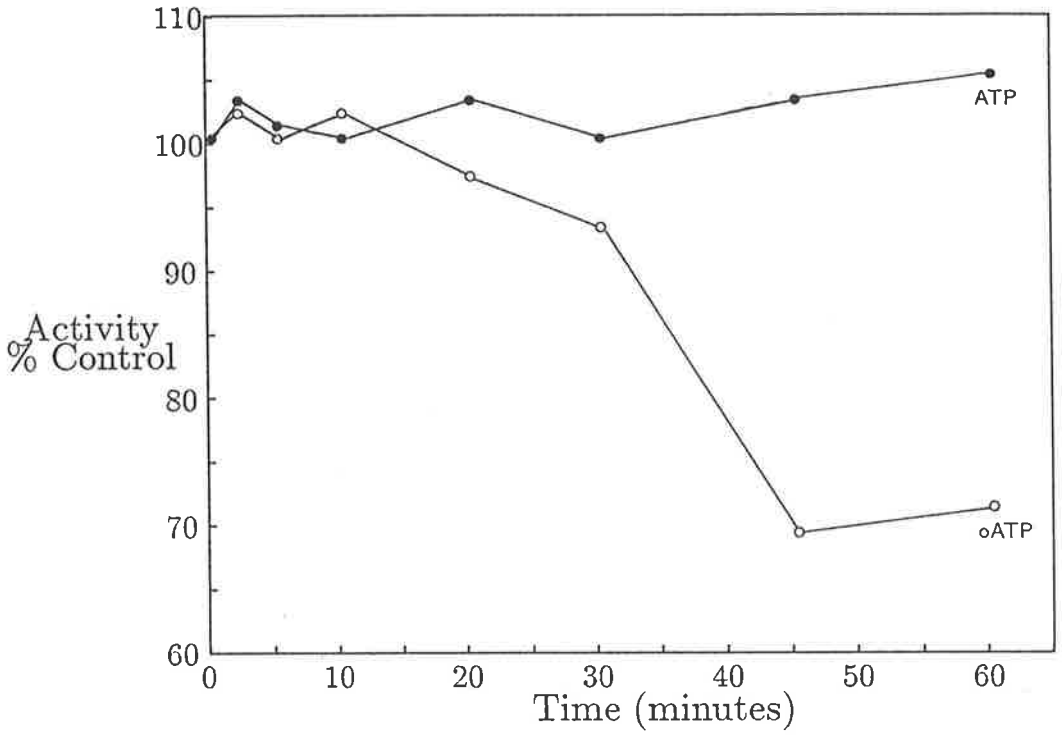

Figure 5.16: **Irreversible inhibition of yeast pyruvate carboxylase by oATP.** After preincubation of pyruvate carboxylase with 1 mM oATP (o) or 1 mM ATP (•) the enzyme/nucleotide complex was reduced with sodium borohydride for the times indicated on the abscissa. A sample was then assayed for catalytic activity by the isotopic method and the results expressed as a percentage of the activity of the unreduced sample.

spotted on paper squares, dried and counted using a toluene scintillant. In Figure 5.17 it can be seen that the experimental data points obtained at low amounts of labelling lie along a line which extrapolates to 1 mol oATP bound per mol enzyme subunit at 100% inactivation. However, at higher labelling ratios the deviation away from this line indicates that nonspecific labelling of the enzyme is occurring. These results indicated that under the conditions used specific labelling of the ATP binding site with oATP could only be achieved with an incorporation of $\leq$0.2 mol oATP/mol enzyme subunit.

In an attempt to further analyse the binding of oATP to yeast pyruvate carboxylase the enzyme was modified with [γ-^{32}P]oATP within the concentration range required to give specific labelling. Electrophoresis of the labelled enzyme on SDS gels followed by autoradiography failed to reveal any radioactivity associated with the pyruvate carboxylase band. Initially this was thought to be due to the loss of the γ-phosphate moiety by enzymatic cleavage and so the experiment was repeated in the presence of carbonic anhydrase. The rationale for this was that in the proposed catalytic mechanism for pyruvate carboxylase (Wallace *et al*, 1985), the phosphoryl transfer reaction cannot occur in the absence of bicarbonate. The carbonic anhydrase would remove any free bicarbonate and thus prevent the loss of the γ-phosphate group from the nucleotide. However, this strategy did not prevent the loss of radiolabel and the most likely explanation is that after conjugation to pyruvate carboxylase oATP is decomposed via a β elimination reaction, as reported for the (Na^+,K^+)-ATPase by Ponzio *et al* (1983), resulting in the loss of the triphosphate. When [5′,8-^{3}H]oATP was used to label yeast pyruvate carboxylase a small amount of radioactivity could be detected in gel slices containing the pyruvate carboxylase band but the specificity of this labelling could not be demonstrated by an absence of labelling in the presence of ATP. Furthermore, when a tryptic digest of the labelled enzyme was subjected to C_{18} reverse phase HPLC, none of the radioactivity was bound to the column and associated with the

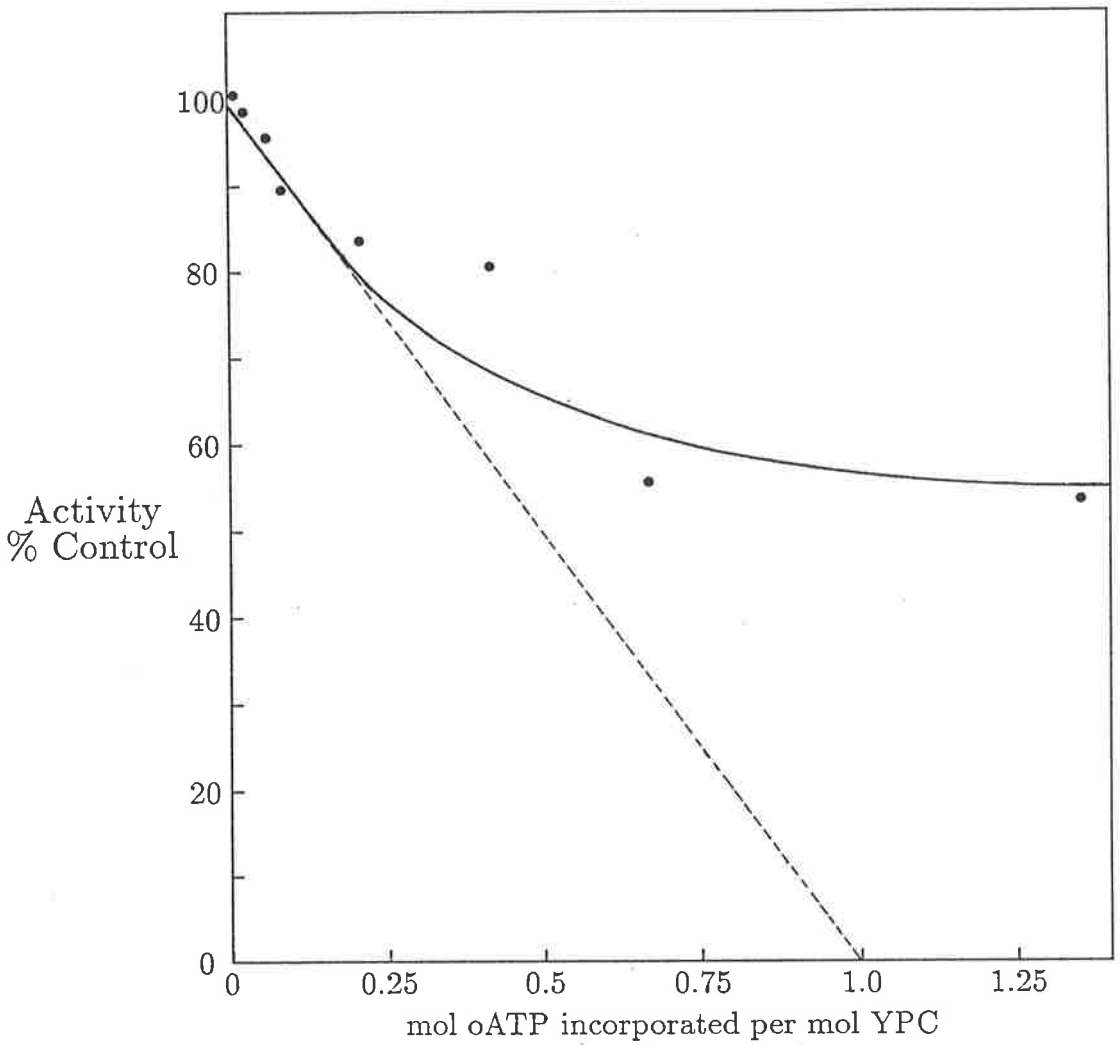

Figure 5.17: **Stoichiometry of inactivation of yeast pyruvate carboxylase by oATP.** Yeast pyruvate carboxylase was modified with varying concentrations of [5′,8-^{3}H]oATP by reduction with sodium borohydride for 40 minutes. After modification an aliquot was assayed for enzyme activity by the spectrophotometric method and the remainder pelleted by precipitation with 15% trichloroacetic acid. After washing with 10% trichloroacetic acid the radioactivity in the pellet was determined by scintillation counting.

peptide fractions. Similar problems have been observed by Lowe and Beechey (1982) who used oATP to label the mitochondrial ATPase. These authors found that not only did decomposition of oATP occur after it had been bound to the enzyme, but that some of the products formed by decomposition of oATP in solution attached to the enzyme more readily and with no specificity for the ATP site. Bezares *et al* (1987) were able to use oADP to isolate a tryptic peptide from the active site of rabbit muscle pyruvate kinase but these authors also found that radioactivity was lost from the final sequenced material.

8-azido-ATP

In view of the apparent instability of oATP after linkage to yeast pyruvate carboxylase another affinity label was investigated. Using the same approach as described above it was found that 8-azido-ADP was a competitive inhibitor of yeast pyruvate carboxylase with respect to ATP, with an apparent K_i of 3.2 mM (F. Occhiodoro, personal communication). Irradiation of the enzyme/8-azido-ADP complex with a broad spectrum ultraviolet lamp resulted in irreversible enzyme inactivation, the specificity of which could be demonstrated by the lack of inactivation obtained in the presence of ATP (F. Occhiodoro, personal communication). However, while specific inactivation of yeast pyruvate carboxylase could be obtained by the use of 8-azido-ADP, the incorporation of [γ-^{32}P]8-azido-ATP into the protein was variable and could not be blocked by the presence of ATP. The radiolabel was however bound to the enzyme in a stable fashion and SDS gel electrophoresis followed by autoradiography revealed a labelled band coincident with the pyruvate carboxylase band (F. Occhiodoro, personal communication). The lack of specificity of labelling is puzzling, in view of the specific nature of inactivation; a possible explanation is that 8-azido-ATP may bind to the enzyme at locations other than the ATP binding site and exert little effect on activity. One

such possibility is that the nucleotide may bind to the acetyl-CoA binding site. This is supported by the observation that the presence of acetyl-CoA decreases the amount of label attached to the enzyme (F. Occhiodoro, personal communication). In an attempt to improve specific incorporation a labelling experiment was performed with the following modifications:

- Acetyl-CoA (250 μM) was present throughout the whole experiment. This was to increase the specificity of labelling by blocking the acetyl-CoA site.
- In the presence of protecting concentrations of ATP (10 mM), the enzyme was first labelled with nonradioactive 8-azido-ADP. This was to block any nonspecific binding sites outside the ATP site normally labelled by the 8-azido-nucleotides.
- after removal of unbound small molecules by buffer exchange (three times through Centricon 30), the enzyme was labelled with [γ-^{32}P]8-azido-ATP as usual. After buffer exchange the enzyme was labelled a second time with [γ-^{32}P]8-azido-ATP. This second labelling was to increase the total amount of radiolabel incorporated.

The net result of these changes was a decrease in the amount of radiolabel incorporated with no increase in specificity.

These results highlight the major difficulty in the use of affinity labels: optimisation of the signal to noise ratio. In order to detect a labelled peptide it is necessary to use as high a ratio of radiolabel to protein as possible. However, this requirement is counterbalanced by the undesirable occurrence of nonspecific labelling at high label to protein ratios. Future work using this technique should be aimed at improving the amount of incorporation under conditions of specific labelling.

Chapter 6

Discussion and Conclusions

The ability to engineer proteins with altered or even new functions by recombinant DNA techniques has emphasised the need for an understanding of the varied aspects of protein structure and function. Some of these principles are well illustrated by this study of pyruvate carboxylase.

6.1 Sequence and Evolution

Apart from being an essential prerequisite for X-ray crystallography studies, the determination of the complete amino acid sequence of yeast pyruvate carboxylase has enabled a detailed comparison of this enzyme with other functionally similar enzymes to begin. In the preceding chapter the approximate boundaries of three domains within the total primary structure were delineated. The origin of the C-terminal biotinyl domain as an independent gene product is supported by partial proteolysis data and sequence similarities with the small biotin-carrying subunits of *P.shermanii* transcarboxylase and *E.coli* acetyl-CoA carboxylase. Furthermore, in the rat pyruvate carboxylase gene, the 3′- exon (which encodes the biotin attachment site) is about the same size as the above-mentioned bacterial biotinyl subunits (Cassady, 1987). The intron separating this from the next exon is possibly a remnant of the 5′- control region of an ancestral gene (Hardie and Coggins, 1986).

The biotinyl carrier domain is common to all biotin enzymes and it appears that

the members of this family have evolved by combination and modification of a basic set of domains. In the scheme depicted in Figure 6.1 the diverse functions of the biotin enzymes are shown to have arisen from divergent evolution (eg. the different specificities of CoA-ester binding in acetyl-CoA carboxylase, transcarboxylase and propionyl-CoA carboxylase) and gene fusion (giving rise to multifunctional polypeptides such as pyruvate carboxylase and acetyl-CoA carboxylase). This is consistent with the concept of domains as "cassettes" (Gilbert, 1978) which may be slotted into genes to confer new functions upon the encoded proteins. The lipoamide transferases and carbamyl phosphate synthetase represent more distantly related enzymes, and although they contain domains which have recognisable structural similarities to those found in the biotin enzymes, the functional similarities among these domains are not as immediately obvious.

6.2 Catalytic Mechanism

The strong homology of the N-terminal region of yeast pyruvate carboxylase with the ATP-binding regions of carbamyl phosphate synthetase has interesting implications about the mechanism of the enzyme. In the first partial reaction the hydrolysis of MgATP to MgADP and Pi is coupled to the carboxylation of biotin. Figure 6.2A shows the stepwise sequence of events proposed by Wallace *et al* (1985) leading to the formation of carboxybiotin. In this scheme bicarbonate is activated by ATP to form a carboxyphosphate intermediate (Figure 6.2B) which then reacts with the N′-atom of the ureido group of the biotin moiety. In support of this mechanism it has been shown that *E.coli* acetyl-CoA carboxylase (Polakis *et al*, 1972) and sheep pyruvate carboxylase (Ashman and Keech, 1975) can catalyse the phosphoryl transfer from carbamyl phosphate (Figure 6.2C), an analogue of carboxyphosphate, to ADP to form ATP. The high degree of sequence homology noted between yeast pyruvate carboxylase and

Figure 6.1: **Hypothetical Scheme for the evolution of the biotin enzymes.** Divergent evolution of a primitive ATP/HCO_3-binding protein may have given rise to proteins with specificities for carbamyl phosphate (C-N-P) and carboxyphosphate (C-O-P).
The CoA-ester binding members of the biotin enzymes shown here fall into two classes: those that bind malonyl-CoA (M-CoA) and those that bind methylmalonyl-CoA (MM-CoA).
Divergence of a primitive carrier protein (CAR) may have given rise to biotinyl proteins (BIO) and lipoyl proteins (LIP).
The multifunctional polypeptides such as eukaryotic acetyl-CoA carboxylase (euk ACC), eukaryotic pyruvate carboxylase (euk PC), the sodium dependent oxaloacetate decarboxylase of *Klebsiella pneumoniae* (OAA DC) and the biotinyl subunits of propionyl-CoA carboxylase and *Pseudomonas citronellolis* pyruvate carboxylase appear to have arisen by fusion of genes coding for monofunctional polypeptides.
Ac-CoA: acetyl-CoA; P-CoA: propionyl-CoA; PYR: pyruvate; OAA: oxaloacetate; the C-terminal portion of eukaryotic acetyl-CoA carboxylase is speculated to be involved in binding of the allosteric activator citrate. The direction of the normally catalysed reaction is indicated in those cases where both substrate and product have been given to show possible evolutionary relationships.

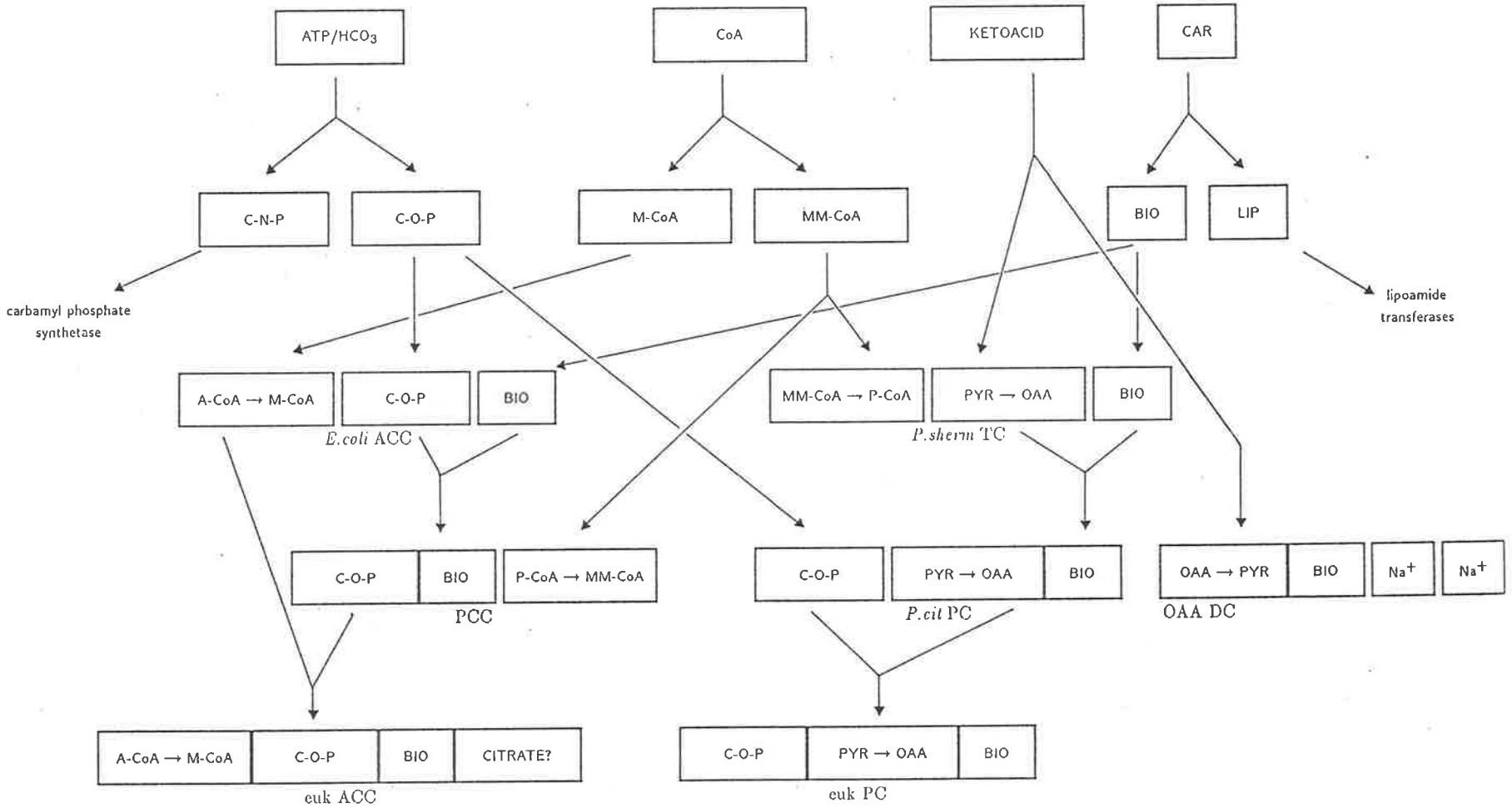
ATP/HCO3
CoA
KETOACID
CAR
C-N-P
C-O-P
M-CoA
MM-CoA
BIO
LIP
carbamyl phosphate synthetase
lipoamide transferases
A-CoA → M-CoA
C-O-P
BIO
E.coli ACC
MM-CoA → P-CoA
PYR → OAA
BIO
P.sherm TC
C-O-P
BIO
P-CoA → MM-CoA
PCC
C-O-P
PYR → OAA
BIO
P.cit PC
OAA → PYR
BIO
Na+
Na+
OAA DC
A-CoA → M-CoA
C-O-P
BIO
CITRATE?
euk ACC
C-O-P
PYR → OAA
BIO
euk PC

A

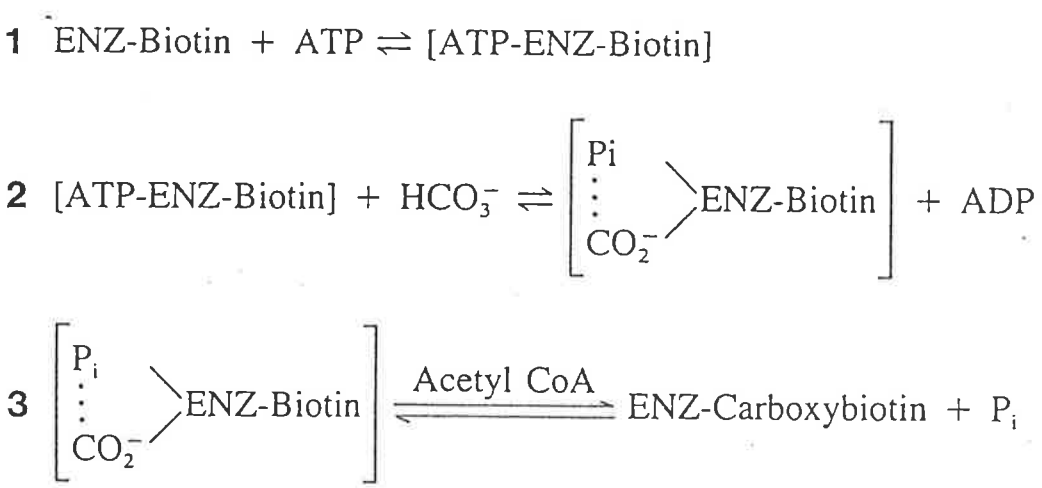

B **C**

Figure 6.2: **The carboxylation of biotin by pyruvate carboxylase** In this scheme (A) proposed by Wallace *et al* (1985) ATP binds to the enzyme (ENZ) first (1) and the subsequent binding of bicarbonate (2) forms an activated carboxyphosphate intermediate (structure C). The transfer of the carboxyl group to biotin (3) is dependent on acetyl-CoA. It can be seen that carbamyl phosphate (structure B) is a close analogue of carboxyphosphate. P_i = inorganic phosphate.

carbamyl phosphate synthetase may well reflect a similarity in the tertiary structures of the ATP/bicarbonate binding sites of these enzymes.

In the same way the sequence homologies noted between the areas surrounding the prosthetic group attachment points in the biotin enzymes and the lipoamide enzymes draws attention to the similar functions of biotin and lipoic acid in these two protein families. Both are connected to the ϵ-amino group of a lysine residue by a 14 Å molecular string (Figure 6.3) which enables them to transport activated groups (CO_2 for biotin and an acetyl group for lipoic acid) from one catalytic subsite to another. In view of the similar structures of biotin and lipoic acid it would appear that there are some very interesting evolutionary relationships between the two enzyme families, the prosthetic groups, and the holoenzyme synthetases which catalyse their attachment.

6.3 Intracellular Location

Although yeast have the subcellular organisation characteristic of eukaryotes, there are a number of important metabolic differences between these organisms and higher eukaryotes such as the vertebrates. For instance, a number of enzymes including glutamate dehydrogenase, carbamyl phosphate synthetase (arginine-specific) and pyruvate carboxylase show differences in their subcellular compartmentation in yeast and in vertebrates.

Pyruvate carboxylase has a mitochondrial location in vertebrate tissues but as shown in Chapter 4 the yeast enzyme is exclusively cytosolic. This is consistent with the absence of a leader sequence in the translation product of the gene sequence, and the failure of antibodies to detect precursor forms of the enzyme on Western blots of total yeast lysates. Despite its different location within the cell, the quaternary structure of yeast pyruvate carboxylase appears to be very similar to that of the vertebrate forms, with four subunits arranged in a tetrahedral configuration. With this structural

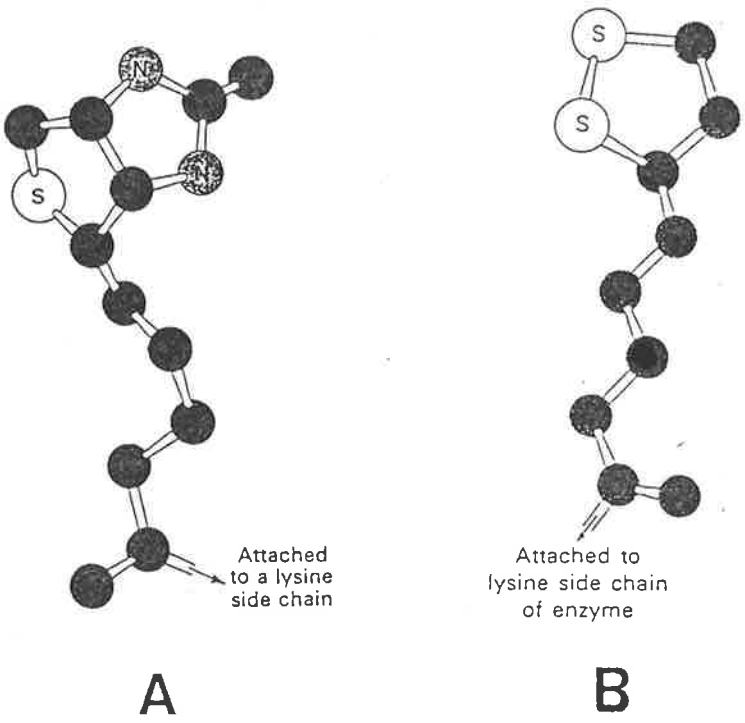

Figure 6.3: **Comparison of the structures of biotin (A) and lipoic acid (B).** These two prosthetic groups are covalently linked to a specific lysine residue in their enzymes by a 14 Å molecular string.

arrangement it seems unlikely that this is a membrane-associated enzyme, since this would require an unequal interaction of subunits with the membrane. Indeed, in pigeon liver, Landriscina *et al* (1970) have used electron microscopy to localise pyruvate carboxylase in a cell extract fraction which was free of membrane, and which they identified as the mitochondrial matrix.

6.4 Allosterism

Eukaryotic pyruvate carboxylases exhibit a considerable stimulation of activity in the presence of acetyl-CoA and it has been proposed (Wallace *et al*, 1985) that it is the transfer of the carboxyl group from carboxyphosphate to biotin which is dependent on acetyl-CoA (Figure 6.2A). The electron microscopic data presented in Chapter 3 show that binding of acetyl-CoA causes the enzyme to become more compact. It is possible that this conformational change is required to bring the carboxyphosphate intermediate close enough to the biotin moiety for carboxyl transfer to occur.

The responses of yeast pyruvate carboxylase to regulatory effectors are different to those of the vertebrate pyruvate carboxylases, reflecting differences in metabolic organisation. In vertebrate liver pyruvate carboxylase is a key enzyme in gluconeogenesis but in nongluconeogenic tissues and microorganisms it still serves an anaplerotic function: regeneration of oxaloacetate whenever the intermediates of the tricarboxylic acid cycle are withdrawn for biosynthesis. However, as discussed in the previous section, metabolic compartmentation differs between the lower and higher eukaryotes. The regulatory properties of several eukaryotic pyruvate carboxylases and their intracellular locations are summarised in Table 6.1. From this data it can be seen that the mitochondrial forms found in vertebrates are activated by acetyl-CoA but not by long chain acyl-CoAs. In contrast the cytosolic pyruvate carboxylases found in fungi are activated by acetyl-CoA as well as long chain CoAs. Additionally the mitochondrial

SOURCE OF ENZYME	INTRACELLULAR LOCALISATION	REGULATORY ACTIVATORS	REGULATORY INHIBITORS
S. cerevisiae	cytosolic	palmitoyl-CoA, acetyl-CoA	L-aspartate, 2-oxo-glutarate
A. nidulans	cytosolic	oleoyl-CoA, acetyl-CoA	L-aspartate, 2-oxo-glutarate
R. arrhizus	cytosolic	palmitoyl-CoA, acetyl-CoA	L-aspartate, 2-oxo-adipate
avian	mitochondrial	acetyl-CoA	L-glutamate, 2-oxo-glutarate
mammalian	mitochondrial	acetyl-CoA	L-glutamate, 2-oxo-glutarate

Table 6.1 **Regulatory effectors and intracellular locations of the fungal and vertebrate pyruvate carboxylases.** (Adapted from Osmani *et al*, 1985).

pyruvate carboxylases are inhibited by L-glutamate and in some cases 2-oxo-glutarate whereas the cytosolic enzymes are sensitive to regulatory inhibition by L-aspartate and in most cases 2-oxo-glutarate.

6.5 A Structural Model

While the three-dimensional description of a protein at the atomic level depends on its successful crystallisation for diffraction studies, it is nevertheless possible to obtain some structural data using other techniques. The electron-microscopic analysis of avidin-pyruvate carboxylase complexes (section 3.2.6) indicates that the C-terminal biotinyl domain of each polypeptide chain is located close to the intersubunit junction. The position of the other two identified domains is uncertain but preliminary data suggests that the ATP/HCO_3 binding domain is at the end of the subunit distal to the intersubunit junction:

- As shown in Chapter 5 limited chymotryptic treatment of yeast pyruvate carboxylase removes this N-terminal domain. When crosslinked tetramers of sheep pyruvate carboxylase were subjected to limited proteolysis with chymotrypsin, electron micrographs revealed complexes with protomers truncated at the distal

end (M. Rohde, personal communication).

- The distal location of the biotin carboxylation active site could explain how an anti-sheep pyruvate carboxylase monoclonal antibody which apparently binds to the distal end of the sheep pyruvate carboxylase subunit, is able to inhibit enzyme activity (K.J. Oliver, personal communication).

Figure 6.3 illustrates a simple structural model which is consistent with the experimental data. Proteolytic removal of the N-terminal ATP/HCO_3 binding domain results in catalytic inactivation and truncation at the distal end of each subunit (Figure 6.3B). Activation of the enzyme by acetyl-CoA occurs via a conformational change which allows carboxylation of biotin to occur. This conformational change also decreases the apparent subunit length, resulting in a more compact appearance for the enzyme tetramer. This phenomenon was also observed by Taylor *et al* (1978) who reported an increase in the S value of yeast pyruvate carboxylase in reacting enzyme sedimentation studies when acetyl-CoA was added.

6.6 Future Work

The work presented in this thesis has been directed towards establishing a convenient system in which mutant biotin enzymes (particularly pyruvate carboxylase) can be synthesised and studied. The selection of mutation sites and the design of experimental approaches will to some extent depend on comparative data obtained by parallel work on other biotin enzymes. In Table 6.2 the status of the work within this laboratory on various biotin enzymes is indicated.

The proposed mutation work has two broad goals: firstly to derive more information about the enzyme, and secondly to design polypeptides to perform specified functions. These two aims are interdependent and several approaches are suggested:

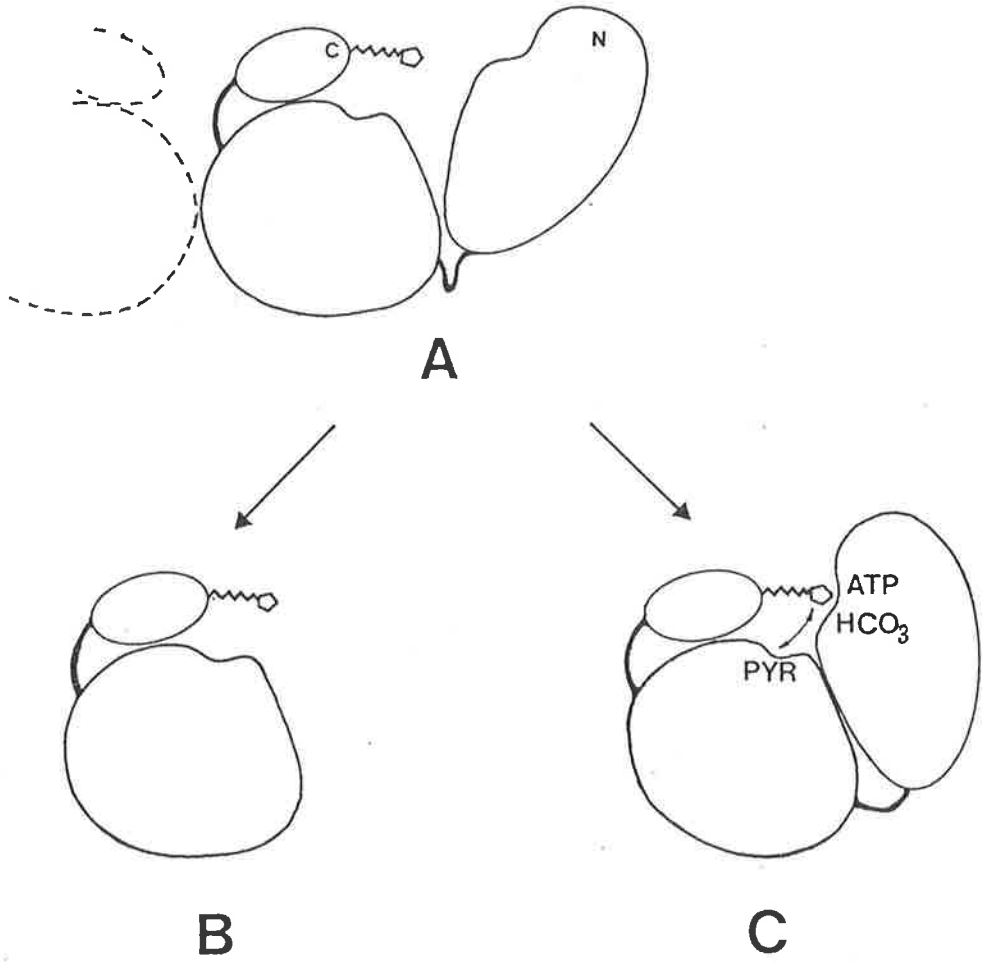

Figure 6.4: **Structural model of yeast pyruvate carboxylase.**

A The C-terminal (C) biotinyl domain is proximal to the junction of the subunit with its dimer partner (dotted lines). The native tetrameric enzyme appears to be composed of two such dimers joined back to back. The N-terminal (N) ATP-binding domain is at the distal end of the subunit.

B Chymotryptic cleavage removes the N-terminal ATP-binding domain, thus shortening the subunit.

C Binding of acetyl-CoA causes a conformational change which enables the biotin moiety to interact with the activated carboxyphosphate in the ATP/HCO_3 domain. The carboxybiotin complex then swings across to the pyruvate (PYR) binding site.

	PROTEIN PURIFIED	PEPTIDES SEQUENCED	ANTIBODIES	CLONES	DNA SEQUENCE	MUTANTS
Chicken PC	yes	yes	polyclonals	—	—	—
Chicken PCC	yes	yes	—	—	—	—
Sheep PC	yes	yes	monoclonals	—	—	—
Sheep PCC	yes	yes	monoclonals	—	—	—
Rat PC	yes	yes	—	partial cDNA	partial	—
Yeast PC	yes	yes	polyclonals	partial genomic complete genomic	complete	in progress
Yeast ACC	—	—	—	putative partial genomic	—	ura$^-$ acc$^-$

Table 6.2 **Status of biotin enzyme work in this laboratory in April 1988.**
PC = pyruvate carboxylase; PCC = propionyl-CoA carboxylase; ACC = acetyl-CoA carboxylase.

In vivo **Mutagenesis** Mutants of *Saccharomyces cerevisiae* induced by ethane-methane-sulphonate or ultraviolet radiation could be screened for putative *pyc* cells based on the inability to grow on glucose unless supplemented by a source of C4 tri-carboxylic acid intermediates. Further screening would be by enzyme assays and immunodetection of pyruvate carboxylase in cell extracts by Western blotting (Lim *et al*, 1987). This approach will reveal essential residues in the protein and will complement the comparative data of other pyruvate carboxylase and biotin enzyme sequences.

Localised Random Mutagenesis As has been described in Chapter 5, it has not been possible to assign by homology the role of acetyl-CoA binding to any specific region(s) in the polypeptide. An alternative approach would be to generate banks of mutants containing base changes in localised regions of the gene using bisulphite mutagenesis (Shortle and Nathans, 1978) with gapped heteroduplex molecules (Kalderon *et al*, 1982). These could then be screened for loss of acetyl-CoA or palmitoyl-CoA activation of the enzyme without concomitant loss of acetyl-CoA independent catalytic activity.

Site-directed Mutagenesis This approach depends on the prior identification of

specific residues of importance in the enzyme based on other studies such as sequence comparisons, affinity labelling and random mutagenesis experiments. Using oligonucleotide-directed mutagenesis methods (Zoller and Smith, 1983) specific substitutions of selected amino acid residues may be made to either confirm the functions assigned to them or to deliberately alter their functions.

For example, the region spanning residues 550–900, which is thought to include the pyruvate binding site (see Section 5.2.5), contains four cysteines. Previous studies (Hudson *et al*, 1975; Bagley *et al*, 1983) have shown an essential role for cysteine residues in the pyruvate-oxaloacetate exchange reaction catalysed by pyruvate carboxylase. Thus, systematic substitution of serine (sterically similar to cysteine) for each of the four cysteines in the putative pyruvate domain may ascertain which is/are involved in catalysis.

Deletions and Fusions The partial proteolysis data (Chapter 5) has indicated the presence of structural domains corresponding to the domains identified by homology studies. In parallel with further partial proteolysis studies to isolate functional fragments, the translation products of deletion and fusion mutants of the pyruvate carboxylase gene could be examined. Besides being useful in identifying functional domains, this approach could have practical benefits. For example, fusion of the recognition site for biotin attachment to a cloned protein may result in a biotinylated expression product, facilitating purification of the protein from yeast cell extracts. Another possible advantage of dissecting yeast pyruvate carboxylase into smaller functional fragments is that each of these may be easier to crystallise than the complete molecule. Since the structures of these components would have to be similar to those found in the native molecule in order to retain activity, the full structure of the enzyme could then be obtained by refinement of the sum of such component structures.

The immediate aim for future work in yeast pyruvate carboxylase is to use the cloned yeast genomic DNA to disrupt the endogenous yeast gene (Rothstein, 1983) and thus create a pyruvate carboxylase-deficient yeast strain. Once such a host background is constructed the expression of plasmids bearing mutated pyruvate carboxylase DNA could begin.

PUBLICATIONS

1. Rohde, M., Lim, F. and Wallace, J.C. (1986) Pyruvate carboxylase from *Saccharomyces cerevisiae*. Quaternary structure, effects of allosteric ligands and binding of avidin *Eur. J. Biochem.* **156**, 15–22.

2. Hughes, B.P., Polverino, A.J., Lim, F. and Barritt, G.J. (1987) Vasopressin decreases total free fatty acids but enhances release of radioactivity from isolated hepatocytes labelled with [^{3}H]Arachidonic Acid *Horm. Metabol. Res.* **19**, 15–20.

3. Morris, C.P., Lim, F. and Wallace, J.C. (1987) Yeast pyruvate carboxylase: gene isolation *Biochem. Biophys. Res. Comm.* **145**, 390–396.

4. Lim, F., Rohde, M., Morris, C.P. and Wallace, J.C. (1987) Pyruvate carboxlase in the yeast *pyc* mutant *Arch. Biochem. Biophys.* **258**, 259–263.

5. Lim, F., Morris, C.P., Occhiodoro, F. and Wallace, J.C. (1988) Sequence and domain structure of yeast pyruvate carboxylase submitted to *J. Biol. Chem.*

Bibliography

[1] Allen, G. (1981) *Sequencing of Proteins and Peptides.* North-Holland Publishing Company Amsterdam.

[2] Artymiuk, P.J., Blake, C.C.F. and Albrecht, E.S. (1981) *Nature* **290**, 287–288.

[3] Ashman, L.K.and Keech, D.B. (1975) *J. Biol. Chem.* **250**, 14–21.

[4] Bagley, C.J., Goss, N.H., Keech, D.B. and Wallace, J.C. (1983) *Proc. Aust. Biochem. Soc.* **15**, 1.

[5] Barden, R.E., Taylor, B.L., Isohashi, F., Frey, W.H., Zander, G.L., Lee, J.C. and Utter, M.F. (1975) *Proc. Natl. Acad. Sci. USA.* **72**, 4308–4312.

[6] Benton, W.D. and Davis, R.W. (1977) *Science* **196**, 180–182.

[7] Bezares, G., Eyzaguirre, J., Hinrichs, M.V., Heinrikson, R.L., Reardon, I., Kemp, R.G., Latshaw, S.P. and Baznes, S. (1987) *Arch. Biochem. Biophys.* **253**, 133–137.

[8] Blake, C.C.F. (1981) *Nature* **291**, 616.

[9] Bradford, M.M. (1976) *Anal. Biochem.* **72**, 248–254.

[10] Brown, R.K. (1967) *Meth. Enzymol.* **11**, 917–927.

[11] Cassady, A.I. *Pyruvate Carboxylase: A Molecular Biological Study* PhD thesis University of Adelaide, Adelaide, South Australia (1987).

[12] Cohen, N.D., Utter, M.F., Wrigley, N.G. and Barrett, A.N. (1979) *Biochemistry* **18**, 2197–2203.

[13] Cryer, D.R., Eccleshall, R. and Marmur, J. (1975) *Meth. Cell Biol.* **12**, 39–44.

[14] Dayhoff, M.O., Schwartz, R.M. and Orcutt, B.C. (1978) *Atlas of Protein Sequence and Structure.* National Biomedical Research Foundation Washington, D.C., USA 5th edition.

[15] de Mey, J., Moeremans, M., Gemeus, G., Moydens, R. and de Brabander, M. (1981) *Cell. Biol. Int. Reports* **5**, 889–899.

[16] Duggleby, R.G. (1980) *Anal. Biochem.* **110**, 9–18.

[17] Duggleby, R.G., Kinns, H. and Rood, J.I. (1981) *Anal. Biochem.* **110**, 49–55.

[18] Easterbrook-Smith, S.B., Wallace, J.C. and Keech, D.B. (1976) *Eur. J. Biochem.* **62**, 125–130.

[19] Ey, P.L., Prowse, S.J. and Jenkin, C.R. (1978) *Immunochemistry* **15**, 429–436.

[20] Fersht, A. (1985) *Enzyme Structure and Mechanism.* W.H. Freeman and Company, New York 2nd edition.

[21] Fothergill-Gilmore, L.A. (1986) Domains of glycolytic enzymes. In Hardie, D.G. and Coggins, J.R., editors, *Multidomain Proteins - Structure and Evolution.* pages 85–174, Elsevier, Amsterdam.

[22] Freytag, S.O. and Collier, K.J. (1984) *J. Biol. Chem.* **259**, 12831–12837.

[23] Fry, D.C., Kuby, S.A. and Mildvan, A.S. (1986) *Proc. Natl. Acad. Sci. USA.* **83**, 907–911.

[24] Gilbert, W. (1978) *Nature* **271**, 501.

[25] Goad, W.B. and Kanehisa, M. (1982) *Nucleic Acids Res.* **10**, 247–263.

[26] Goss, N.H. *Pyruvate Carboxylase* PhD thesis University of Adelaide, Adelaide, South Australia (1978).

[27] Goss, N.H., Dyer, P.Y., Keech, D.B. and Wallace, J.C. (1979) *J. Biol. Chem.* **254**, 1734–1739.

[28] Guest, J.R., Lewis, H.M., Graham, L.D., Packman, L.C. and Perham, R.N. (1985) *J. Mol. Biol.* **185**, 743–754.

[29] Haarasilta, S. and Taskinen, L. (1977) *Arch. Microbiol.* **113**, 159–161.

[30] Haase, F.C., Henrikson, K.P., Treble, D.H. and Allen, S.H.G. (1982) *J. Biol. Chem.* **257**, 11994–11999.

[31] Henrikson, K.P., Allen, S.H.G. and Maloy, W.L. (1979) *Anal. Biochem.* **94**, 366–370.

[32] Hudson, P.J., Keech, D.B. and Wallace, J.C. (1975) *Biochem. Biophys. Res. Comm.* **65**, 213–219.

[33] Hunkapiller, M.W., Hewick, R.M., Dreyer, W.J. and Hood, L.E. (1983) *Methods Enzymol.* **91**, 399–413.

[34] Ikemura, T. (1982) *J. Mol. Biol.* **158**, 573–597.

[35] Irias, J.J., Olmsted, M.R. and Utter, M.F. (1969) *Biochemistry* **8**, 5136–5140.

[36] Johannssen, W., Attwood, P.V., Wallace, J.C. and Keech, D.B. (1983) *Eur. J. Biochem.* **133**, 201–206.

[37] Julin, D.A. and Lehman, I.R. (1987) *J. Biol. Chem.* **262**, 9044–9051.

[38] Kalderon, D., Oostra, B.A., Ely, B.K. and Smith, A.E. (1982) *Nucleic Acids Res.* **10**, 5161–5171.

[39] Kalnins, A., Otto, K., Ruther, U. and Muller-Hill, B. (1983) *EMBO J.* **2**, 593–597.

[40] Khew-Goodall, Y.S. *Pyruvate Carboxylase: Its Interactions with Acetyl-CoA* PhD thesis University of Adelaide, Adelaide, South Australia (1985).

[41] Klotz, I.M. and Darnall, D.W. (1969) *Science* **166**, 126–151.

[42] Knight, K.L. and McEntee, K. (1986) *Proc. Natl. Acad. Sci. USA.* **83**, 9289–9293.

[43] Knuth, D.E. (1984) *The TEXbook.* Addison-Wesley Publishing Company Reading, Massachusetts.

[44] Kohanski, R.A. and Lane, M.D. (1985) Blank In Dakshinamurti, K. and Bhagavan, H.N., editors, *Biotin.* pages 373–385 Annals of the New York Academy of Sciences, New York, USA, Volume 447.

[45] Kraus, J.P., Firgaira, F., Novotný, J., Kalousek, F., Williams, K.R., Williamson, C., Ohura, T. and Rosenberg, L.E. (1986) *Proc. Natl. Acad. Sci. USA.* **83**, 8049–8053.

[46] Laemmli, U.K. (1970) *Nature* **227**, 680–685.

[47] Lamhonwah, A-M., Barankiewicz, T.J., Willard, H.F., Mahuran, D.J., Quan, F. and Gravel, R.A. (1986) *Proc. Natl. Acad. Sci. USA.* **83**, 4864–4868.

[48] Lamhonwah, A-M., Quan, F. and Gravel, R.A. (1987) *Arch. Biochem. Biophys.* **254**, 631–636.

[49] Lamport, L. (1986) LATEX. Addison-Wesley Publishing Company Reading, Massachusetts.

[50] Lau, E.P., Cochran, B.C., Munson, L. and Fall, R.R. (1979) *Proc. Natl. Acad. Sci. USA.* **76**, 214–218.

[51] Layne, E. (1957) *Meth. Enzymol.* **3**, 447–454.

[52] Libor, S., Sundaram, T.K., Warwick, R., Chapman, J.A. and Grundy, S.M.W. (1979) *Biochemistry* **18**, 3647–3653.

[53] Lim, F., Rohde, M., Morris, C.P. and Wallace, J.C. (1987) *Arch. Biochem. Biophys.* **258**, 259–264.

[54] Losada, M., Canovas, J.L. and Ruiz-Amil, M. (1964) *Biochem. Z.* **340**, 60–64.

[55] Lowe, P.N. and Beechey, R.B. (1982) *Biochemistry* **21**, 4073–4082.

[56] Lusty, C.J., Widgren, E.E., Broglie, K.E. and Nyunoya, H. (1983) *J. Biol. Chem.* **258**, 14466–14472.

[57] Lynen, F. (1975) Structures of biotin carboxylases. In Richter, D., editor, *Energy regulation and biosynthesis in molecular biology.* pages 671–698, W. de Gruyter, Berlin, West Gremany.

[58] Maniatis, T., Fritsch, E.F. and Sambrook, J. (1982) *Molecular Cloning. (A Laboratory Manual).* Cold Spring Harbor Laboratory, Cold Spring Harbor, NY, USA.

[59] Mayer, F., Wallace, J.C. and Keech, D.B. (1980) *Eur. J. Biochem.* **112**, 265–272.

[60] Mornet, D., Ue, K. and Morales, F. (1984) *Proc. Natl. Acad. Sci. USA.* **81**, 736–742.

[61] Morris, C.P., Lim, F. and Wallace, J.C. (1987) *Biochem. Biophys. Res. Comm.* **145**, 390–396.

[62] Moss, J. and Lane, M.D. (1971) *Adv. Enzymol.* **35**, 321–442.

[63] Murtif, V.L., Bahler, C.R. and Samols, D. (1985) *Proc. Natl. Acad. Sci. USA.* **82**, 5617–5621.

[64] Murtif, V.L. and Samols, D. (1987) *J. Biol. Chem.* **262**, 11813–11816.

[65] Myers, D.E., Tolbert, B. and Utter, M.F. (1983) *Biochemistry* **22**, 5090–5096.

[66] Needleman, S.B. and Wunsch, C.D. (1970) *J. Mol. Biol.* **48**, 443–453.

[67] Nyunoya, H., Broglie, K.E., Widgren, E.E. and Lusty, C.J. (1985) *J. Biol. Chem.* **260**, 9346–9356.

[68] Nyunoya, H. and Lusty, C.J. (1983) *Proc. Natl. Acad. Sci. USA.* **80**, 4629–4633.

[69] Nyunoya, H. and Lusty, C.J. (1984) *J. Biol. Chem.* **259**, 9790–9798.

[70] Obermayer, M. and Lynen, F. (1976) *Trends Biochem. Sci.* **1**, 169–171.

[71] O'Brien, R.W., Chuang, D.T., Taylor, B.L. and Utter, M.F. (1977) *J. Biol. Chem.* **252**, 1257–1262.

[72] Osmani, S.A., Mayer, F., Marston, F.A.O., Selmes, I.P. and Scrutton, M.C. (1984) *Eur. J. Biochem.* **139**, 509–518.

[73] Osmani, S.A. and Scrutton, M.C. (1985) *Eur. J. Biochem.* **147**, 119–128.

[74] Osmani, S.A. and Scrutton, M.C. (1983) *Eur. J. Biochem.* **133**, 551–560.

[75] Osmani, S.A., Scrutton, M.C. and Mayer, F. (1985) The structure and regulation of fungal pyruvate carboxylases. In Dakshinamurti, K. and Bhagavan, H.N., editors, *Biotin.* pages 169–188 Annals of the New York Academy of Sciences, New York, USA, Volume 447.

[76] Palczewski, K. and Kochman, M. (1987) *Biochemistry* **26**, 3466–3471.

[77] Paranjape, S., Shenoy, B.C., Kumar, G.K., Samols, D. and Wood, H.G. (1988) *Fed. Proc.* , in press.

[78] Perham, R.N. and Wilkie, A.O.M. (1980) *Biochem. Internatl.* **1**, 470–477.

[79] Polakis, S.E., Guchhait, R.B. and Lane, M.D. (1972) *J. Biol. Chem.* **247**, 1335–1337.

[80] Ponzio, G., Rossi, B. and Lazdunski, M. (1983) *J. Biol. Chem.* **258**, 8201–8205.

[81] Porter, R.R. (1959) *Biochem. J.* **73**, 119–126.

[82] Powers-Lee, S.G. and Corina, K. (1987) *J. Biol. Chem.* **262**, 9052–9056.

[83] Radding, C.M. and Shreffler, D.C. (1966) *J. Mol. Biol.* **18**, 251–261.

[84] Rigby, P.W.J., Dieckmann, C., Rhodes, C. and Berg, P. (1977) *J. Mol. Biol.* **113**, 237–251.

[85] R.L., Potter and Taylor, S.S. (1980) *J. Biol. Chem.* **255**, 9706–9712.

[86] Rohde, M., Lim, F. and Wallace, J.C. (1986) *Eur. J. Biochem.* **156**, 15–22.

[87] Rothstein, R.J. (1983) *Meth. Enzymol.* **101**, 202–211.

[88] Ruiz-Amil, M., de Torrontegui, G., Palacian, E., Catalina, L. and Losada, M. (1965) *J. Biol. Chem.* **183**, 3485–3492.

[89] Rylatt, D.B., Keech, D.B. and Wallace, J.C. (1977) *Arch. Biochem. Biophys.* **183**, 113–122.

[90] Rylatt, D.B. and Parish, C.R. (1982) *Anal. Biochem.* **121**, 213–214.

[91] Samols, D., Thornton, C.G., Murtif, V.L., Ganesh, K., Kumar, F., Haase, C. and Wood, H.G. (1988) *J. Biol. Chem.* , in press.

[92] Sanger, F., Nicklen, S. and Coulson, A.R. (1977) *Proc. Natl. Acad. Sci. USA.* **74**, 5463–5467.

[93] Scrutton, M.C. and Utter, M.F. (1965) *J. Biol. Chem.* **240**, 1–8.

[94] Scrutton, M.C., Young, M.R. and Utter, M.F. (1970) *J. Biol. Chem.* **245**, 6220–6227.

[95] Shortle, D. and Nathans, D. (1978) *Proc. Natl. Acad. Sci. USA.* **75**, 2170–2174.

[96] Simon, E.J. and Shemin, D. (1953) *J. Amer. Chem. Soc.* **75**, 2520–2523.

[97] Skinner, V.M. and Armitt, S. (1972) *FEBS Lett.* **20**, 16–18.

[98] Slot, J.W. and Geuze, H.J. (1981) *J. Cell. Biol.* **90**, 533–536.

[99] Srivastava, G., Borthwick, I.A., Brooker, J.D., Wallace, J.C., May, B.K. and Elliott, W.H. (1983) *Biochem. Biophys. Res. Comm.* **117**, 344–349.

[100] Staden, R. (1982) *Nucleic Acids Res.* **10**, 4731–4751.

[101] Staden, R. (1984) *Nucleic Acids Res.* **12**, 551–567.

[102] Struhl, K. (1987) *Cell* **49**, 295–297.

[103] Sundaram, T.K. (1973) *J. Bacteriol.* **113**, 549–552.

[104] Svboda, M., Meuris, S. and Christophe, J. (1985) *Anal. Biochem.* **151**, 16–23.

[105] Takai, T., Wada, K. and Tanabe, T. (1987) *FEBS Lett.* **212**, 98–102.

[106] Taylor, B.L, Frey, W.H., Barden, R.E., Scrutton, M.C. and Utter, M.F. (1978) *J. Biol. Chem.* **253**, 3062–3069.

[107] Wallace, J.C. (1985) Distribution and biological functions of pyruvate carboxylase in nature. In Keech, D.B. and Wallace, J.C., editors, *Pyruvate Carboxylase.* pages 5–64, CRC Series in Enzyme Biology, CRC Press, Boca Raton, USA.

[108] Wallace, J.C. and Easterbrook-Smith, S.B. (1985) The structure of pyruvate carboxylase. In Keech, D.B. and Wallace, J.C., editors, *Pyruvate Carboxylase.* pages 65–108, CRC Series in Enzyme Biology, CRC Press, Boca Raton, USA.

[109] Wallace, J.C., Phillips, N.B., Snoswell, M.A., Goodall, G.J., Attwood, P.V. and Keech, D.B. (1985) Pyruvate carboxylase: mechanisms of the partial reactions. In Dakshinamurti, K. and Bhagavan, H.N., editors, *Biotin.* pages 169–188 Annals of the New York Academy of Sciences, New York, USA, Volume 447.

[110] Wilbur, W.J. and Lipman, D.J. (1983) *Proc. Natl. Acad. Sci. USA.* **80**, 726–730.

[111] Wills, C. and Melham, T. (1985) *Arch. Biochem. Biophys.* **236**, 782–791.

[112] Wood, H.G. and Barden, R.E. (1977) *Annu. Rev. Biochem.* **46**, 385–413.

[113] Wood, H.G. and Kumar, G.K. (1985) Transcarboxylase: Its quaternary structure and the role of the biotinyl subunit in the assembly of the enzyme and in catalysis. In Dakshinamurti, K. and Bhagavan, H.N., editors, *Biotin.* pages 1–22, Annals of the New York Academy of Sciences, New York, USA, Volume 447.

[114] Young, M.R., Tolbert, B. and Utter, M.F. (1969) *Meth. Enzymol.* **13**, 250–258.

[115] Zoller, M.J. and Smith, M. (1983) *Meth. Enzymol.* **100**, 468–500.